# 3-D Seismic Delineation of the North Anatolian Fault System Shear Zone in the Western Half of Marmara Basin, Türkiye

Ö. Yilmaz, Z. Özer, D. T. Beşevli, J. E. L. Wu, C. Özsoy, S. Sevinç, K. B. Bakioglu, M. B. Ercengiz, Ö. K. Şahin, B. Dadak, T. Hastürk, Ö. Yapar, H. Dalabasmaz, N. Ö. Sipahioglu, C. Demirci, R. Ö. Temel, M. F. Akalın, and M. S. B. Sadioglu

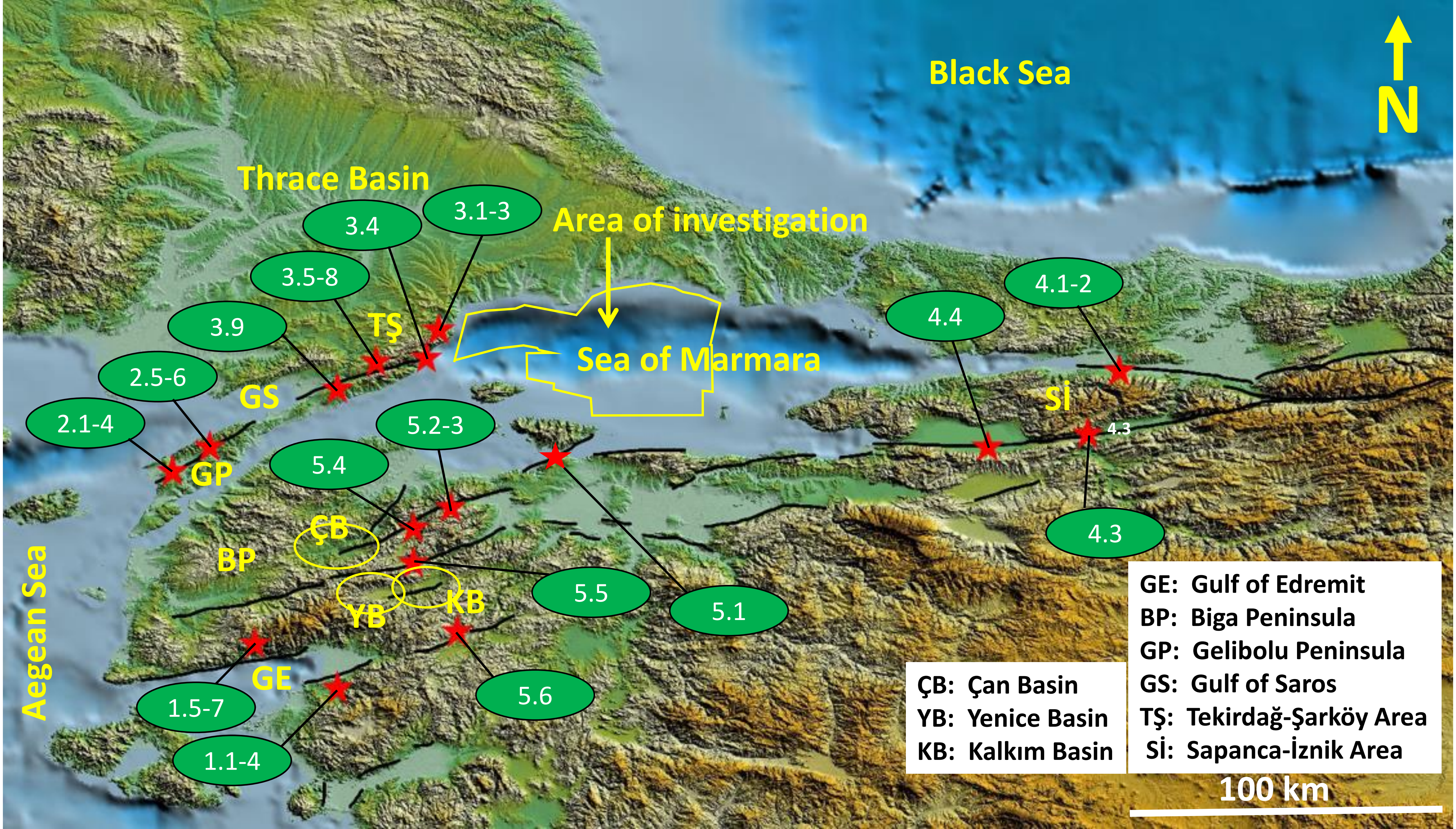

Black Sea
N
Thrace Basin
Area of investigation
Sea of Marmara
3.4
3.1-3
3.5-8
TŞ
3.9
2.5-6
GS
2.1-4
GP
5.2-3
5.4
ÇB
BP
5.5
5.1
YB
KB
GE
1.5-7
1.1-4
5.6
Aegean Sea
4.1-2
4.4
Sİ
4.3
4.3
GE: Gulf of Edremit
BP: Biga Peninsula
GP: Gelibolu Peninsula
GS: Gulf of Saros
TŞ: Tekirdağ-Şarköy Area
Sİ: Sapanca-İznik Area
ÇB: Çan Basin
YB: Yenice Basin
KB: Kalkım Basin
100 km

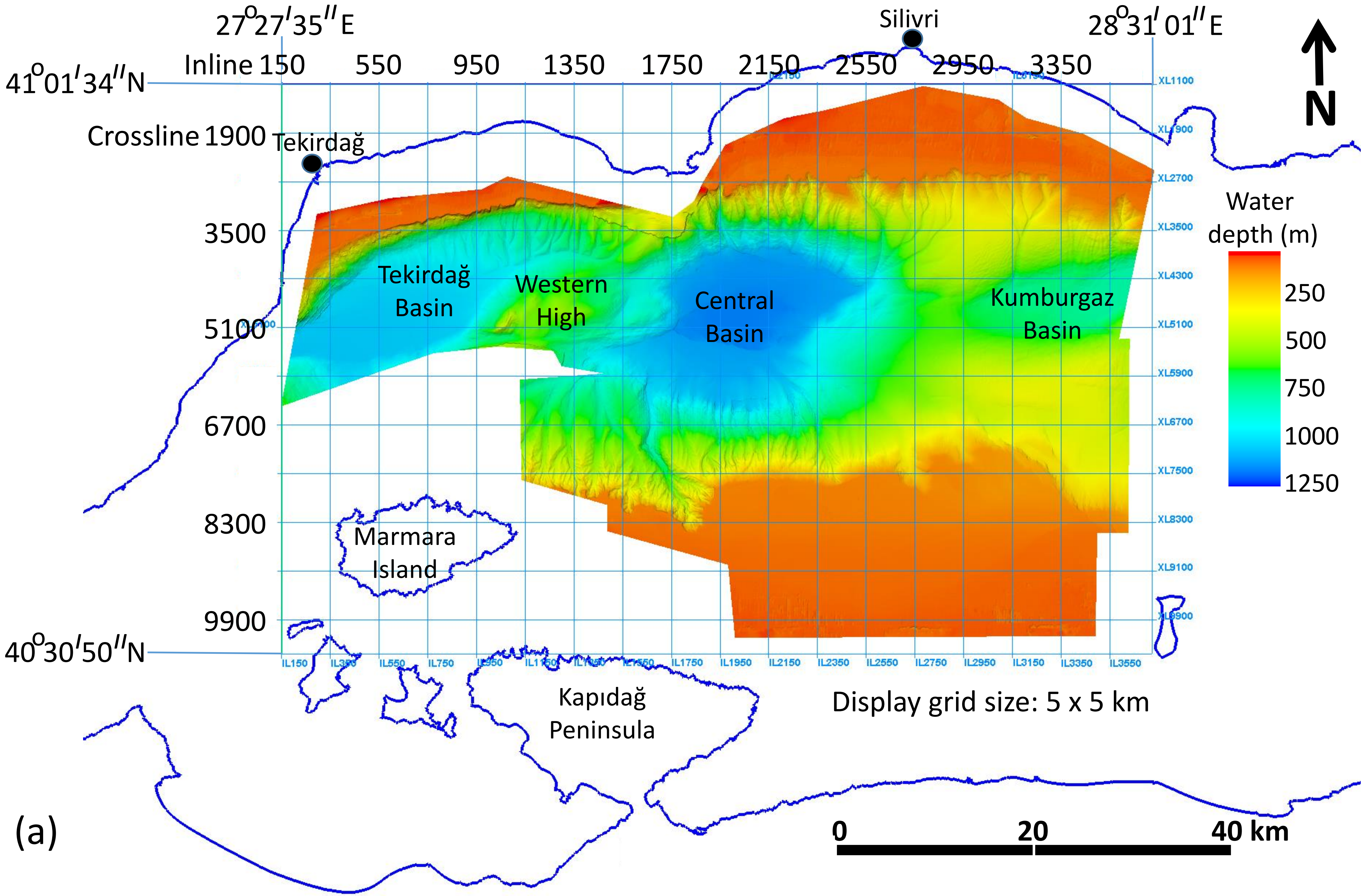
27°27′35″E
Silivri
28°31′01″E
N
41°01′34″N
Inline 150
550
950
1350
1750
2150
2550
2950
3350
Crossline 1900
Tekirdağ
3500
5100
6700
8300
9900
40°30′50″N
Tekirdağ Basin
Western High
Central Basin
Kumburgaz Basin
Water depth (m)
250
500
750
1000
1250
Marmara Island
Kapıdağ Peninsula
Display grid size: 5 x 5 km
0
20
40 km
(a)

# 1988

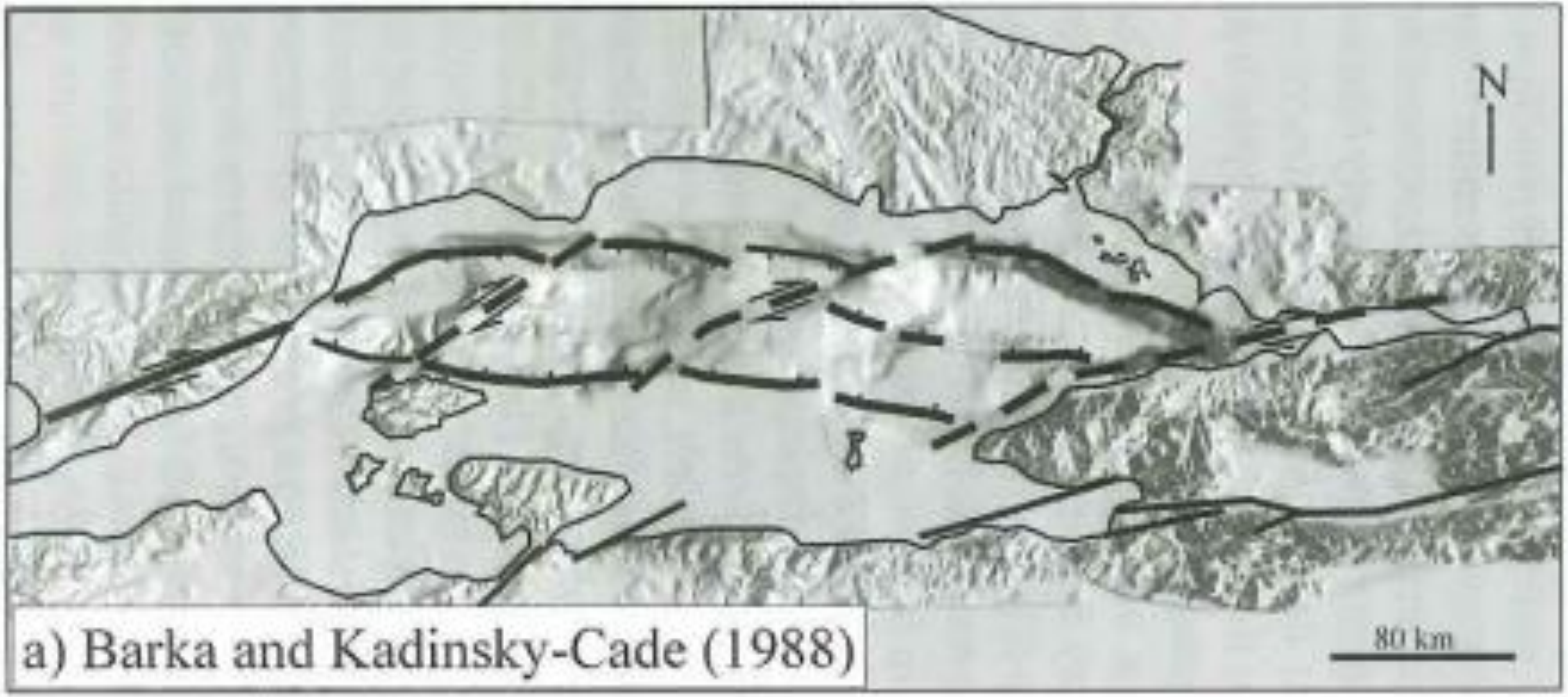

a) Barka and Kadinsky-Cade (1988)

Barka, A. A. and Kadinsky-Cade, K. (1988). Strike-slip fault geometry in Turkey and its influence on earthquake activity. *Tectonics*, **(7)** 3**,** 663–684.

Figure 11 of paper 69 Yilmaz, Y., Gökaşan, E., & Erbay, A. Y. (2010), Morphotectonic development of the Marmara Region. *Tectonophysics*, 488, 51-70.

# 1999

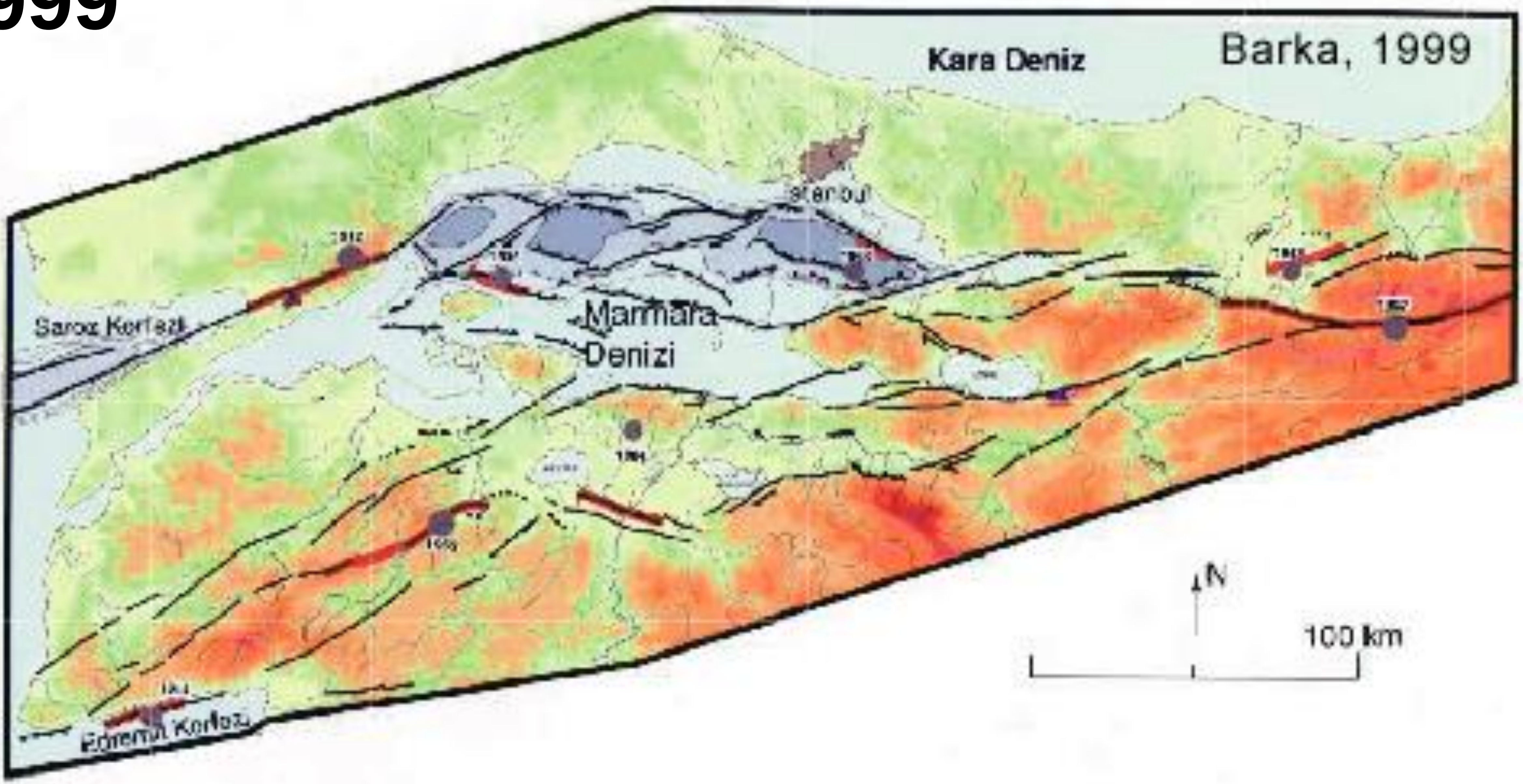
Barka, 1999
Kara Deniz
Saroz Korfezi
Marmara
Denizi
Edremit Korfezi
N
100 km

# 1999

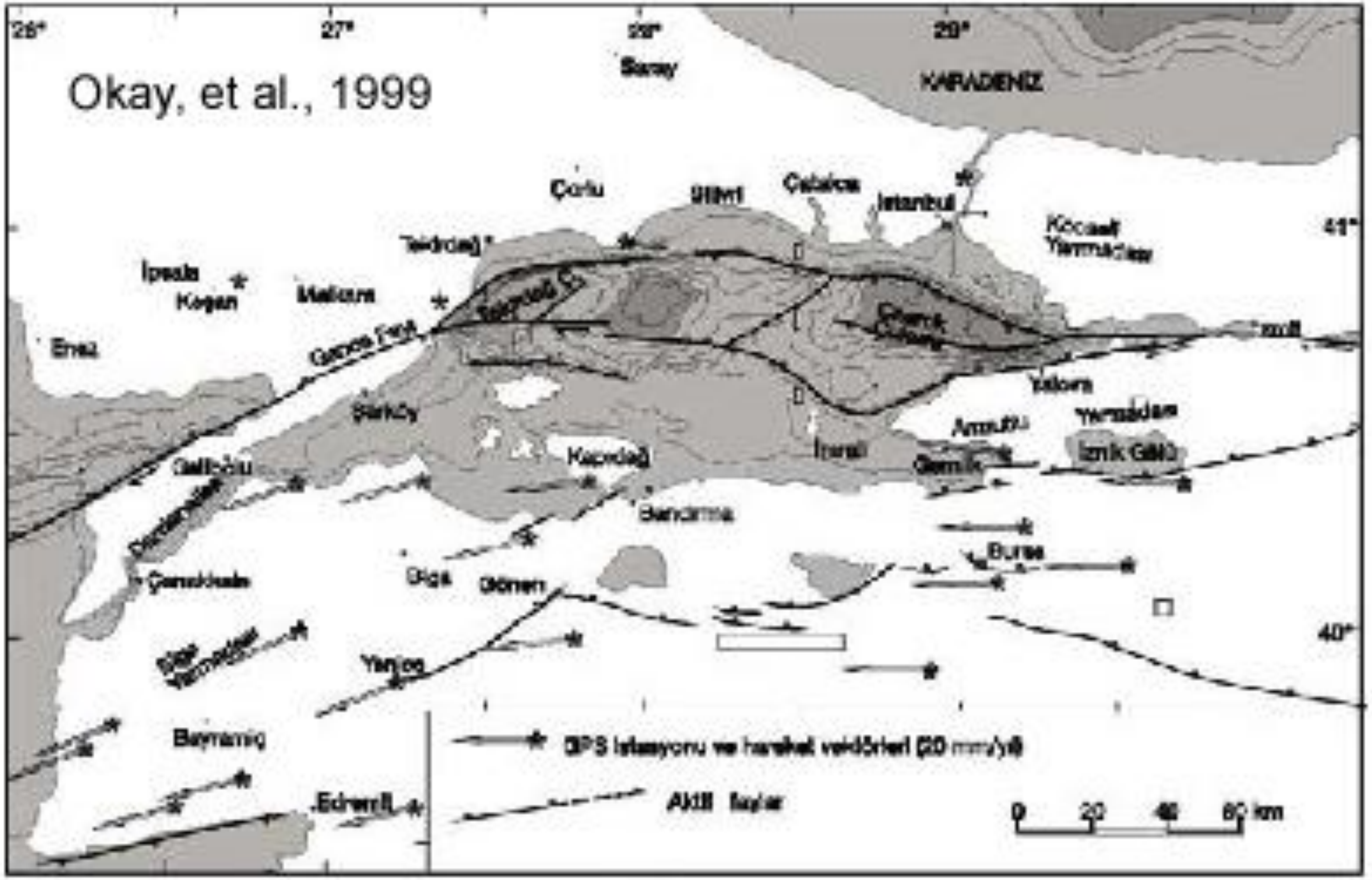


Okay, A. I., Demirbağ, E., Kurt, H., Okay, N. and Kuşçu, İ. (1999). An active, deep marine strike-slip basin along the North Anatolian Fault in Turkey. *Tectonics*, **(18)** 1, 129-147.

# 1999

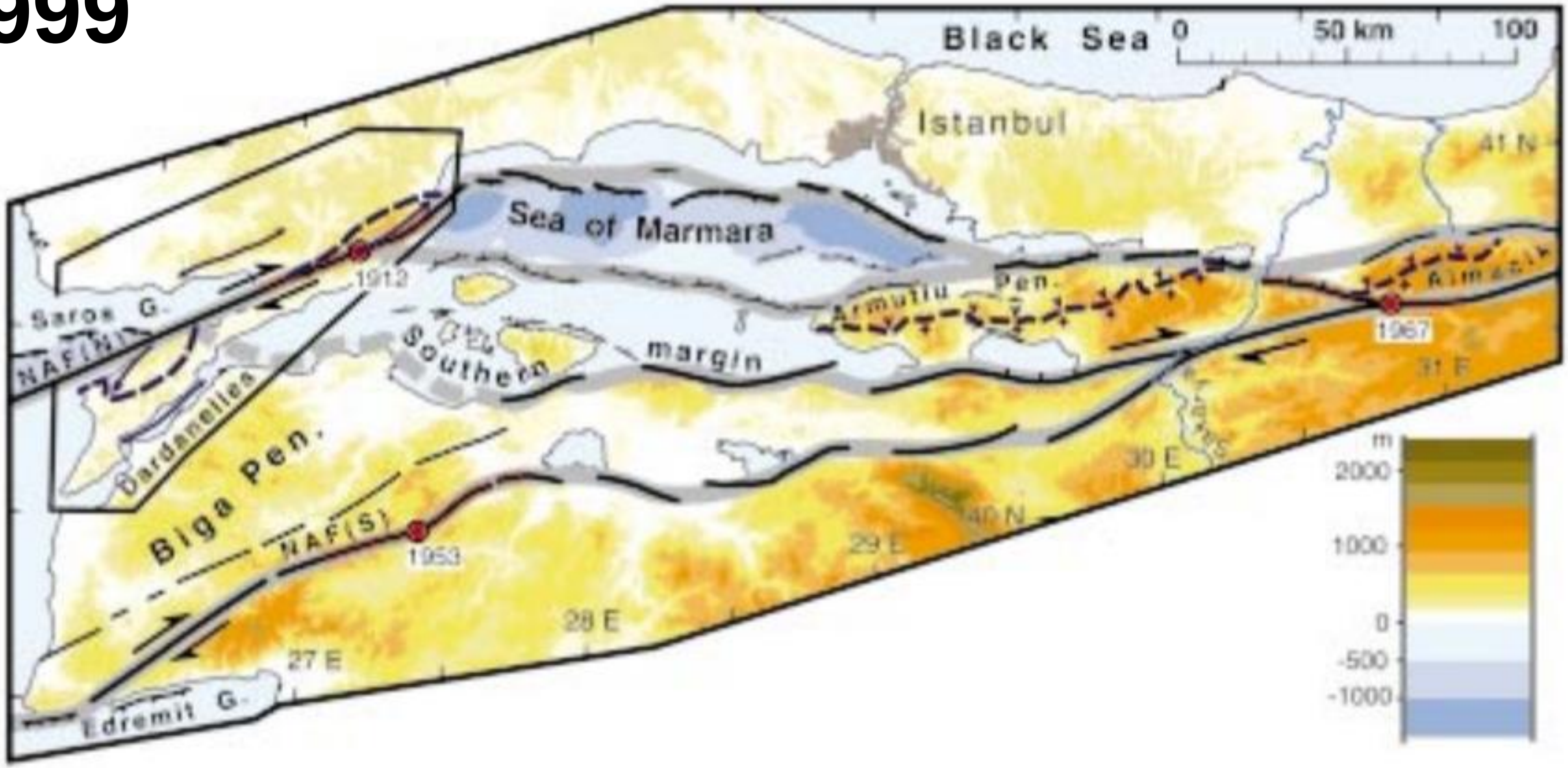


Figure 2 of paper 65

Armijo, R., Meyer, B., Hubert, A. & Barka, A. (1999), Westward propagation of the North Anatolian fault into the northern Aegean: Timing and kinematics. *Geology,* **(27)** 3; 267–270.

# 1999

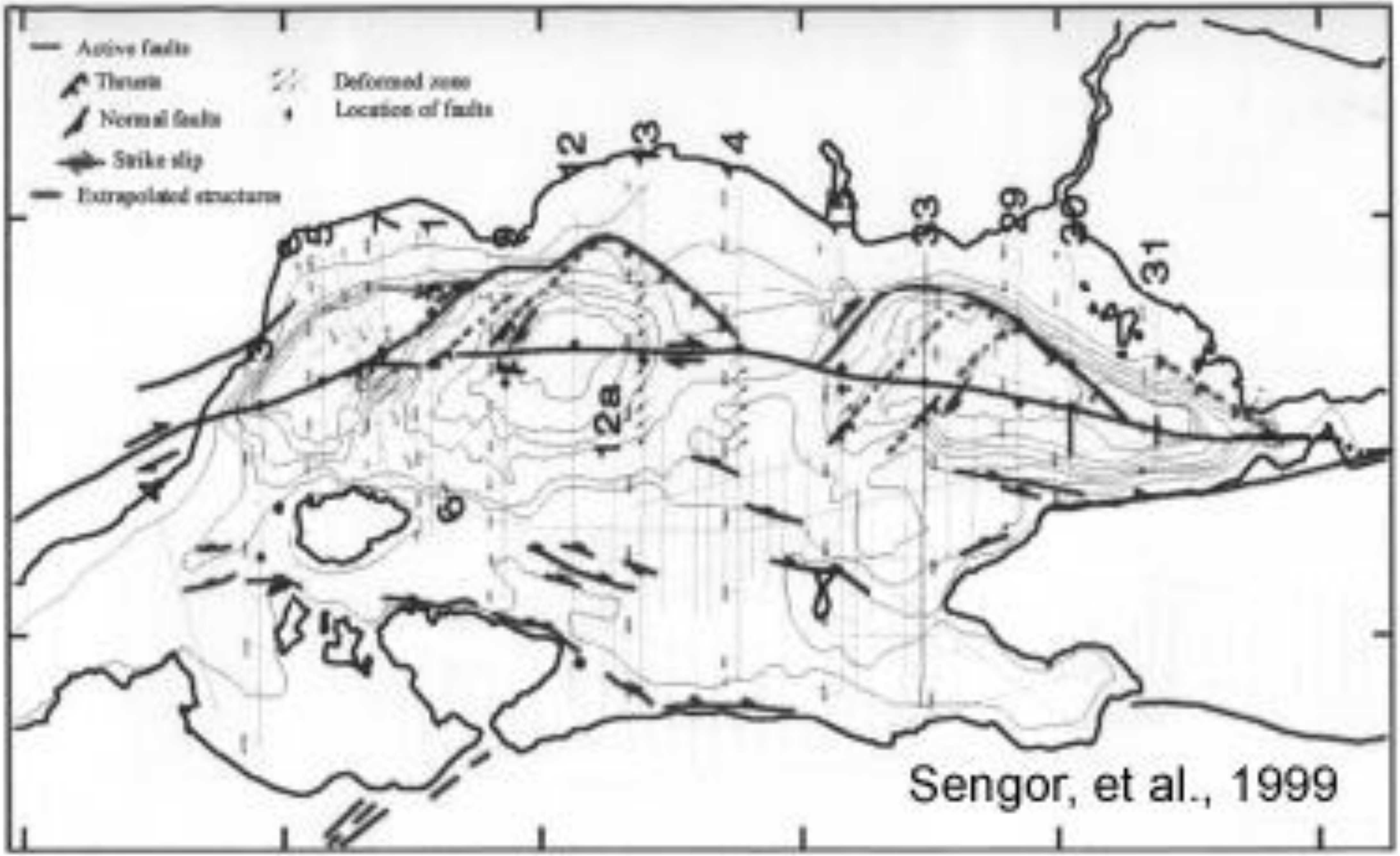

Active faults
Thrusts
Normal faults
Strike slip
Extrapolated structures
Deformed zone
Location of faults
Sengor, et al., 1999

# 2000

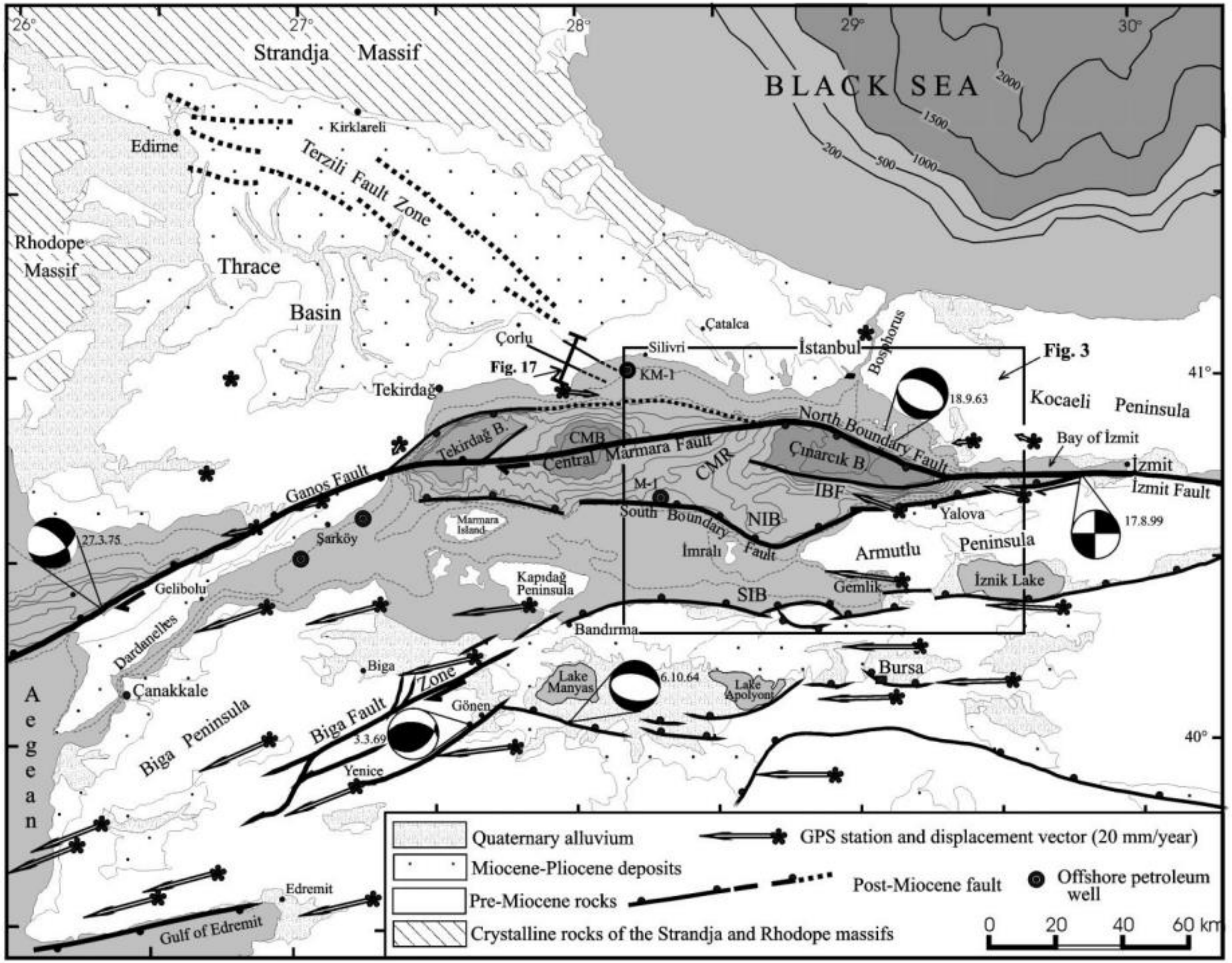


Figure 2 of paper 36 Okay, A. I., Kaşlılar-Özcan, A., İmren, C., Boztepe-Güney, A., Demirbağ, E. & Kuşçu, I. (2000), Active faults and evolving strike-slip basins in the Marmara Sea, northwest Turkey: a multichannel seismic reflection study. *Tectonophysics*, **321**, 189-218.

# 2000

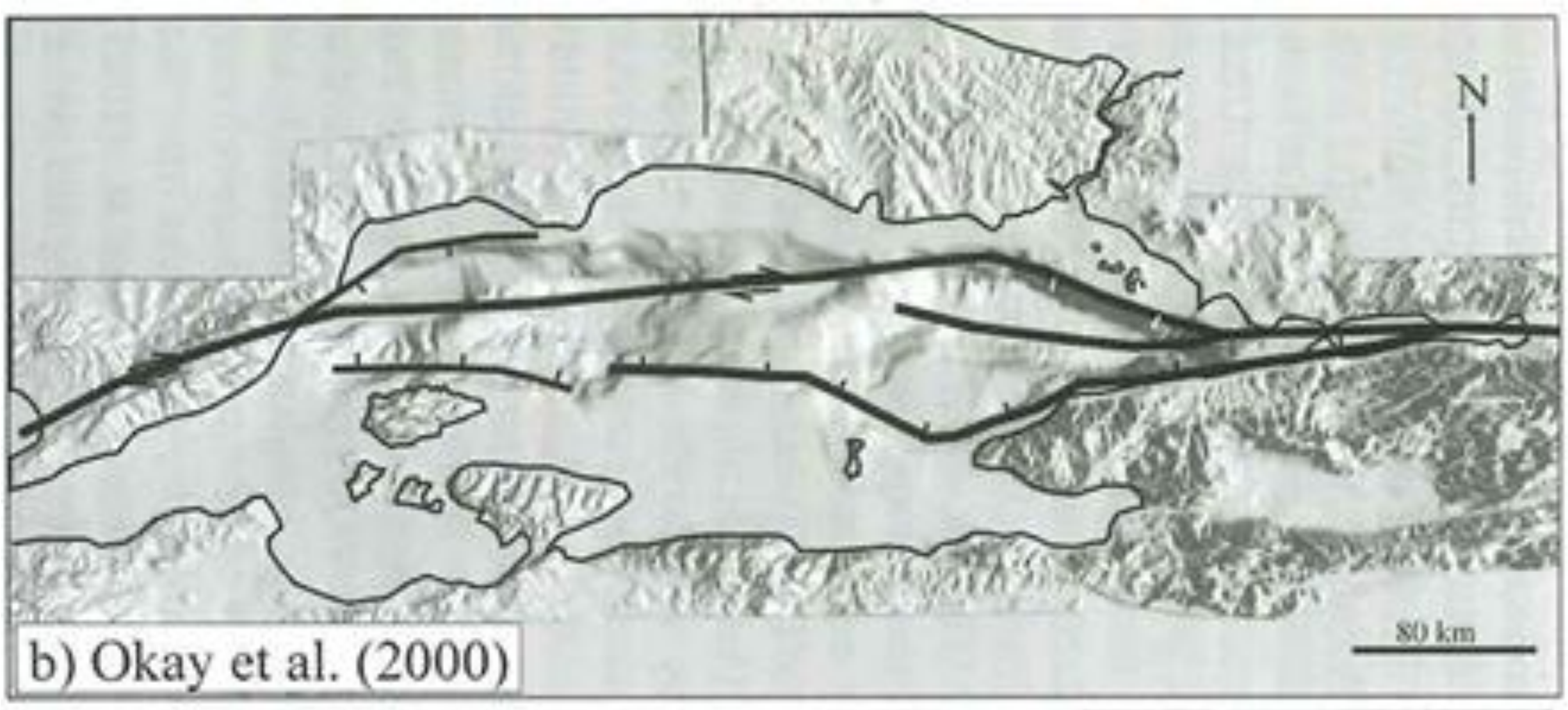


Okay, A. I., Kaşlılar-Özcan, A., İmren, C., Boztepe-Güney, A., Demirbağ, E. and Kuşçu, I. (2000). Active faults and evolving strike-slip basins in the Marmara Sea, northwest Turkey: a multichannel seismic reflection study. *Tectonophysics*, **321**, 189-218.

Figure 11 of paper 69

Yilmaz, Y., Gökaşan, E., & Erbay, A. Y. (2010), Morphotectonic development of the Marmara Region. *Tectonophysics,* 488, 51-70.

# 2000

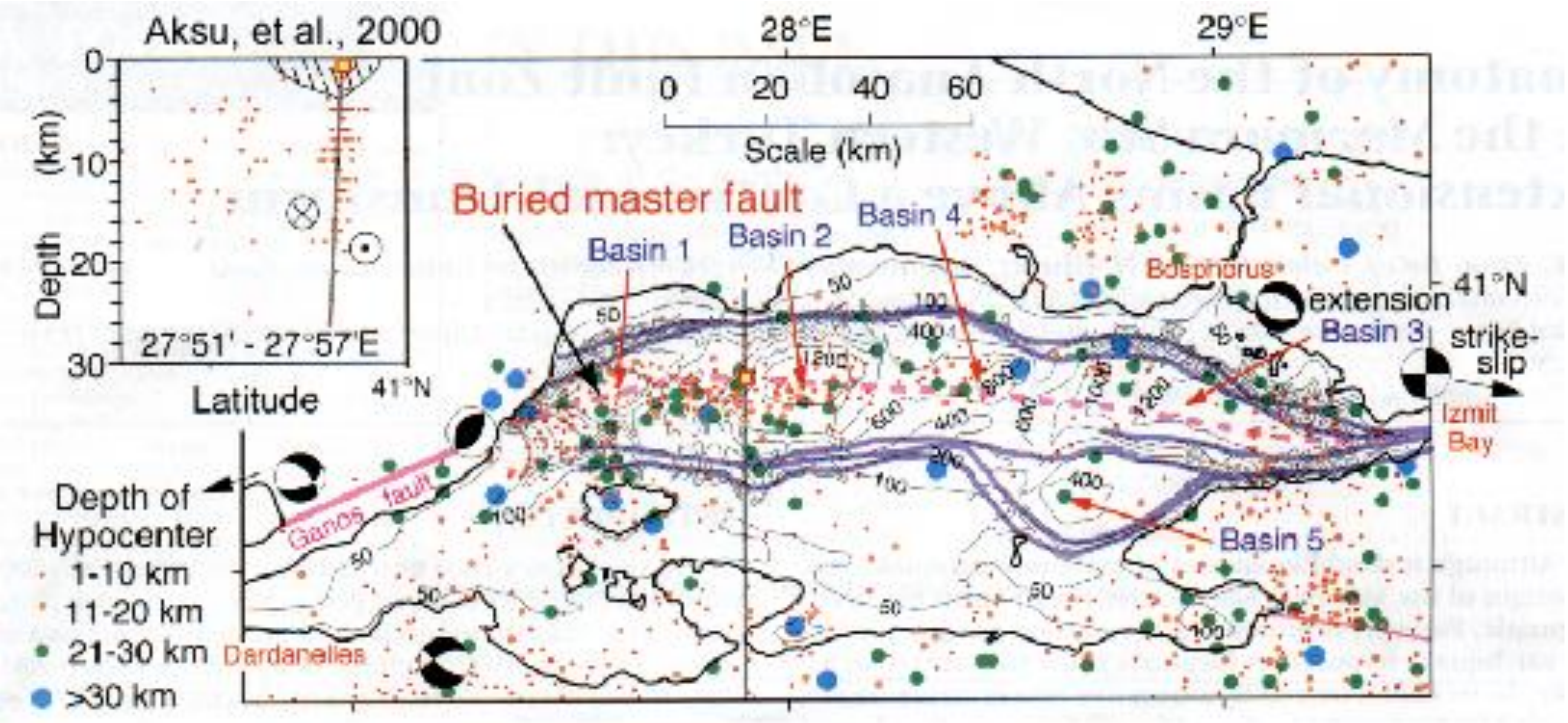

Aksu, et al., 2000
Depth (km)
27°51' - 27°57'E
28°E
29°E
0 20 40 60
Scale (km)
Buried master fault
Basin 1
Basin 2
Basin 4
Basin 3
Basin 5
Bosphorus
extension
strike-slip
41°N
Izmit Bay
Latitude
Depth of Hypocenter
1-10 km
11-20 km
21-30 km
>30 km
Ganos fault
Dardanelles

# 2001

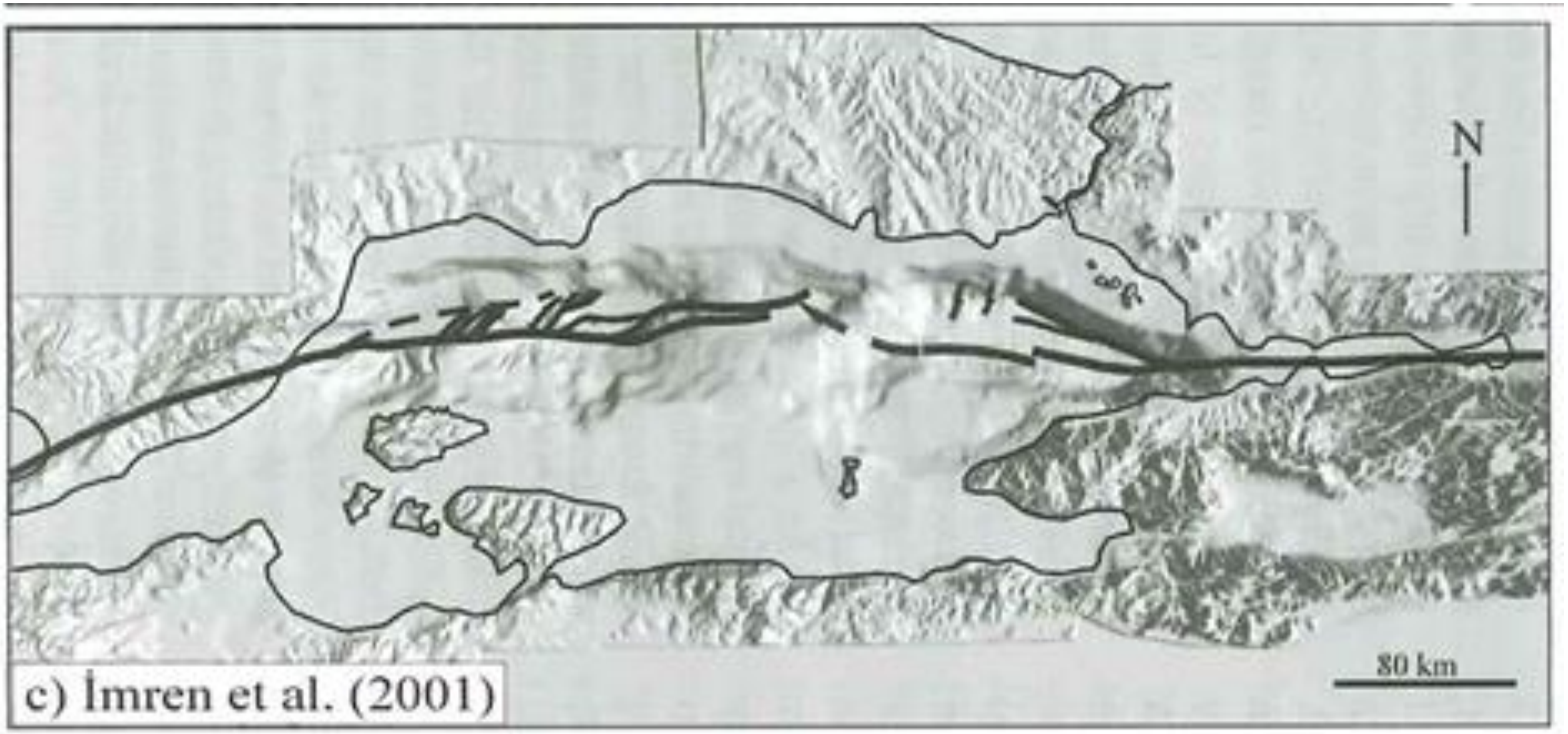


Imren, C., Le Pichon, X., Rangin, C., Demirbağ, E., Ecevitoğlu, B. and Görür, N. (2001). The North Anatolian Fault within the Sea of Marmara: a new evaluation based on multichannel seismic and multi-beam data. *Earth Planet. Sci. Lett.* **186,** 143-158.

Figure 11 of paper 69 Yilmaz, Y., Gökaşan, E., & Erbay, A. Y. (2010), Morphotectonic development of the Marmara Region. *Tectonophysics*, 488, 51-70.

# 2001

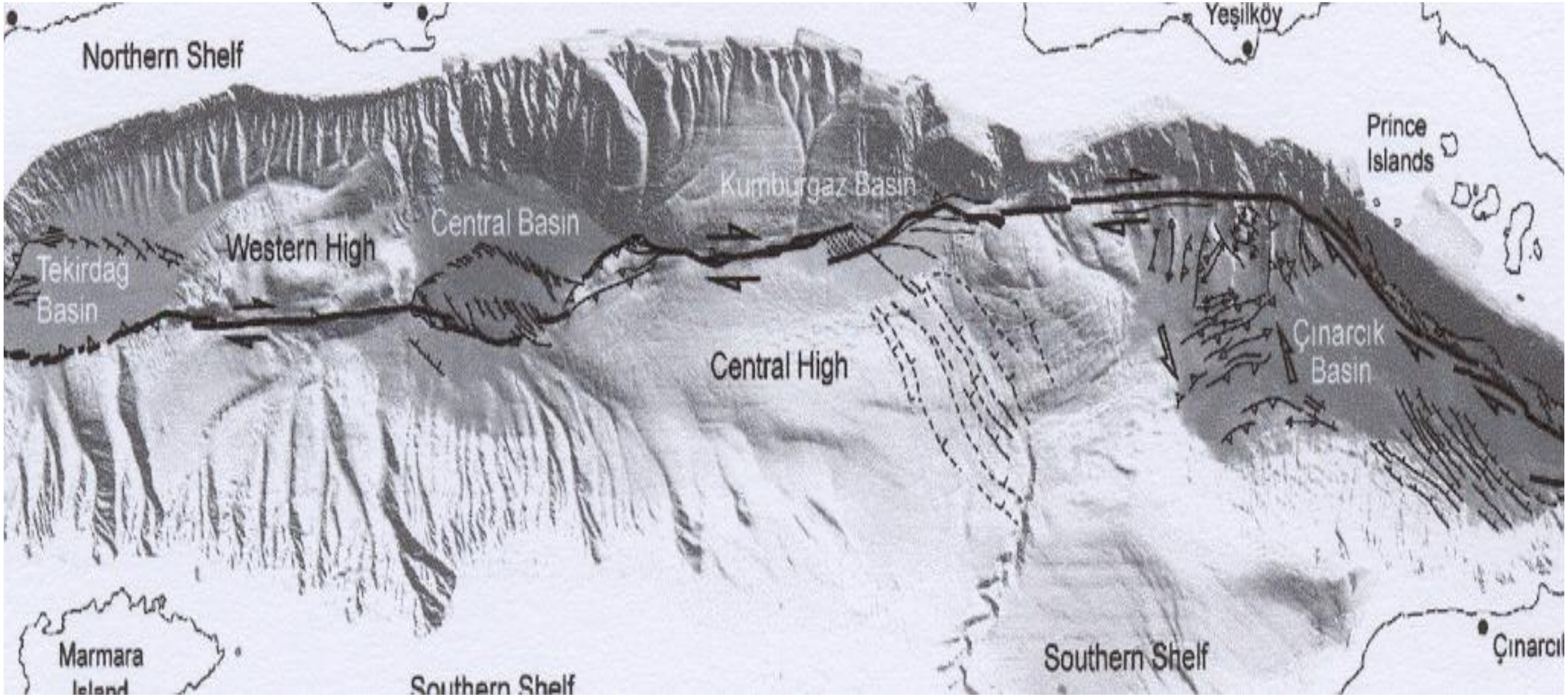


Le Pichon, X., Şengör, A.M.C., Demirbağ, E., Rangin, C., Imren, C., Armijo, R., Görür, N. and Çağatay, N., Mercier de Lepinay, B., Meyer, B., Saatcilar, R. and Tok, B. (2001). The active main Marmara fault. *Earth Planet. Sci. Lett.*, **192**, 595–616.

**(Le Pichon et al., 2001)**

# 2001

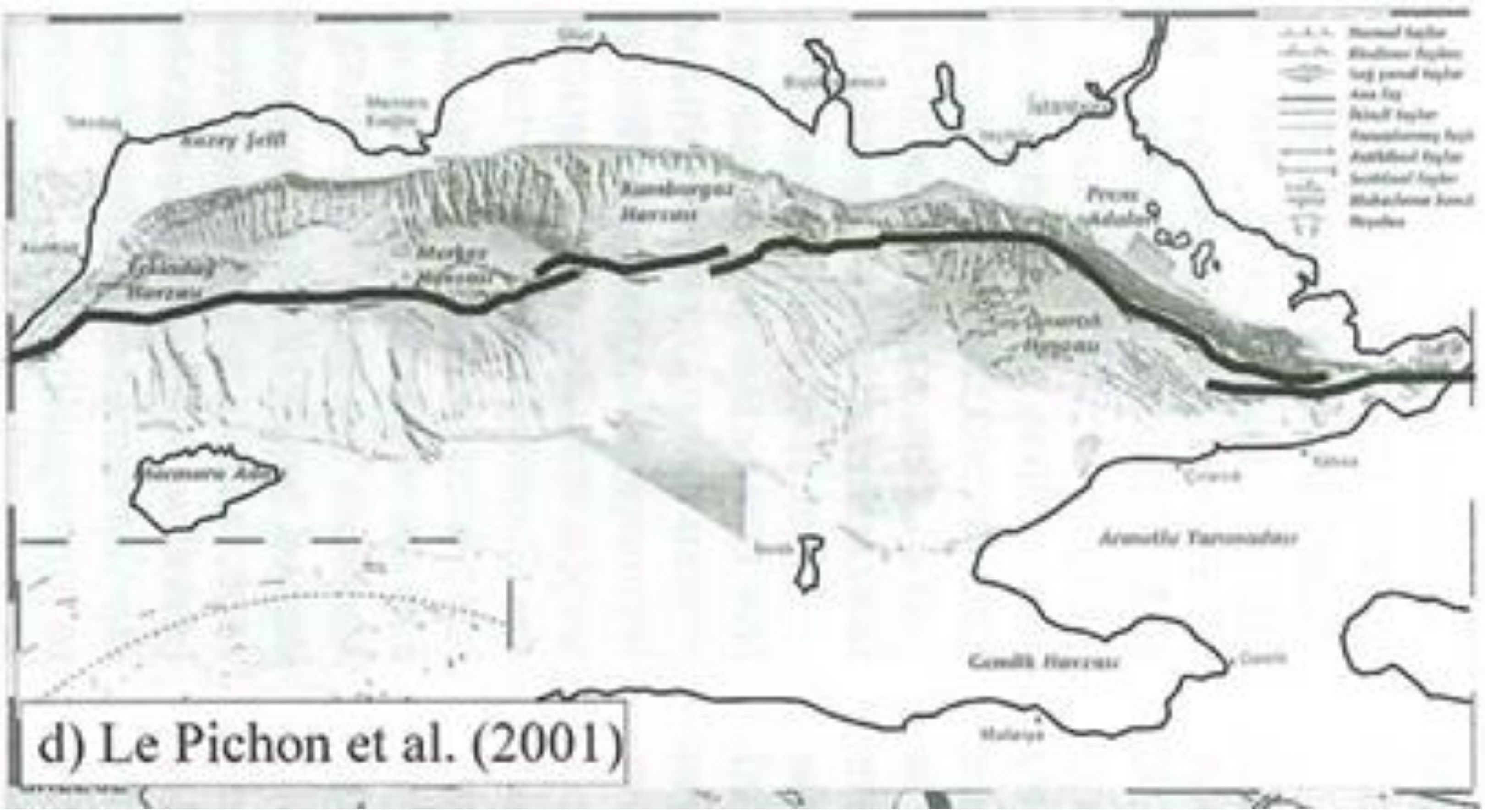


Le Pichon, X., Şengör, A.M.C., Demirbağ, E., Rangin, C., Imren, C., Armijo, R., Görür, N. and Çağatay, N., Mercier de Lepinay, B., Meyer, B., Saatcilar, R. and Tok, B. (2001). The active main Marmara fault. *Earth Planet. Sci. Lett.*, **192**, 595–616.

Figure 11 of paper 69

Yilmaz, Y., Gökaşan, E., & Erbay, A. Y. (2010), Morphotectonic development of the Marmara Region. *Tectonophysics*, 488, 51-70.

# 2002

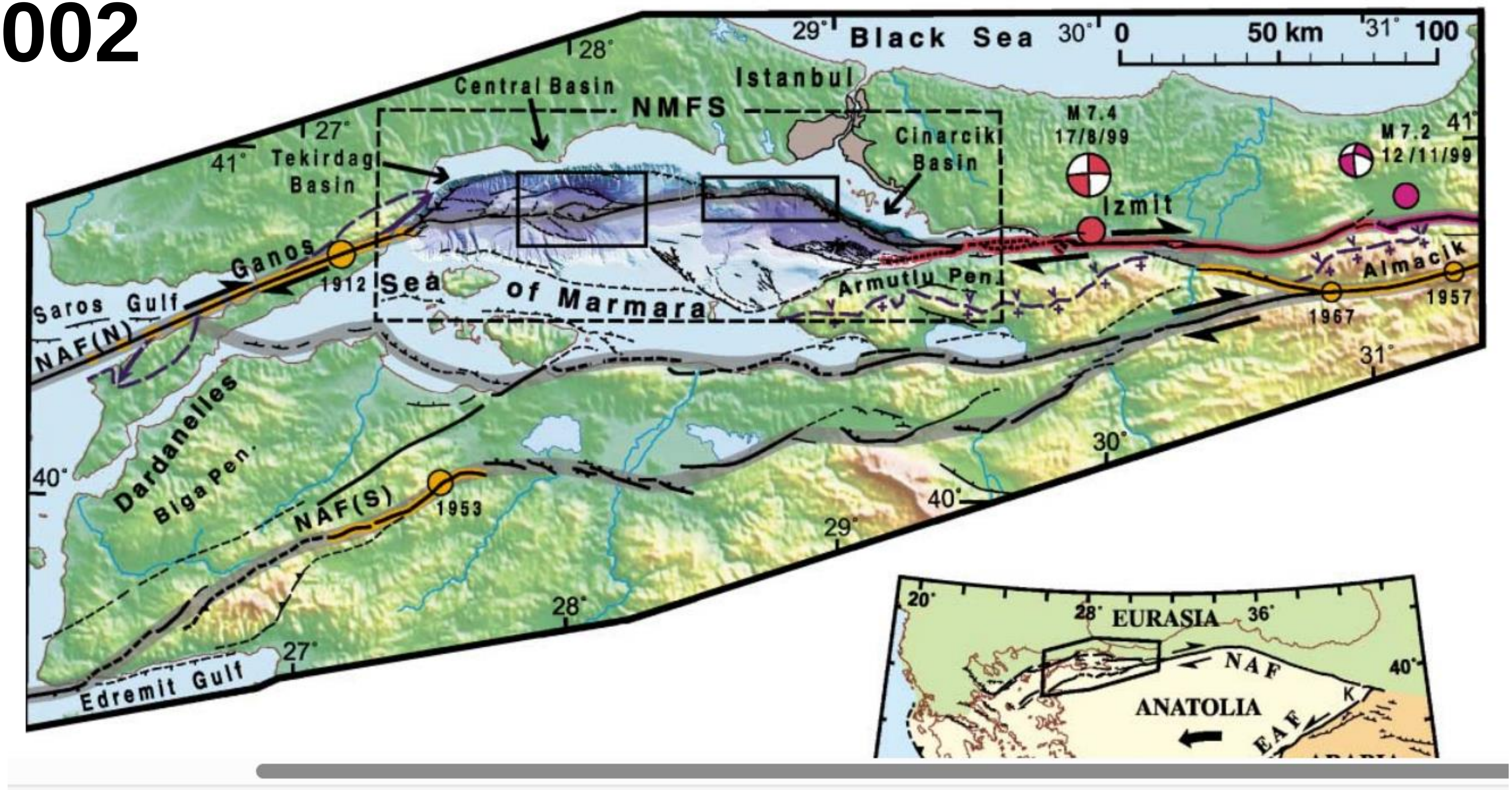


Figure 1 of paper 62 Armijo, R., Meyer, B., Navarro, S., King, G. & Barka, A. (2002), Asymmetric slip partitioning in the Sea of Marmara pull-apart: a clue to propagation processes of the North Anatolian Fault. *Terra Nova*, 14 (2), 80–86.

# 2002

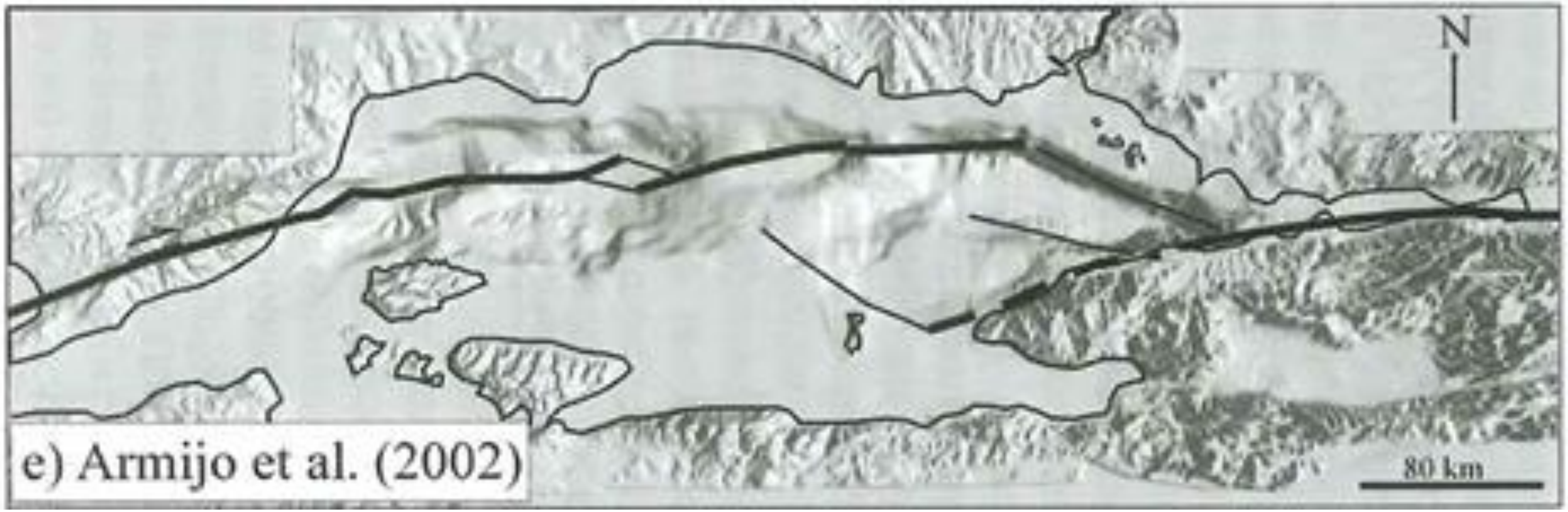



Armijo, R., Meyer, B., Navarro, S., King, G. and Barka, A. (2002), Asymmetric slip partitioning in the Sea of Marmara pull-apart: a clue to propagation processes of the North Anatolian Fault. *Terra Nova*, 14 (2), 80–86.


Figure 11 of paper 69


Yilmaz, Y., Gökaşan, E., & Erbay, A. Y. (2010), Morphotectonic development of the Marmara Region. *Tectonophysics*, 488, 51-70.

# 2002

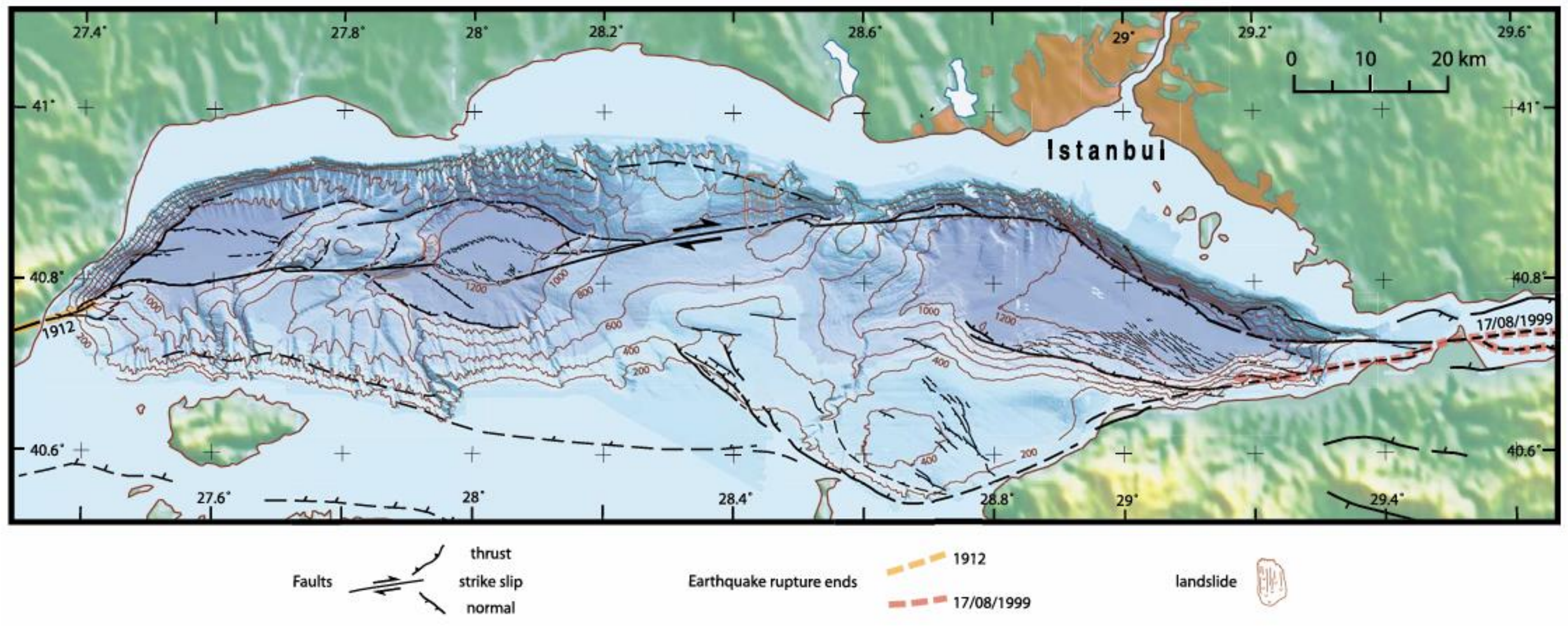


Armijo, R., Meyer, B., Navarro, S., King, G. and Barka, A. (2002), Asymmetric slip partitioning in the Sea of Marmara pull-apart: a clue to propagation processes of the North Anatolian Fault. *Terra Nova*, 14 (2), 80–86.

# 2002

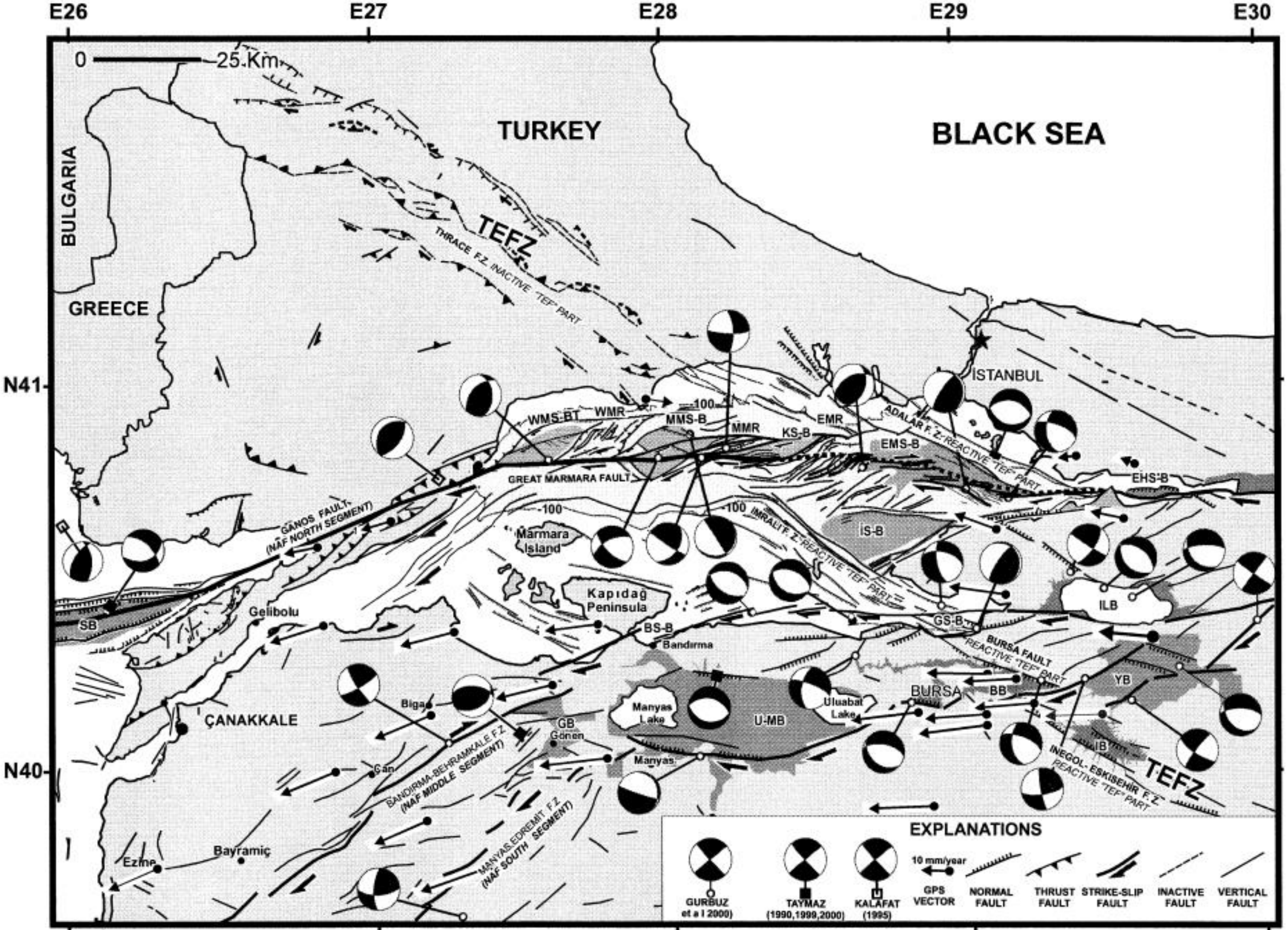


Figure 10 of paper 43 Yaltırak, C. (2002), Tectonic evolution of the Marmara Sea and its surroundings. *Marine Geology,* **(190)** 1-2, 493-529.

# 2002

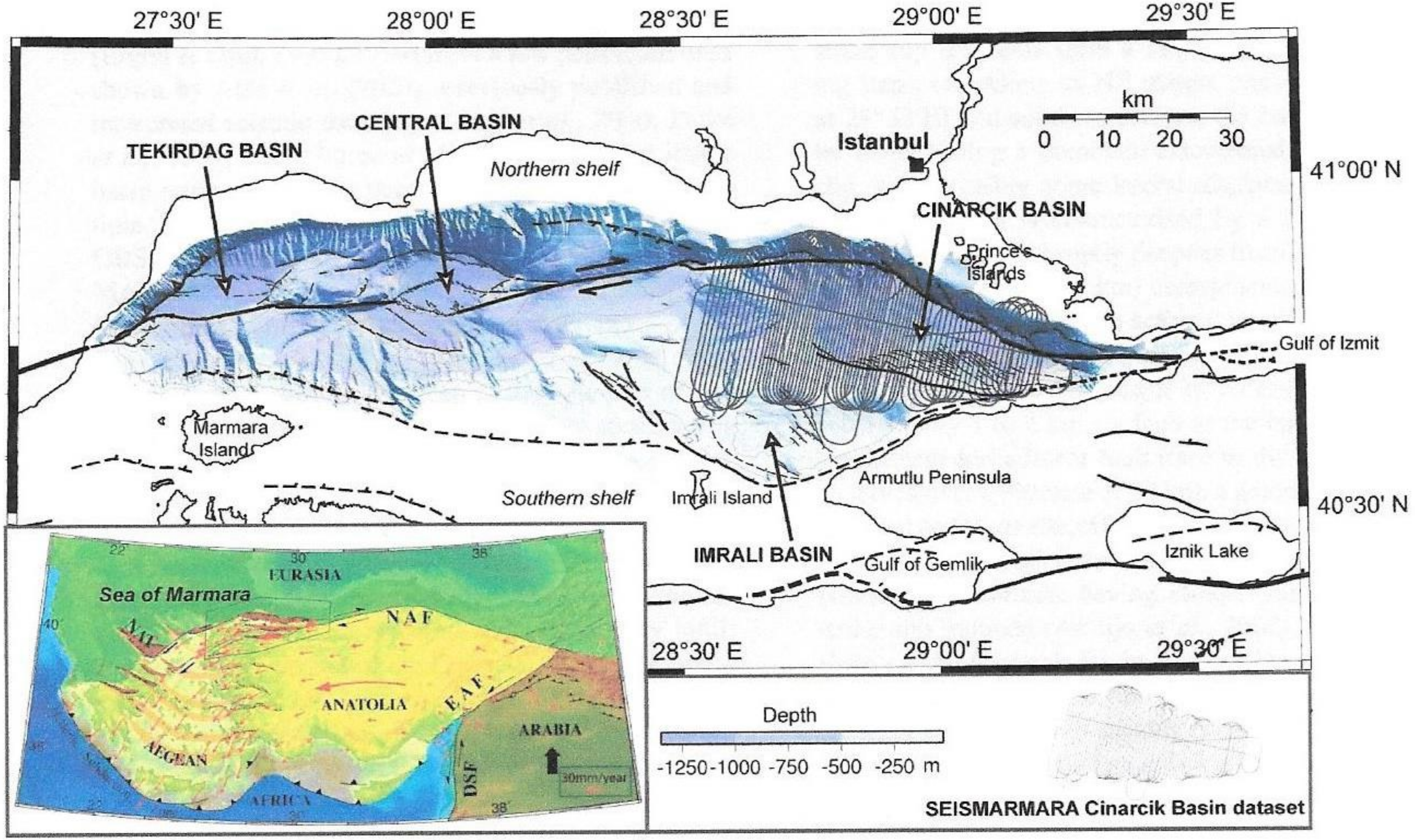


**(Armijo et al., 2002)**

# 2003

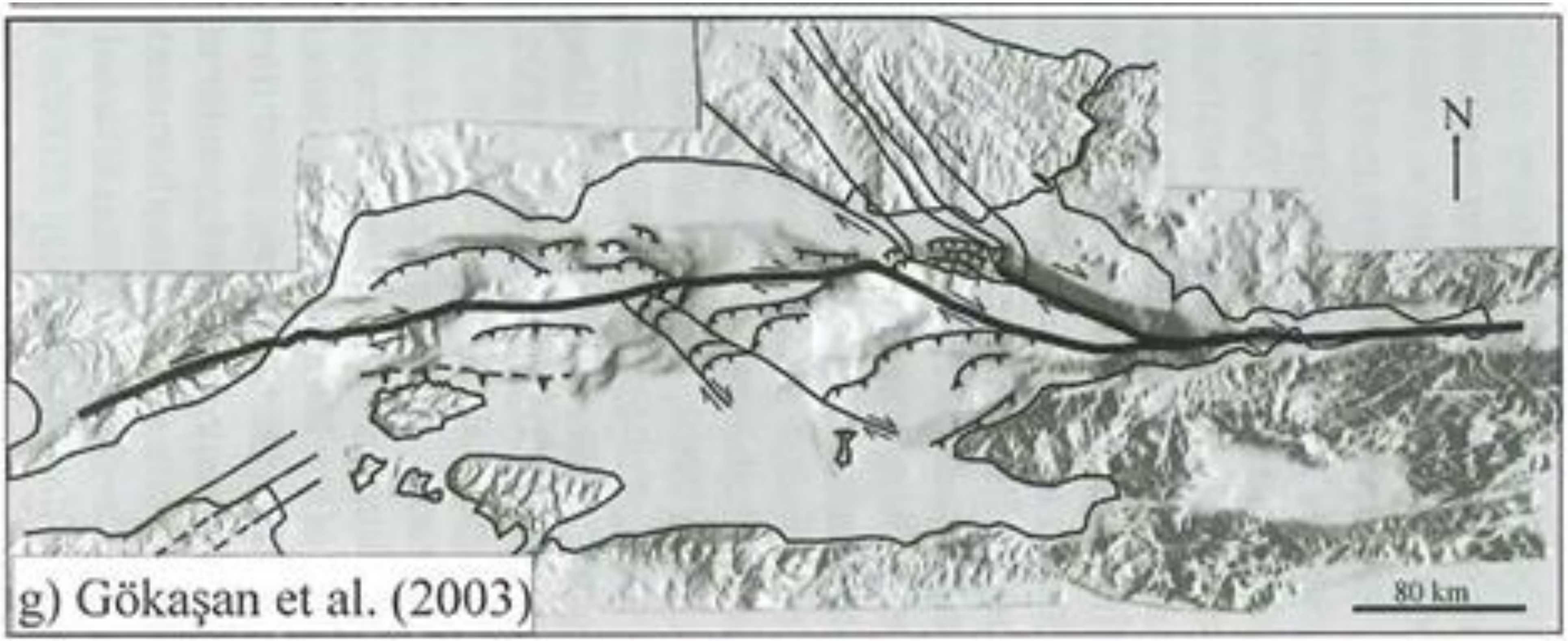

g) Gökaşan et al. (2003)

Gökaşan, E., Ustaömer, T., Gazioglu, C, Yucel, Z. Y., Ozturk, K., Tur, H., Ecevitoglu, B. and Tok, B. (2003). Morphotectonic evolution of the Marmara Sea inferred from multi-beam bathymetric and seismic data. *Geo-Mar. Lett.* **(23)** 1, 19-33.

Figure 11 of paper 69

Yilmaz, Y., Gökaşan, E., & Erbay, A. Y. (2010), Morphotectonic development of the Marmara Region. *Tectonophysics,* 488, 51-70.

# 2003

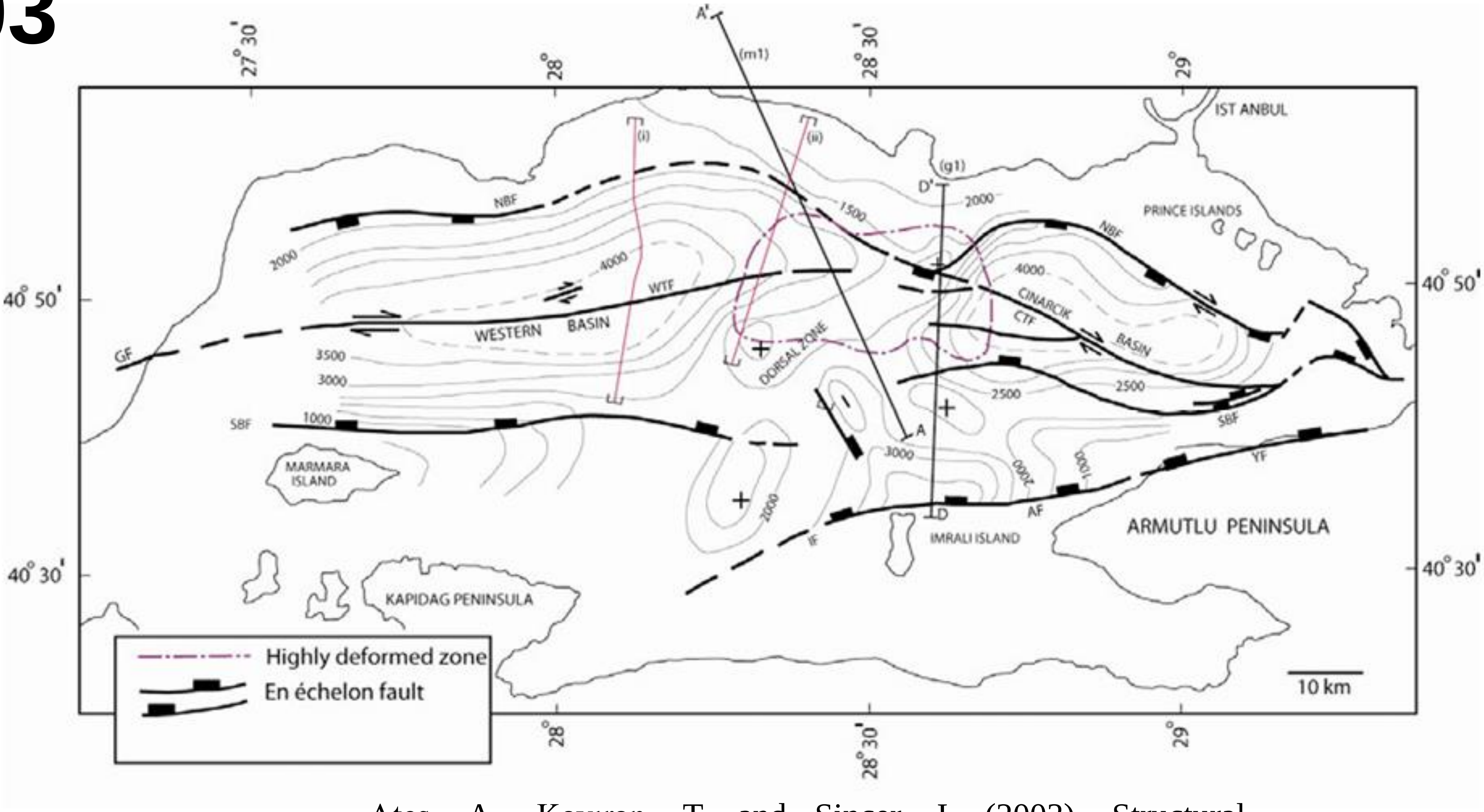


Ateş, A., Kayıran, T. and Sincer, I. (2003). Structural interpretation of the Marmara region, NW Turkey, from aeromagnetic, seismic, and gravity data. *Tectonophysics*, 367, 41-99.

# 2003

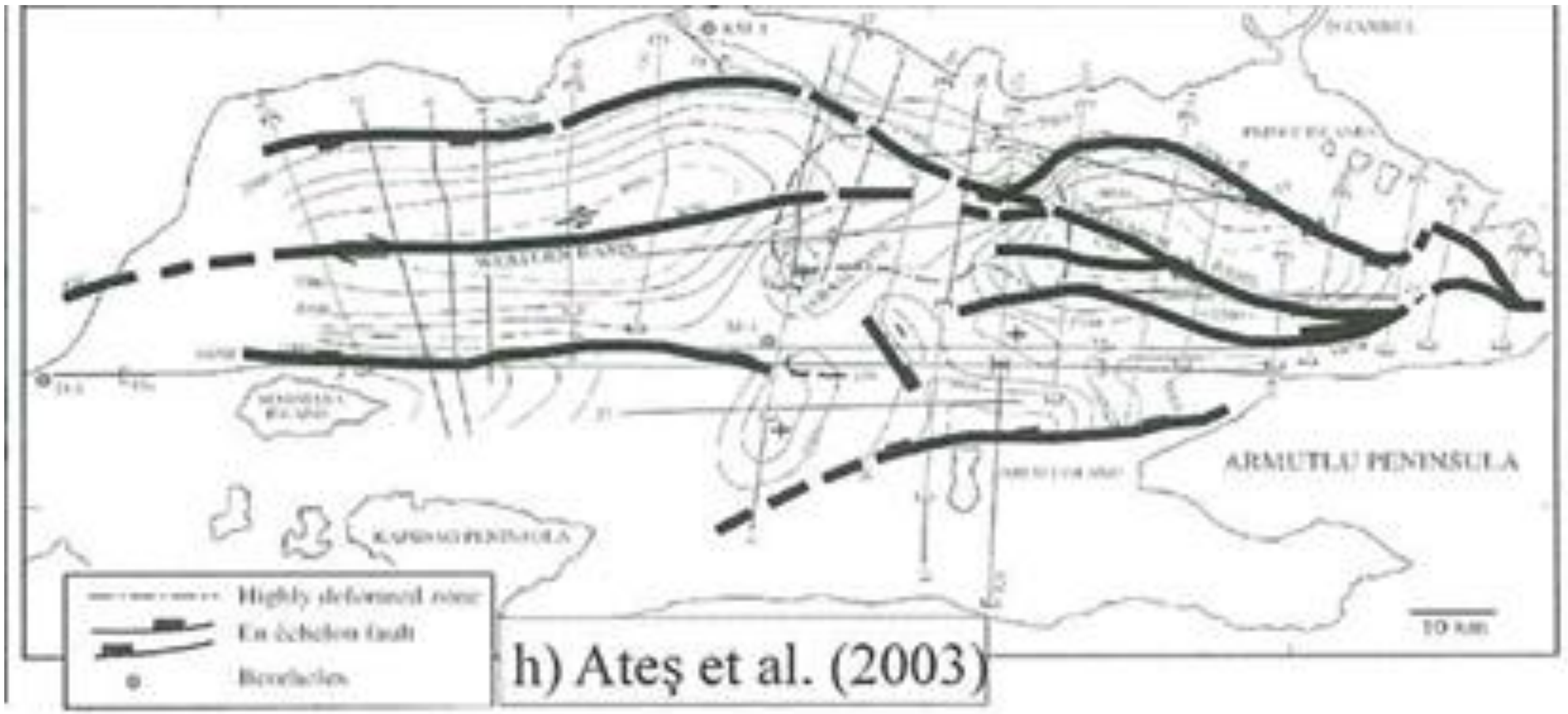


Ateş, A., Kayıran, T. and Sincer, I. (2003). Structural interpretation of the Marmara region, NW Turkey, from aeromagnetic, seismic, and gravity data. *Tectonophysics*, 367, 41-99.

Figure 11 of paper 69

Yilmaz, Y., Gökaşan, E., & Erbay, A. Y. (2010), Morphotectonic development of the Marmara Region. *Tectonophysics*, 488, 51-70.

# 2009

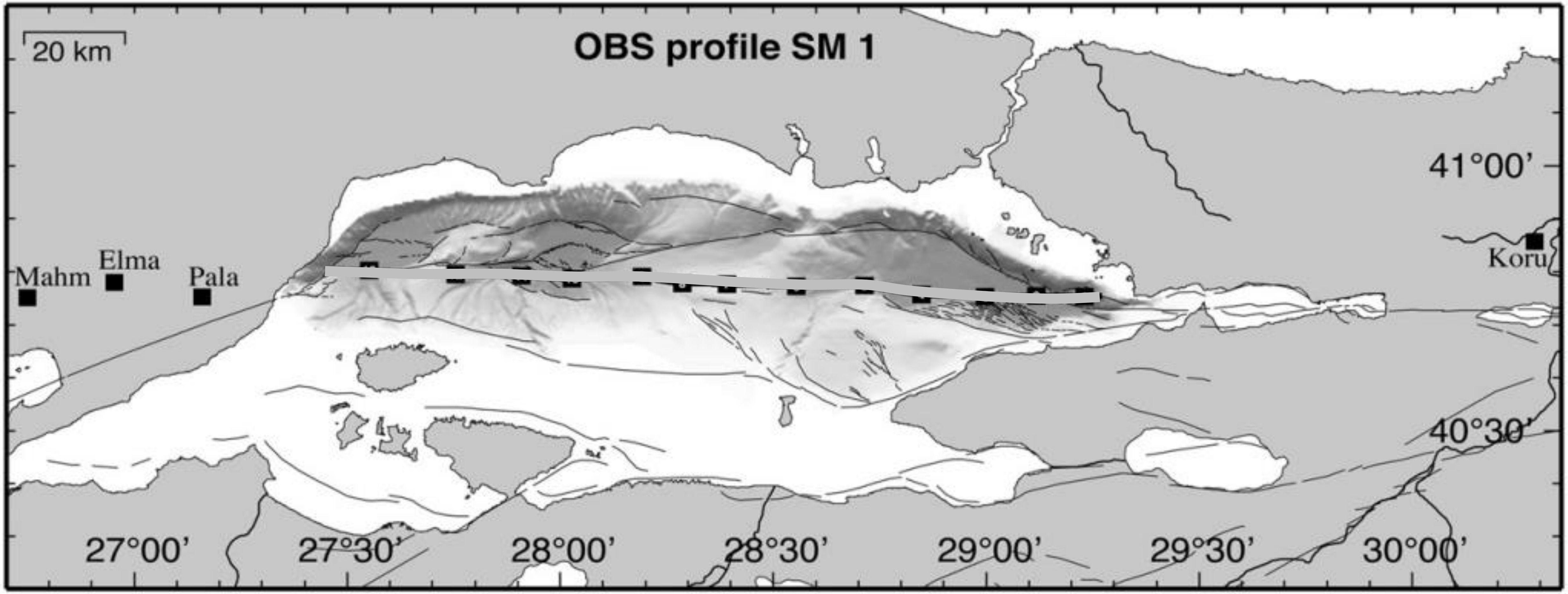


Figure 3 of paper 02 Bécel, A., Laigle, M., de Voogd, B., Hirn, A., Taymaz, T., Galvé, A., Shimamura, H., Murai, Y., Lépine, J-C., Sapin, M., & Özalaybey, S. (2009), Moho, crustal architecture and deep deformation under the North Marmara Trough, from the SEISMARMARA Leg 1 offshore–onshore reflection–refraction survey. *Tectonophysics*, 467, 1–21.

# 2010



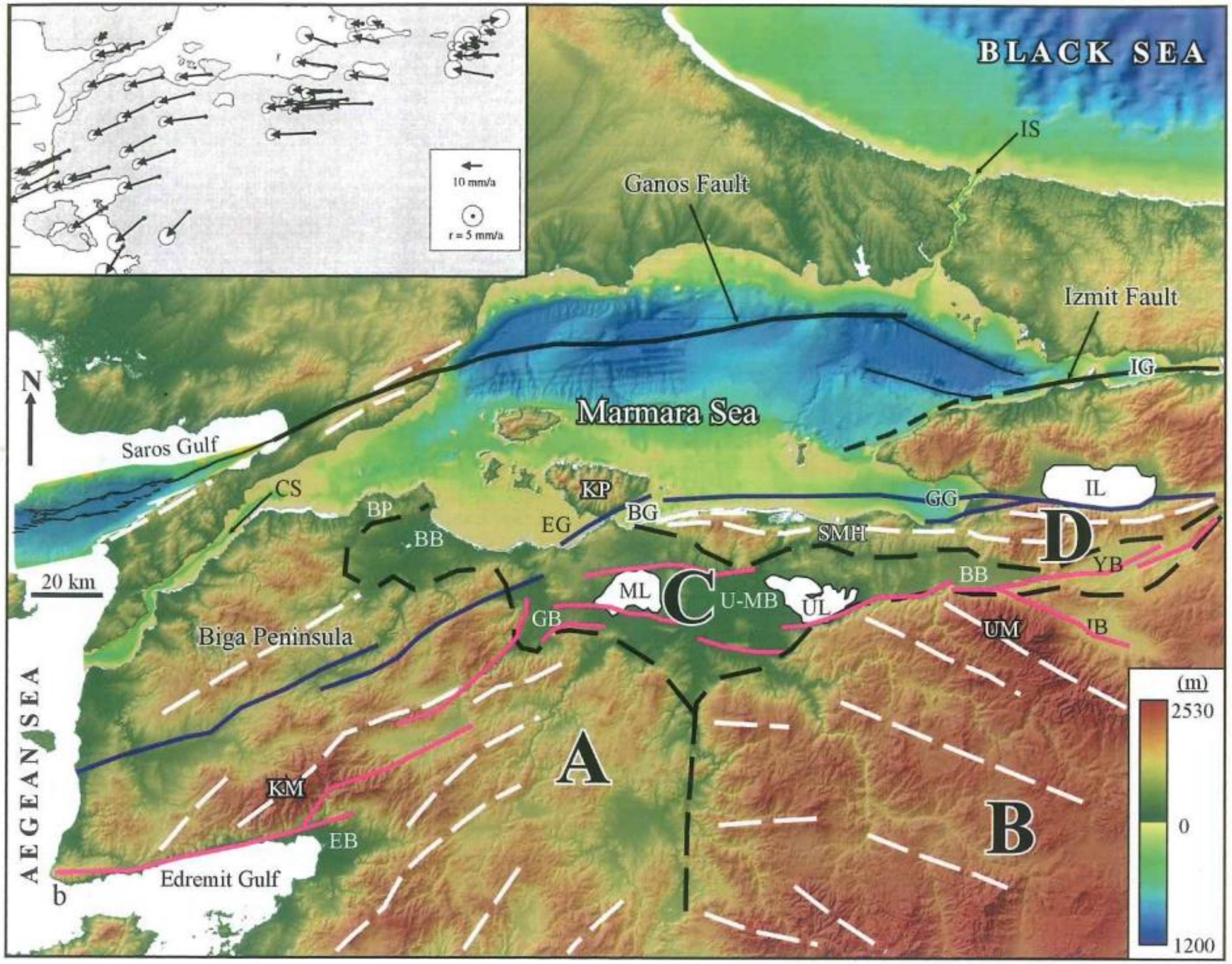


Figure 8 of paper 69 Yilmaz, Y., Gökaşan, E., & Erbay, A. Y. (2010), Morphotectonic development of the Marmara Region. *Tectonophysics*, 488, 51-70.

# 2014

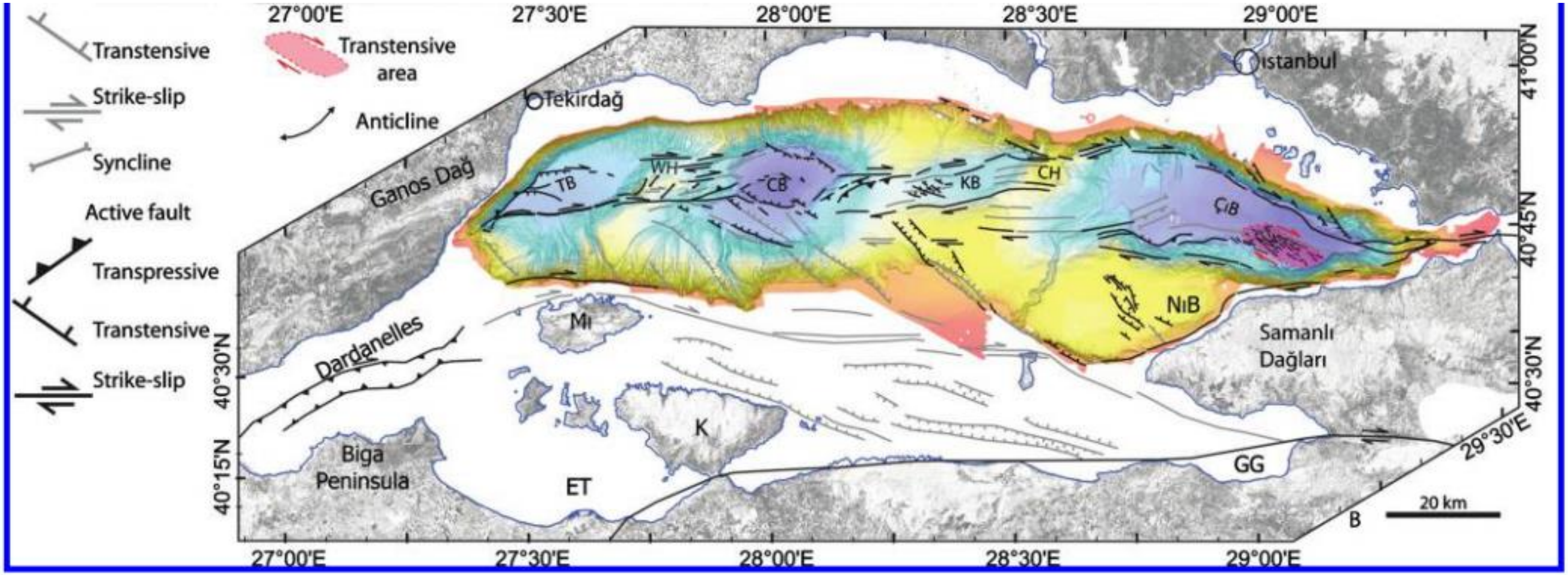


Figure 5 of paper 26 Şengör, A. M. C., Grall, C., Imren, C., Le Pichon, X., Görür, N., Henry, P., Karabulut, H. & Siyako, M. (2014), The geometry of the North Anatolian transform fault in the Sea of Marmara and its temporal evolution: implications for the development of intracontinental transform faults. *Can. J. Earth Sci.* 51:222–242, dx.doi.org/10.1139/cjes-2013-016.

# 2001

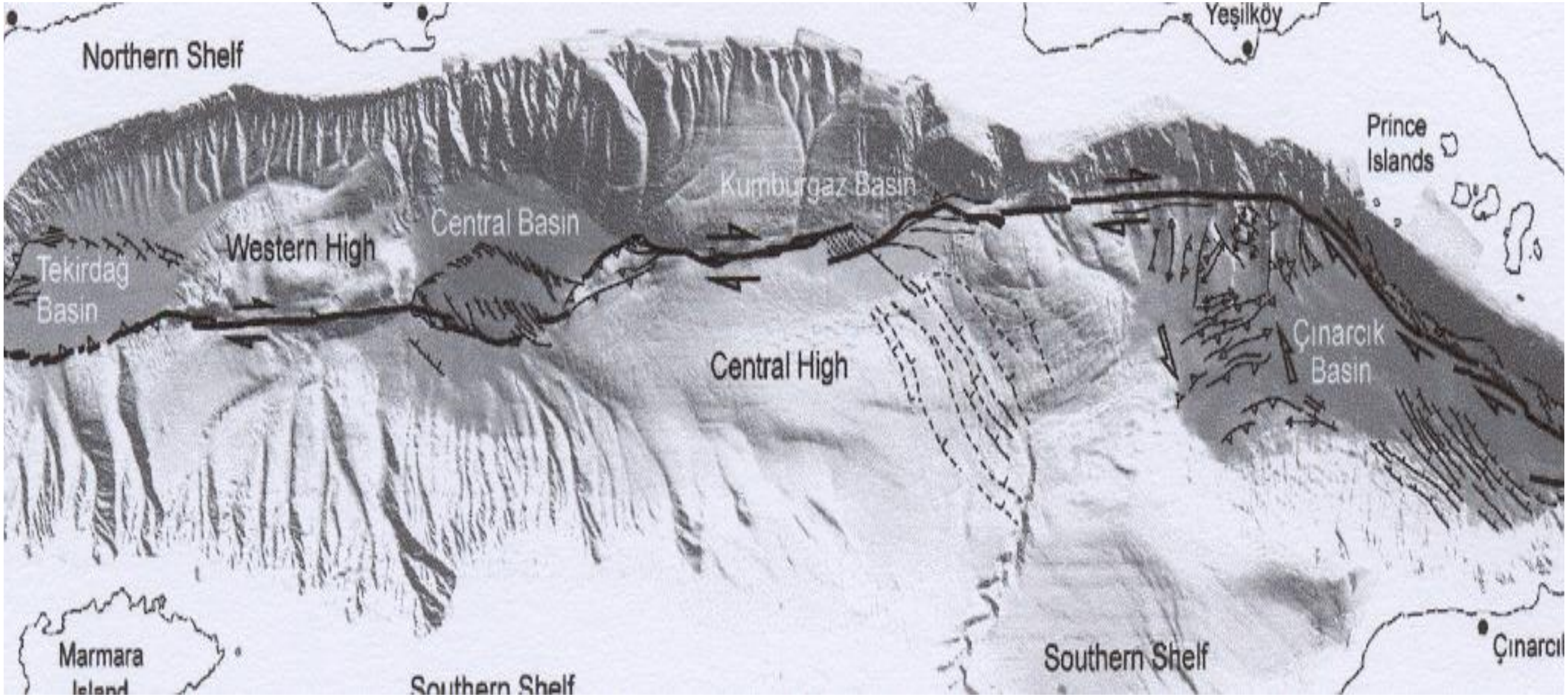


Le Pichon, X., Şengör, A.M.C., Demirbağ, E., Rangin, C., Imren, C., Armijo, R., Görür, N. and Çağatay, N., Mercier de Lepinay, B., Meyer, B., Saatcilar, R. and Tok, B. (2001). The active main Marmara fault. *Earth Planet. Sci. Lett.*, **192**, 595–616.

**(Le Pichon et al., 2001)**

# 1999

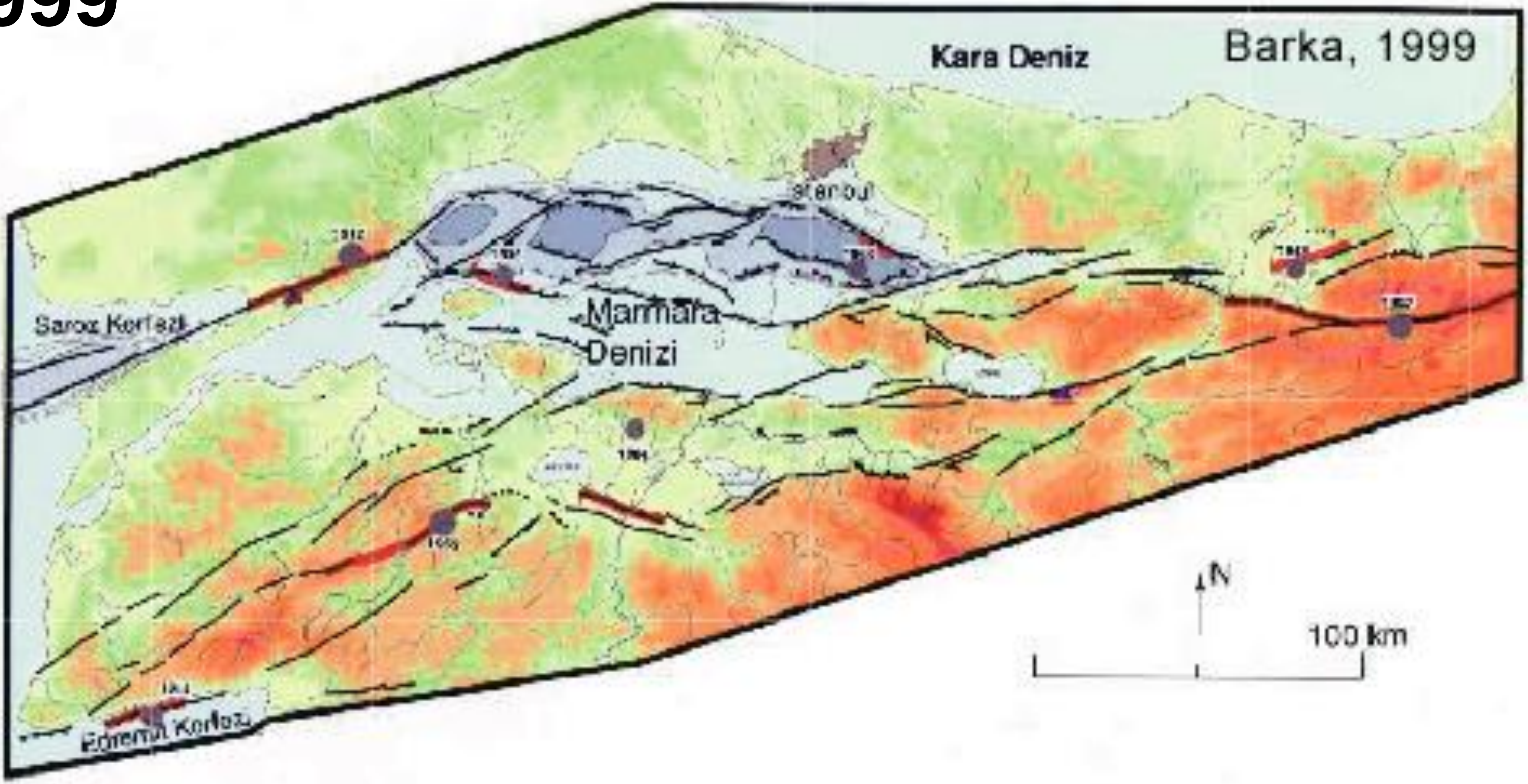
Barka, 1999
Kara Deniz
Saroz Körfezi
Marmara
Denizi
Edremit Körfezi
N
100 km

# 2-D seismic surveys during the period 1976-2014

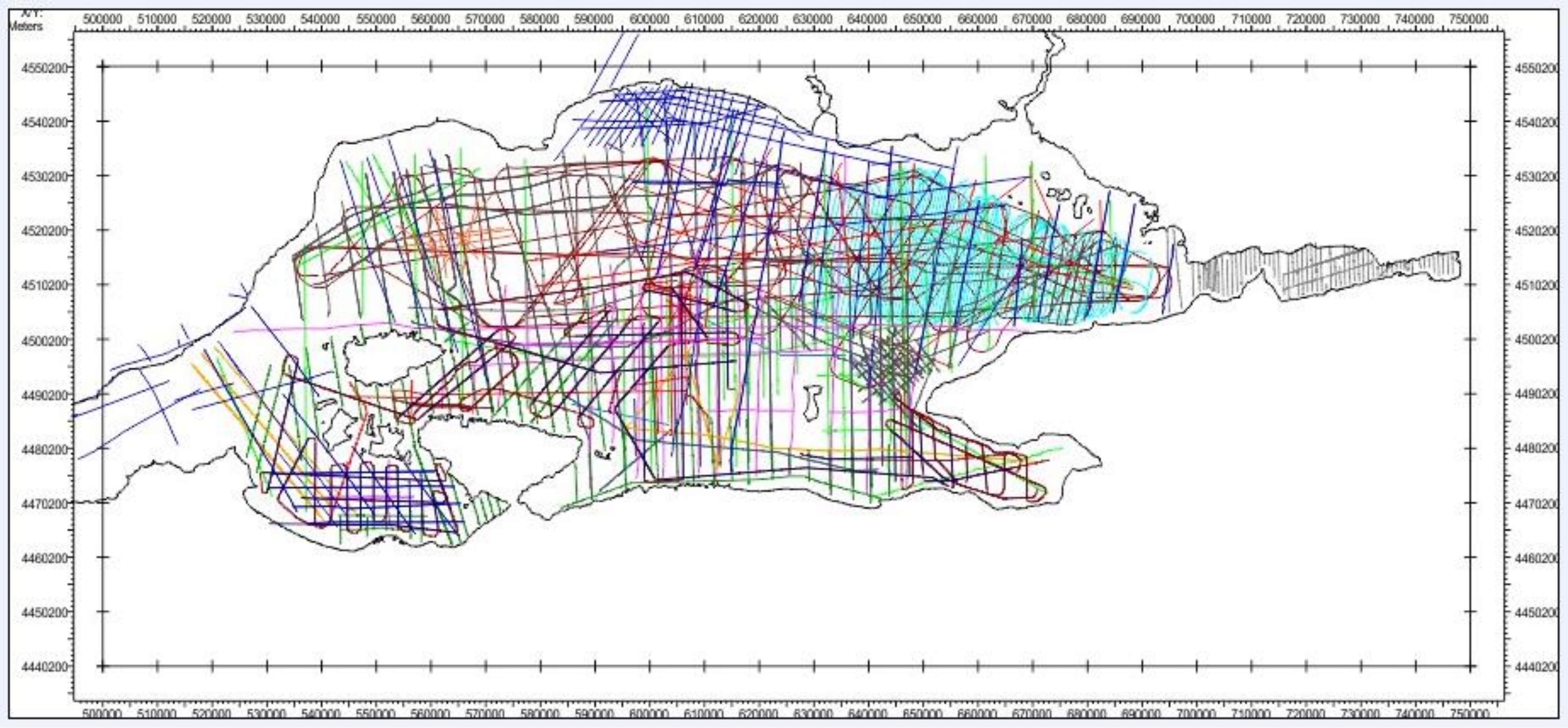

- TPAO : 1976 - 1982
- Marathon : 1988 – 1995 Marathon Oil Company
- MTA : 1997 - 1999
- Piri : DBTE- Colombia Üniversitesi - 2008
- SeisMarmara (Leg 1) : IFREMER - 2001
- SeisMarmara (Leg 2) : IFREMER - 2001
- PirMarmara : DBTE - 2010
- PirMarmara : DBTE - 2010
- PirMarmara : DBTE - 2010
- Somar : DBTE - 2013 (Chirp)
- Somar : DBTE - 2013
- Somar : DBTE - 2013 (Sparker)
- Somar : DBTE - 2014 (Sparker)

DBTE : Deniz Bilimleri ve Teknoloji Enstitüsü

IFREMER : Fransız Deniz Araştırma Enstitüsü

**(Courtesy Günay Çifçi)**

discontinuity volume: inline 2128 and time slice 1740 ms

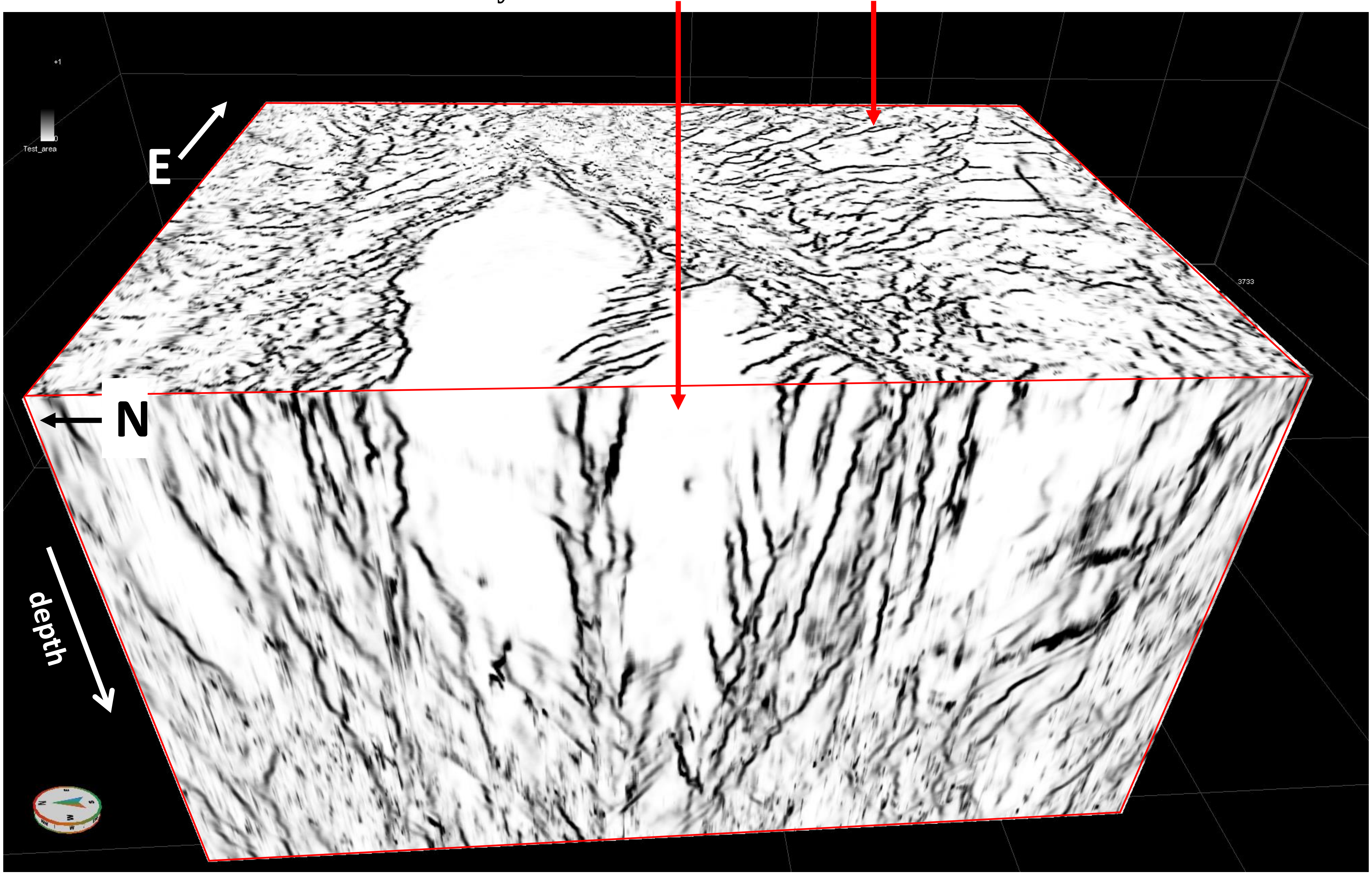

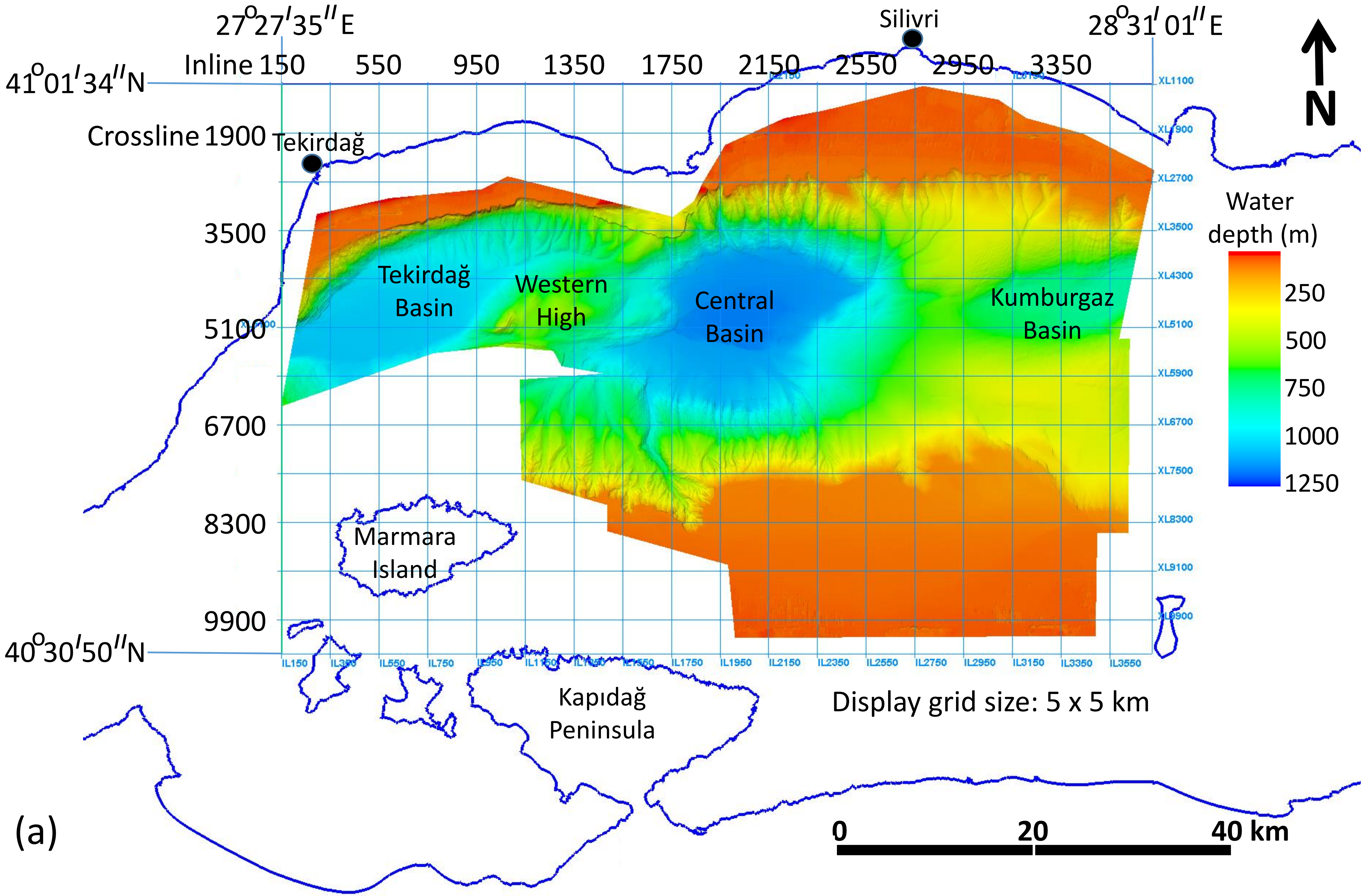

27°27′35″E
Silivri
28°31′01″E
N
41°01′34″N
Inline 150
550
950
1350
1750
2150
2550
2950
3350
Crossline 1900
Tekirdağ
3500
5100
6700
8300
9900
40°30′50″N
Tekirdağ Basin
Western High
Central Basin
Kumburgaz Basin
Water depth (m)
250
500
750
1000
1250
Marmara Island
Kapıdağ Peninsula
Display grid size: 5 x 5 km
0
20
40 km
(a)

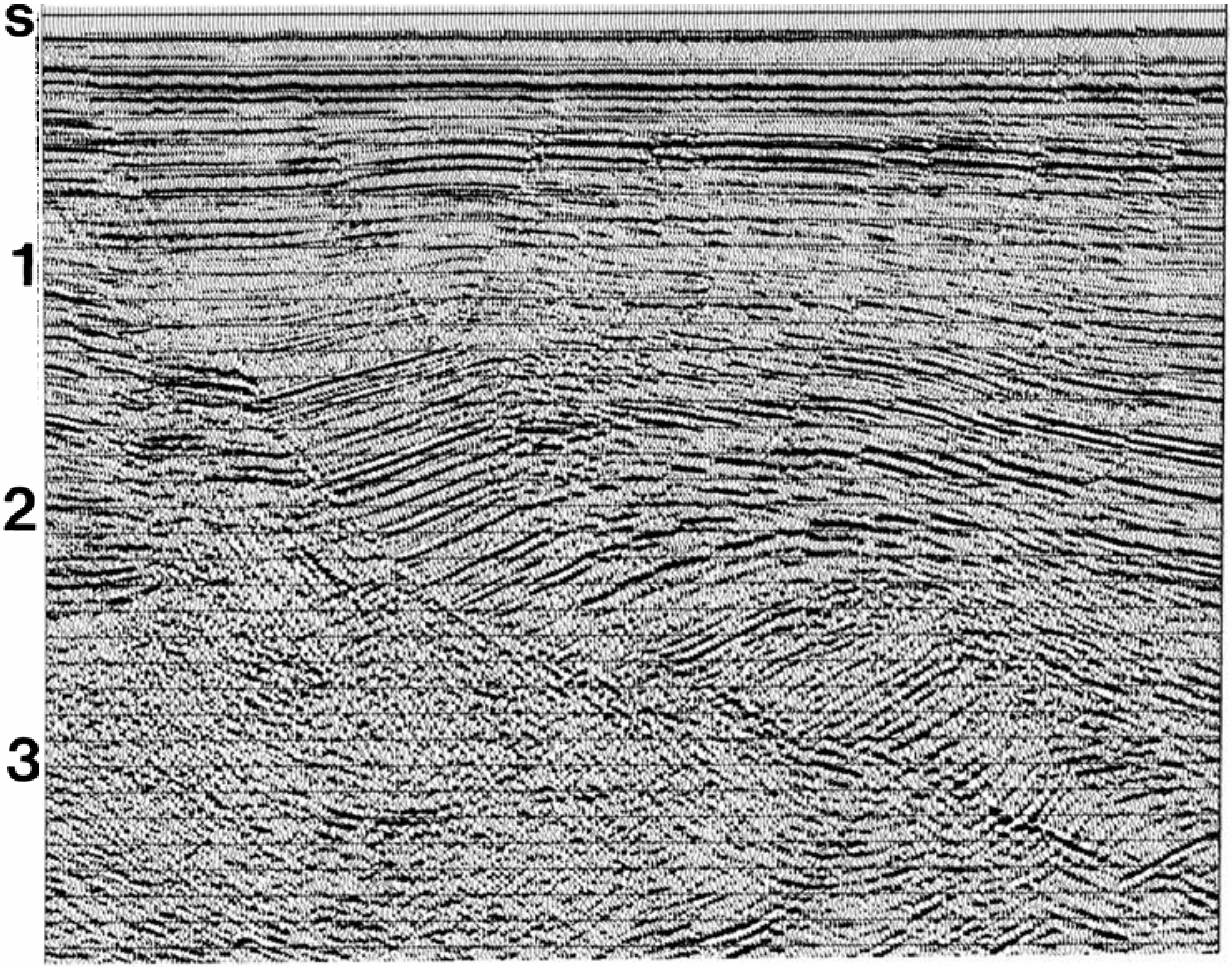


(Yilmaz, 2001)

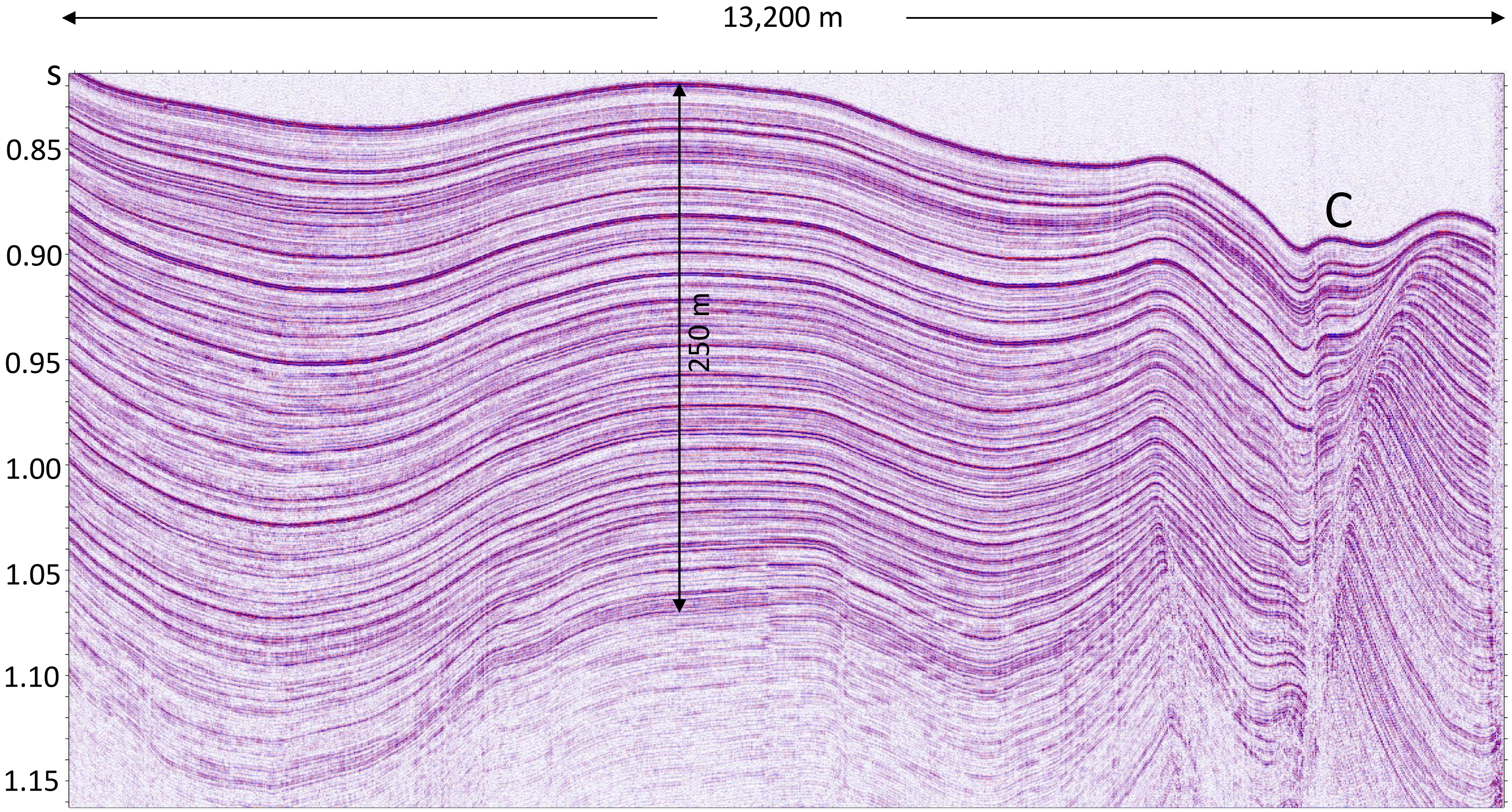


**(Data from offshore Akkuyu, Mersin, courtesy Derinsu; Yılmaz, 2015)**

Feature C represents an incipent compressional structure resulting an initial faulting with a likely strike-slip component.

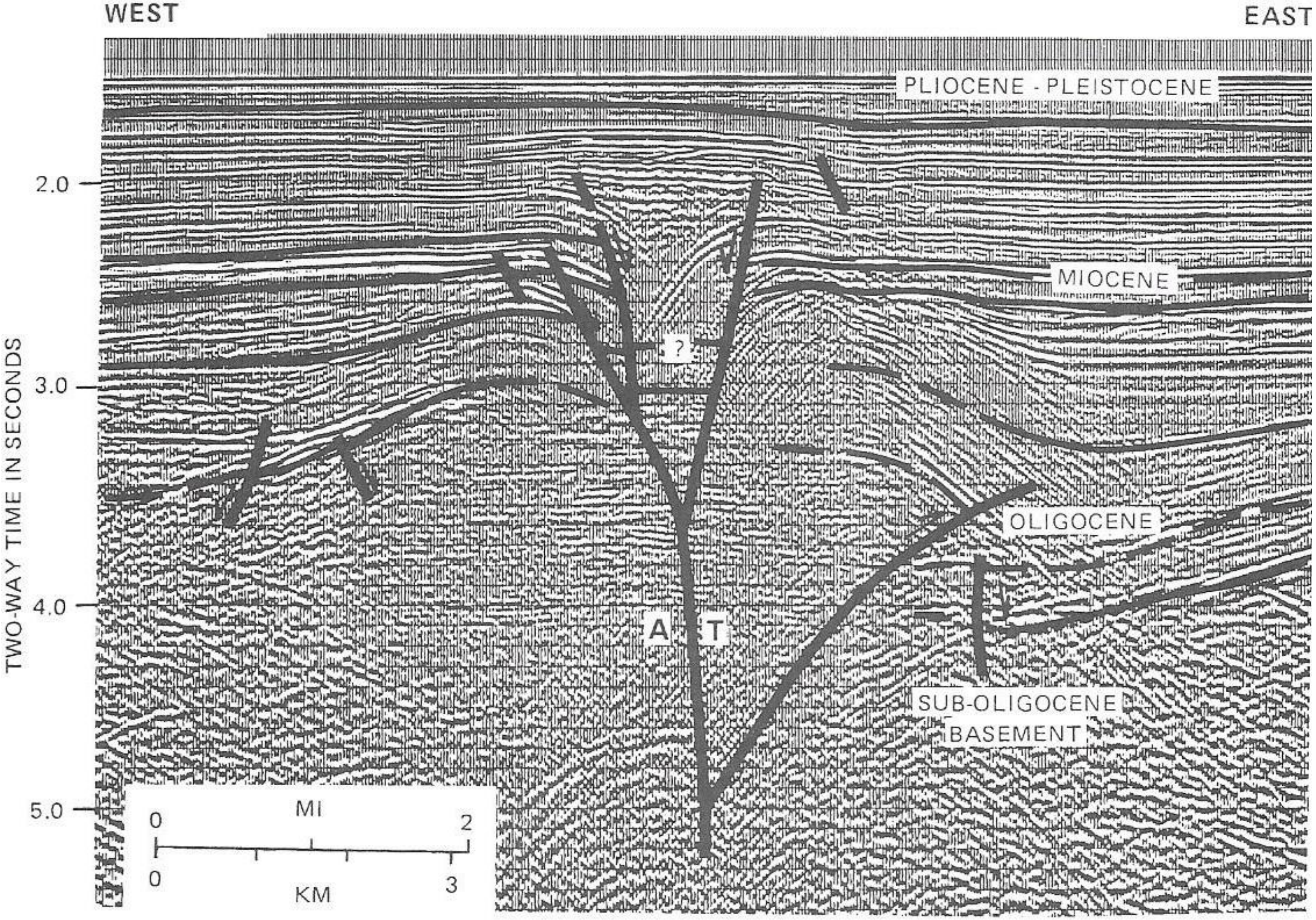


Example of a negative flower structure from an extensional duplex on a dextral strike-slip fault from the Andaman Sea between India and Malay peninsula.

(Twiss and Moores, 2007)

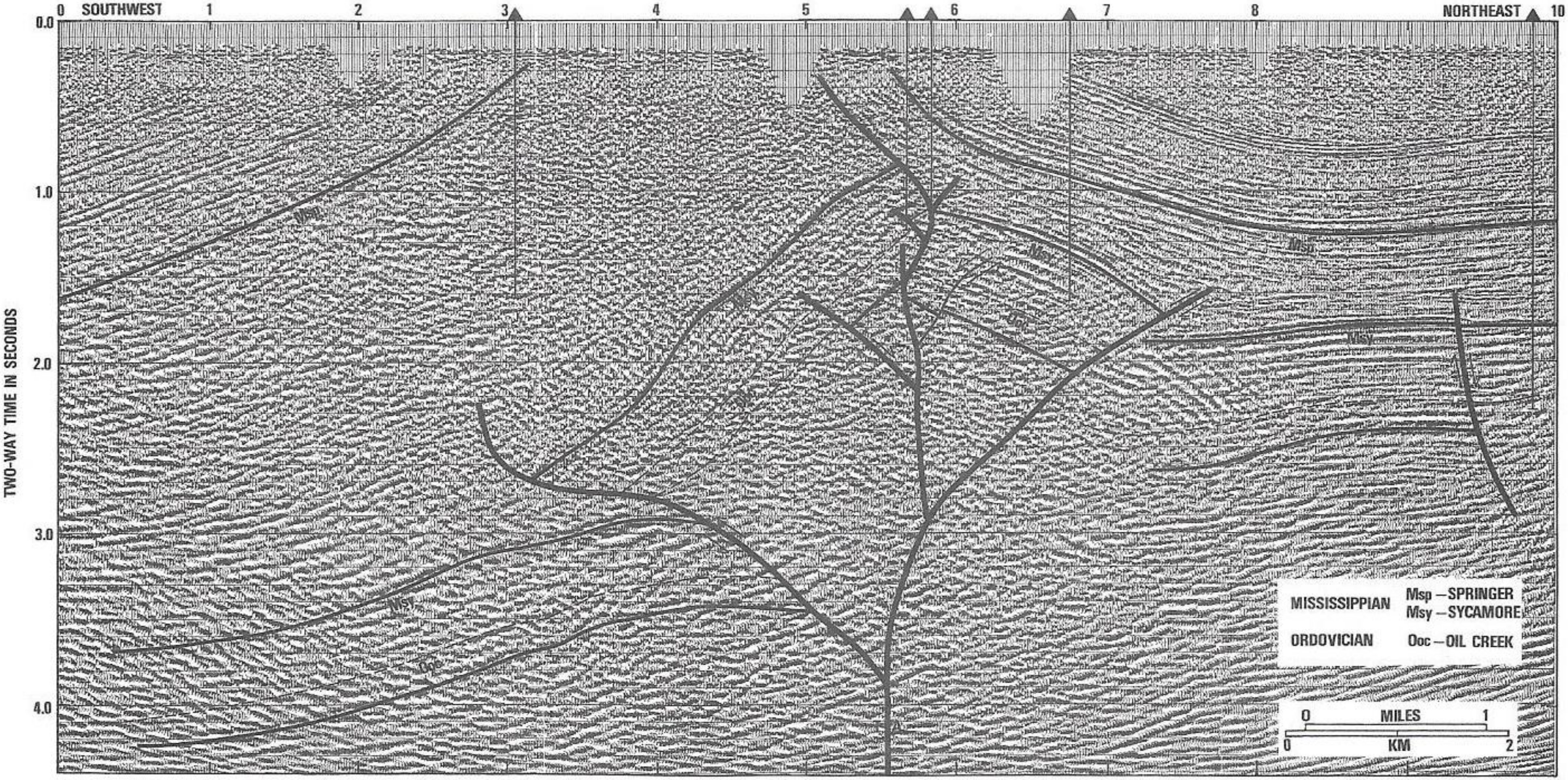


Example of a positive flower structure from a contractional duplex on a sinistral strike-slip fault in the Ardmore Basin, Oklahoma.

(Twiss and Moores, 2007)

# wrench tectonism

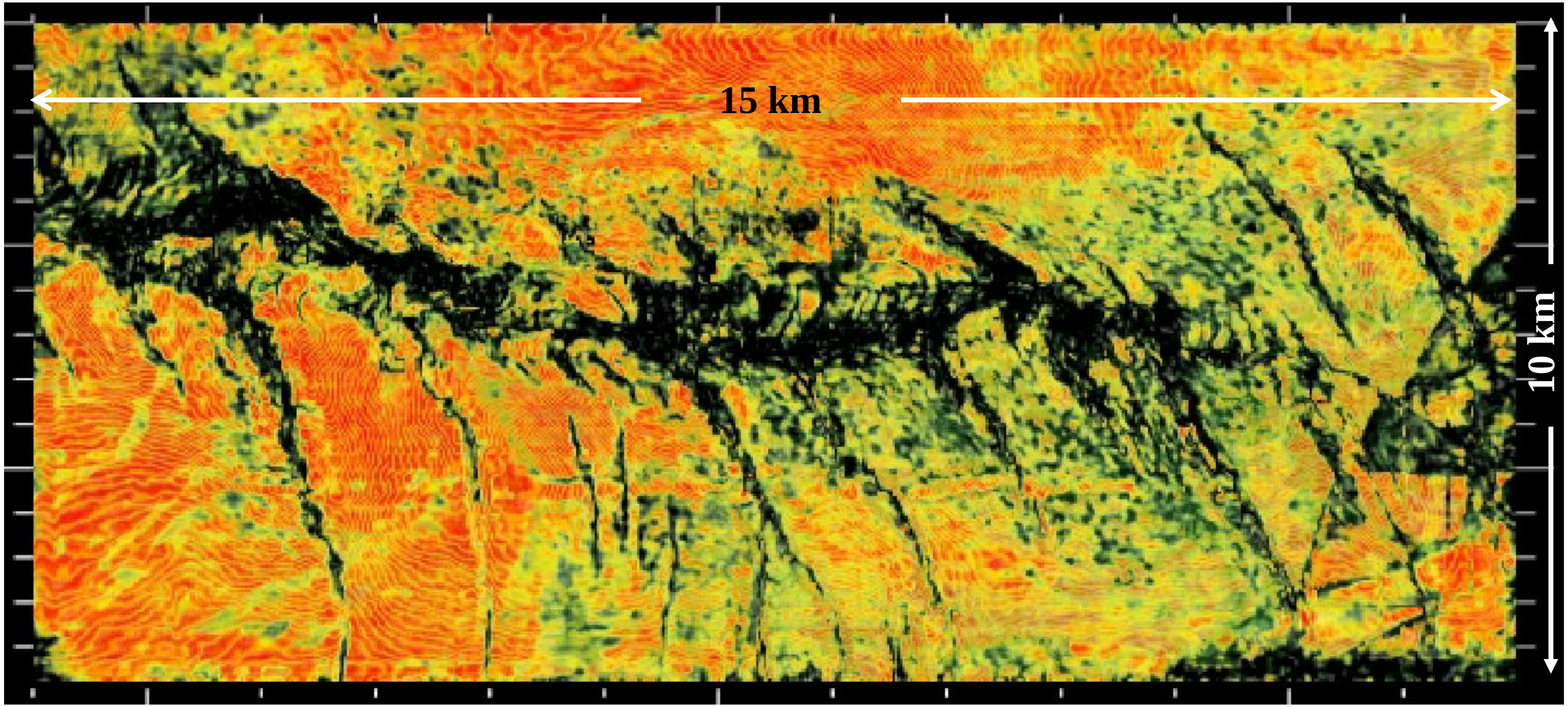


(Data from offshore Indonesia courtesy Clyde Petroleum; Yılmaz, 2001)

# 2-D CMP stack

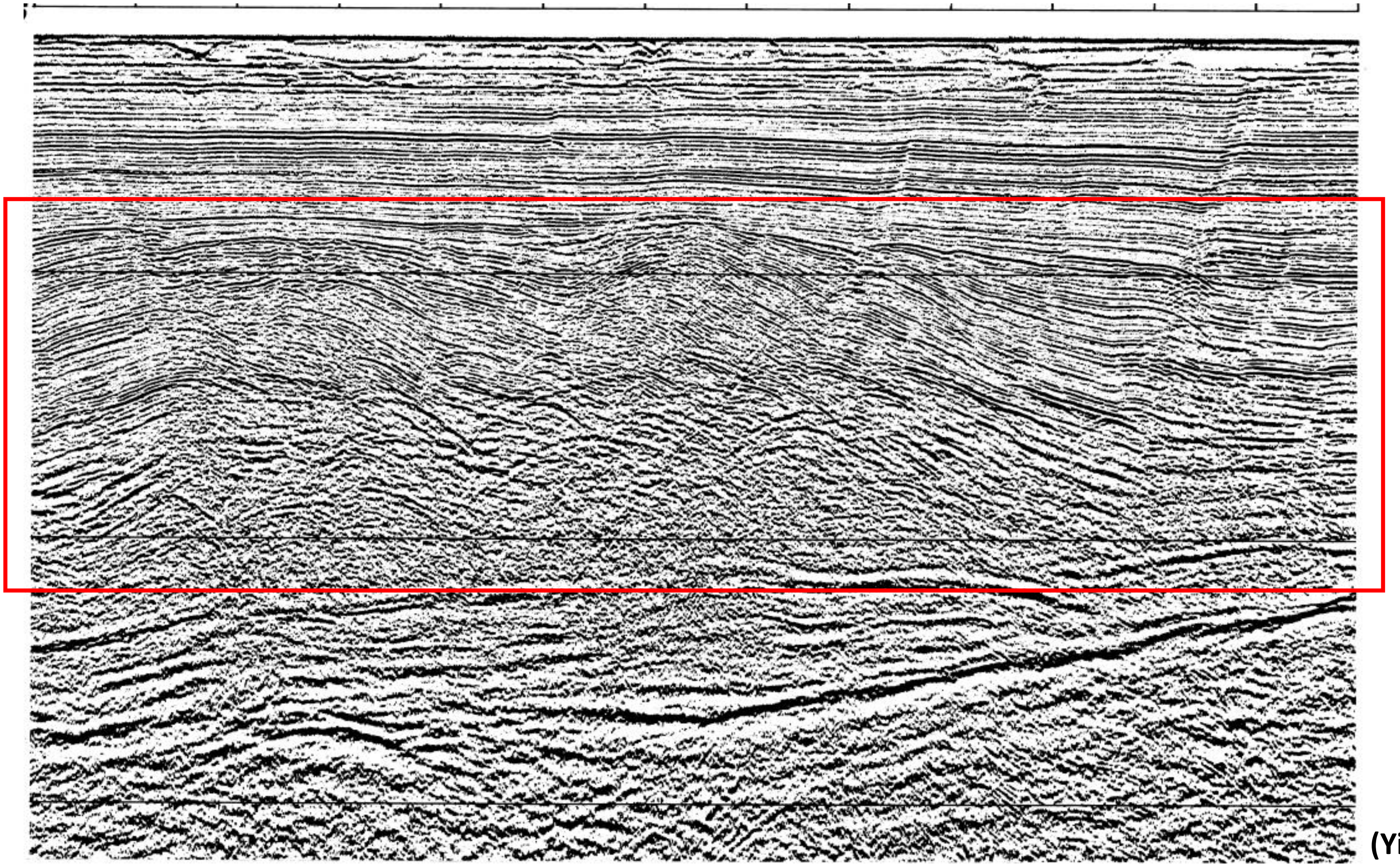

(Yilmaz, 2001)

# 2-D poststack time migration

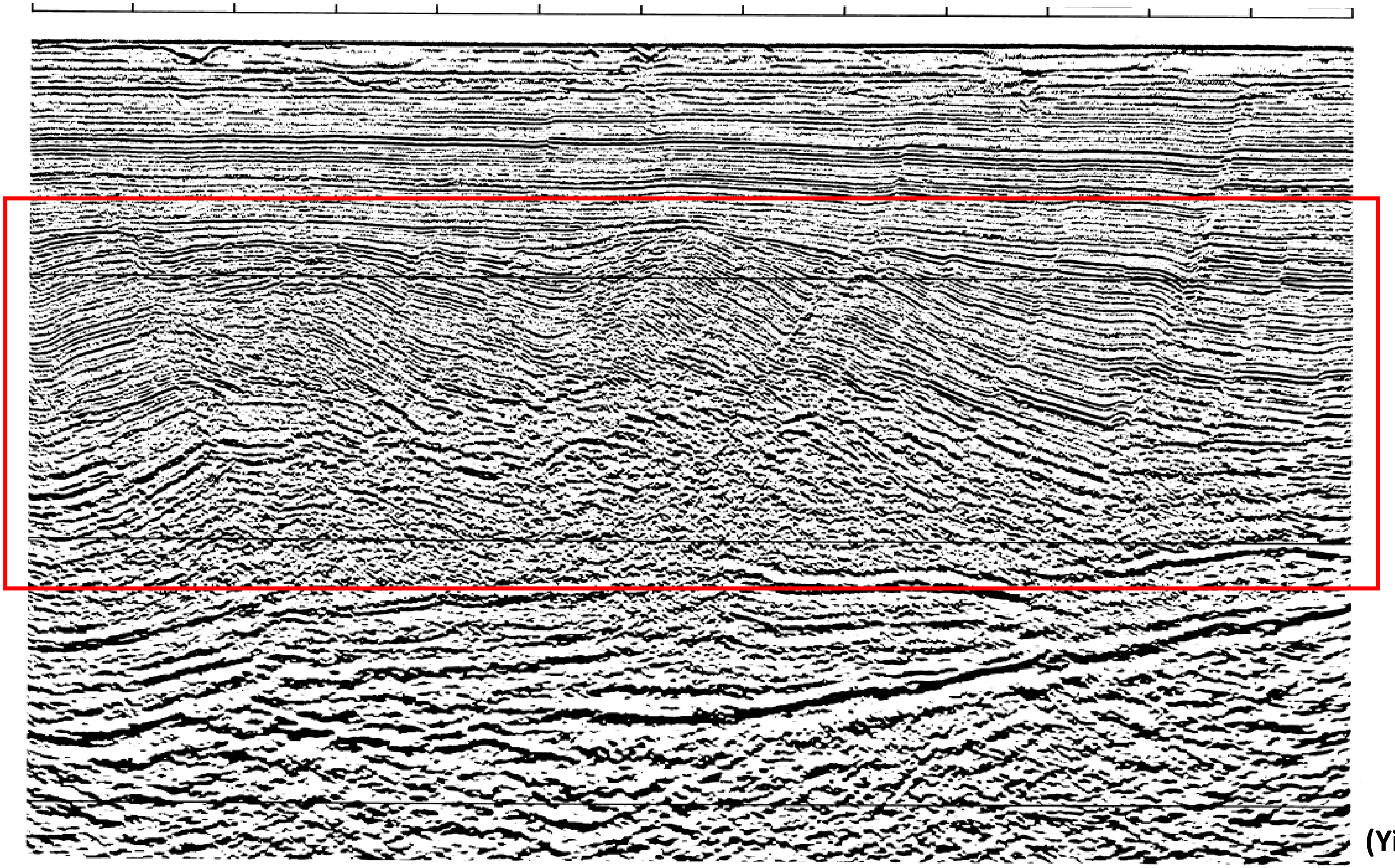

(Yilmaz, 2001)

# 3-D prestack time migration

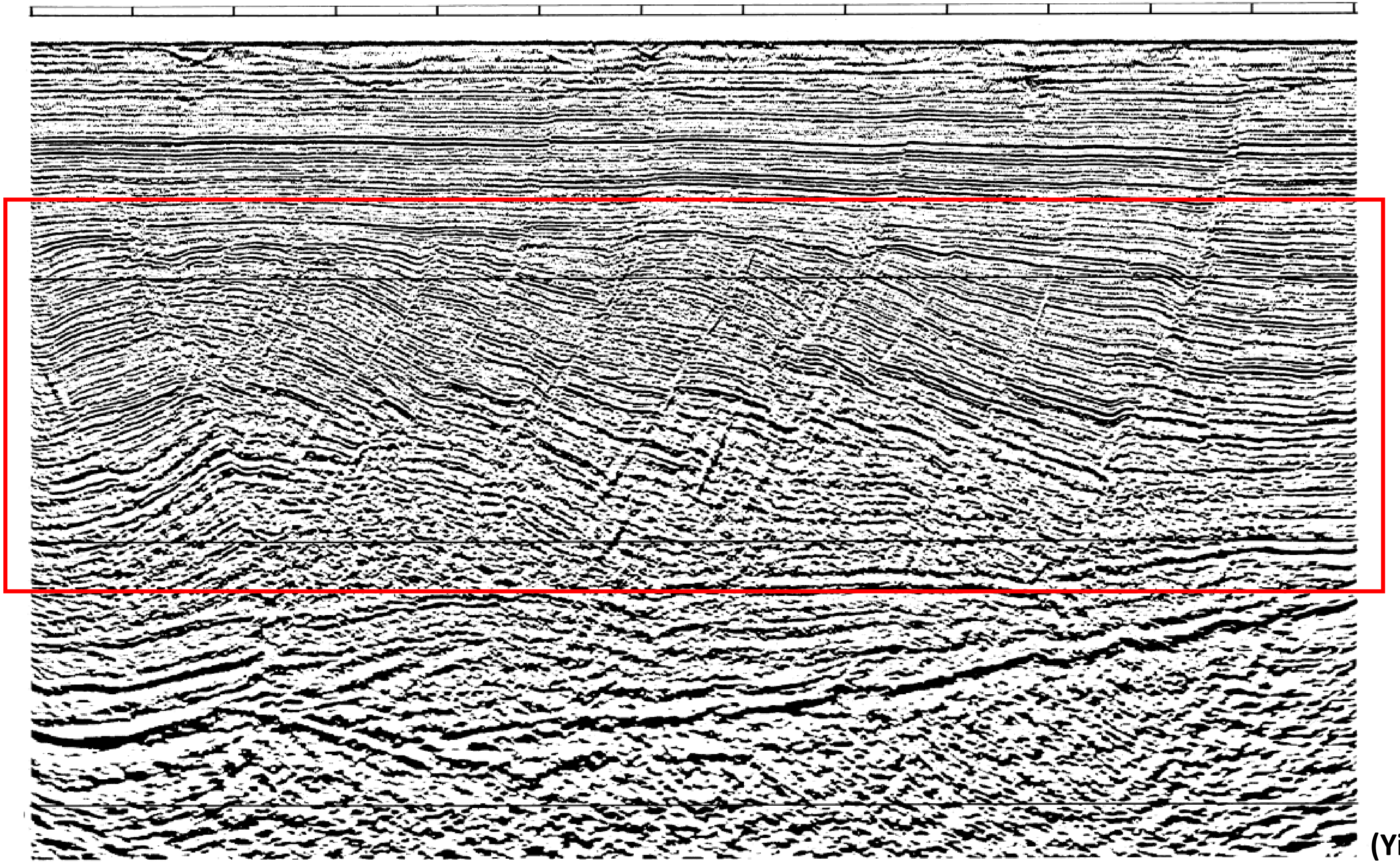

(Yilmaz, 2001)

# 2-D CMP stack

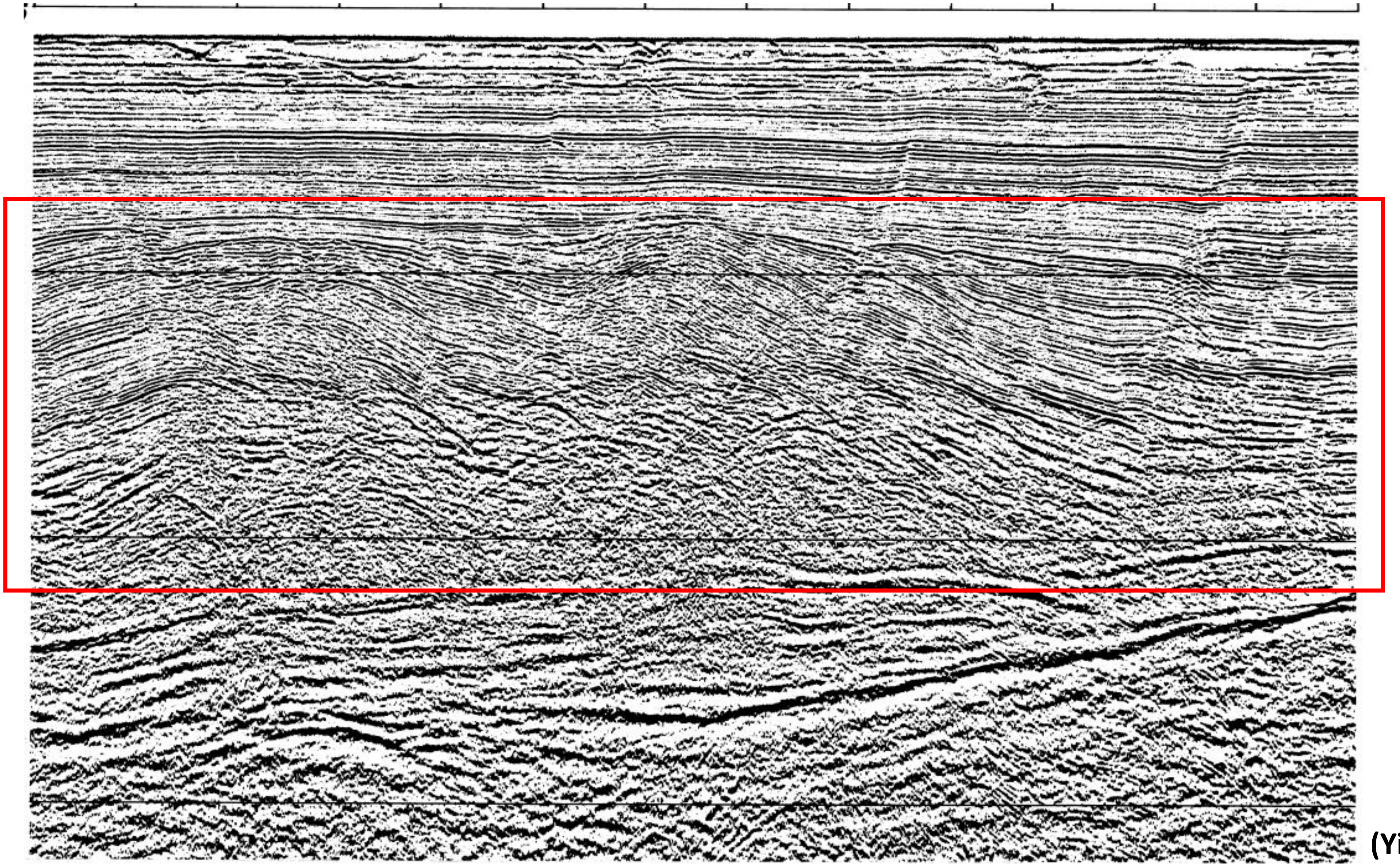

(Yilmaz, 2001)

# 2-D poststack time migration

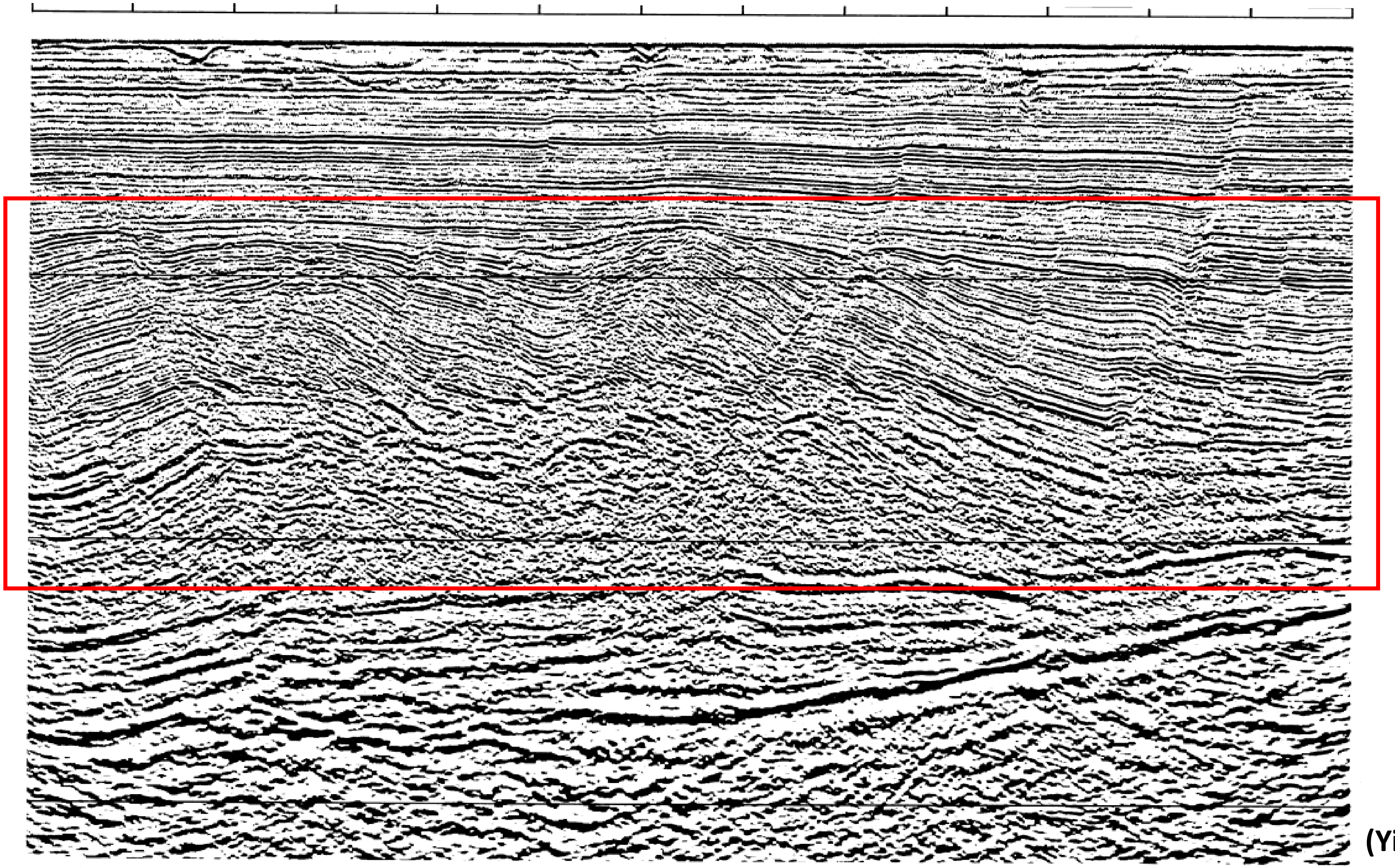

(Yilmaz, 2001)

# 3-D prestack time migration

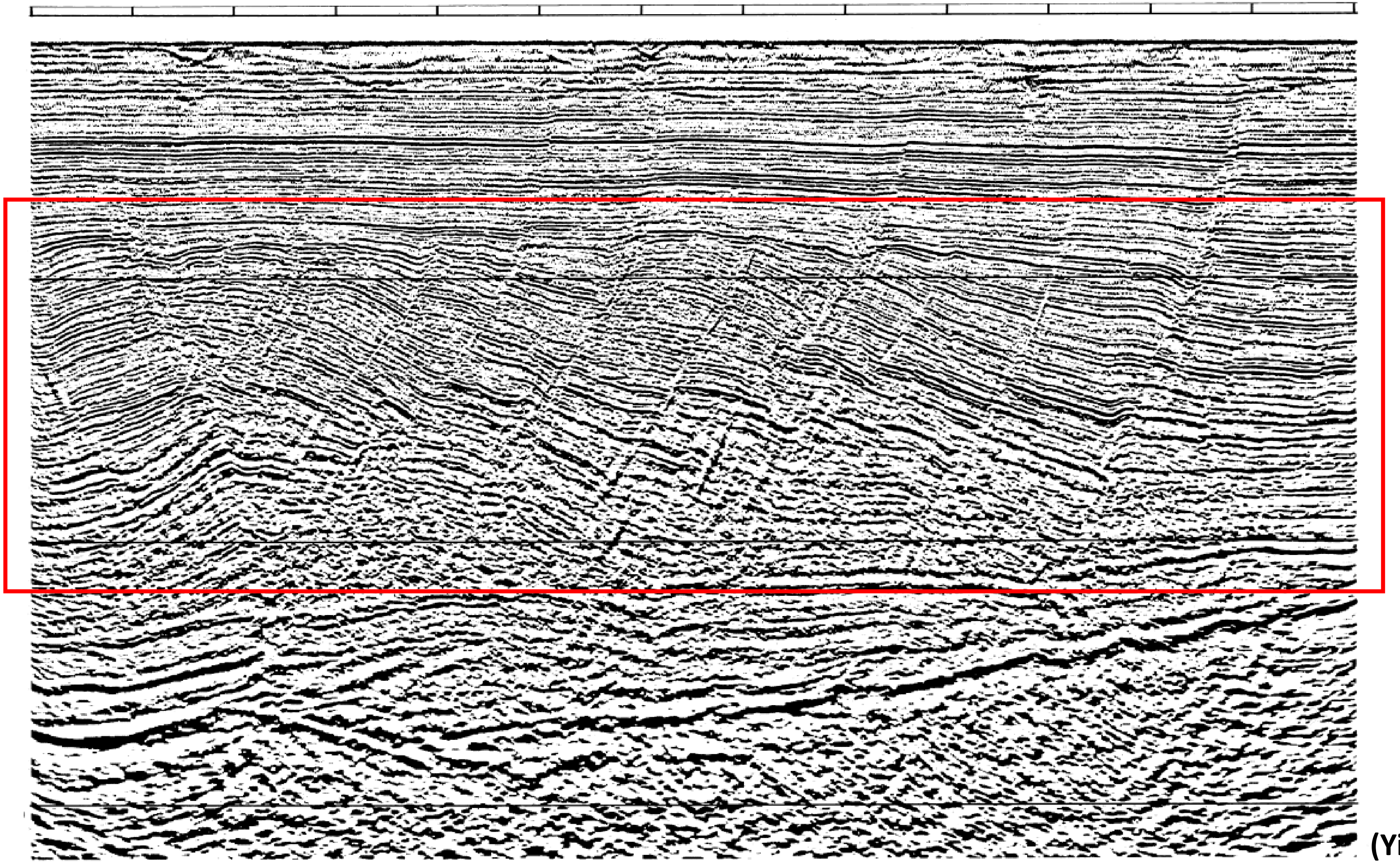

(Yilmaz, 2001)

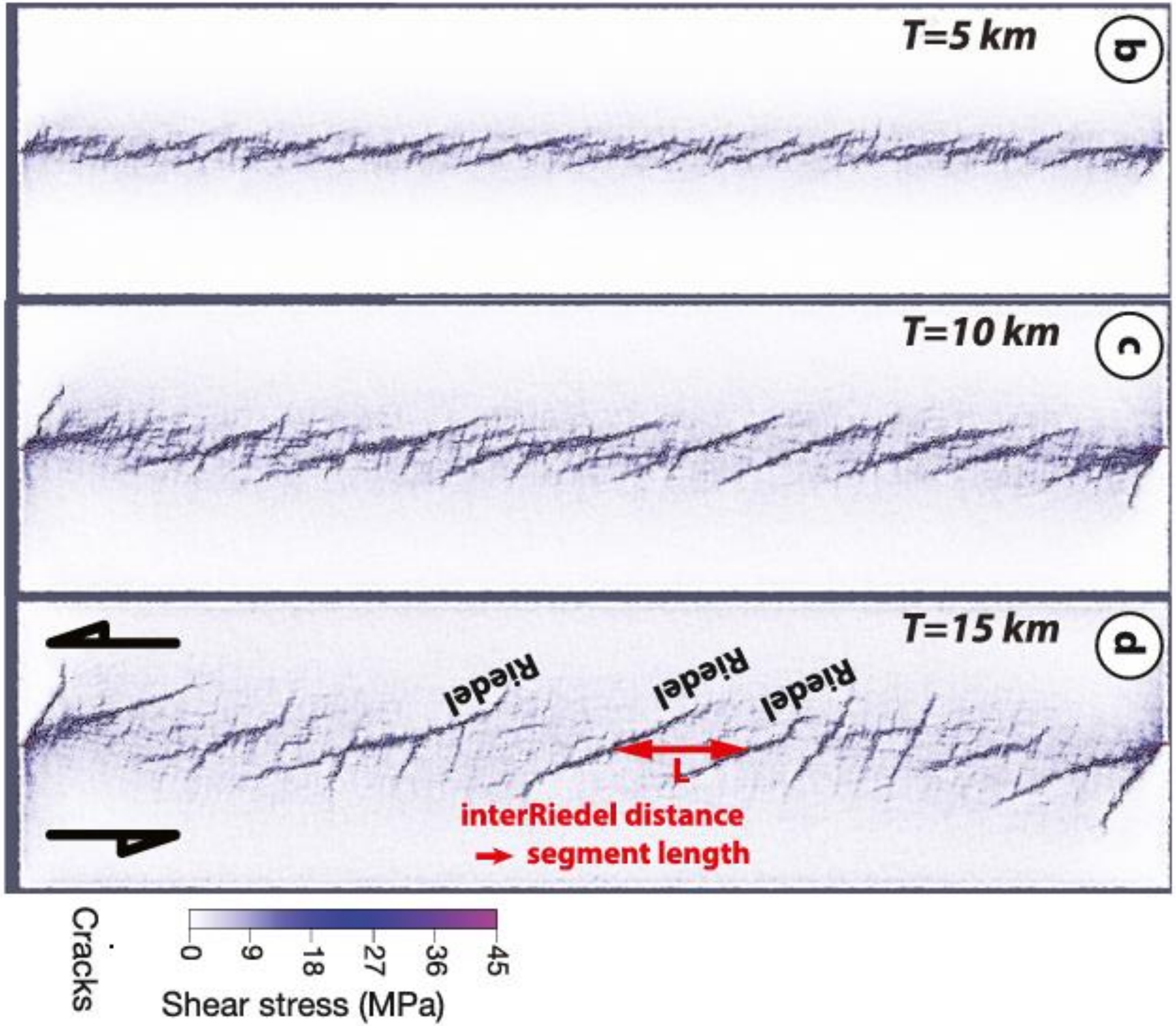


# Numerical modeling of brittle continental crust with different thickness *T*

**The separation between the shear strands increases with increasing thickness of the brittle crust.**

**(Jiao et al., 2021)**

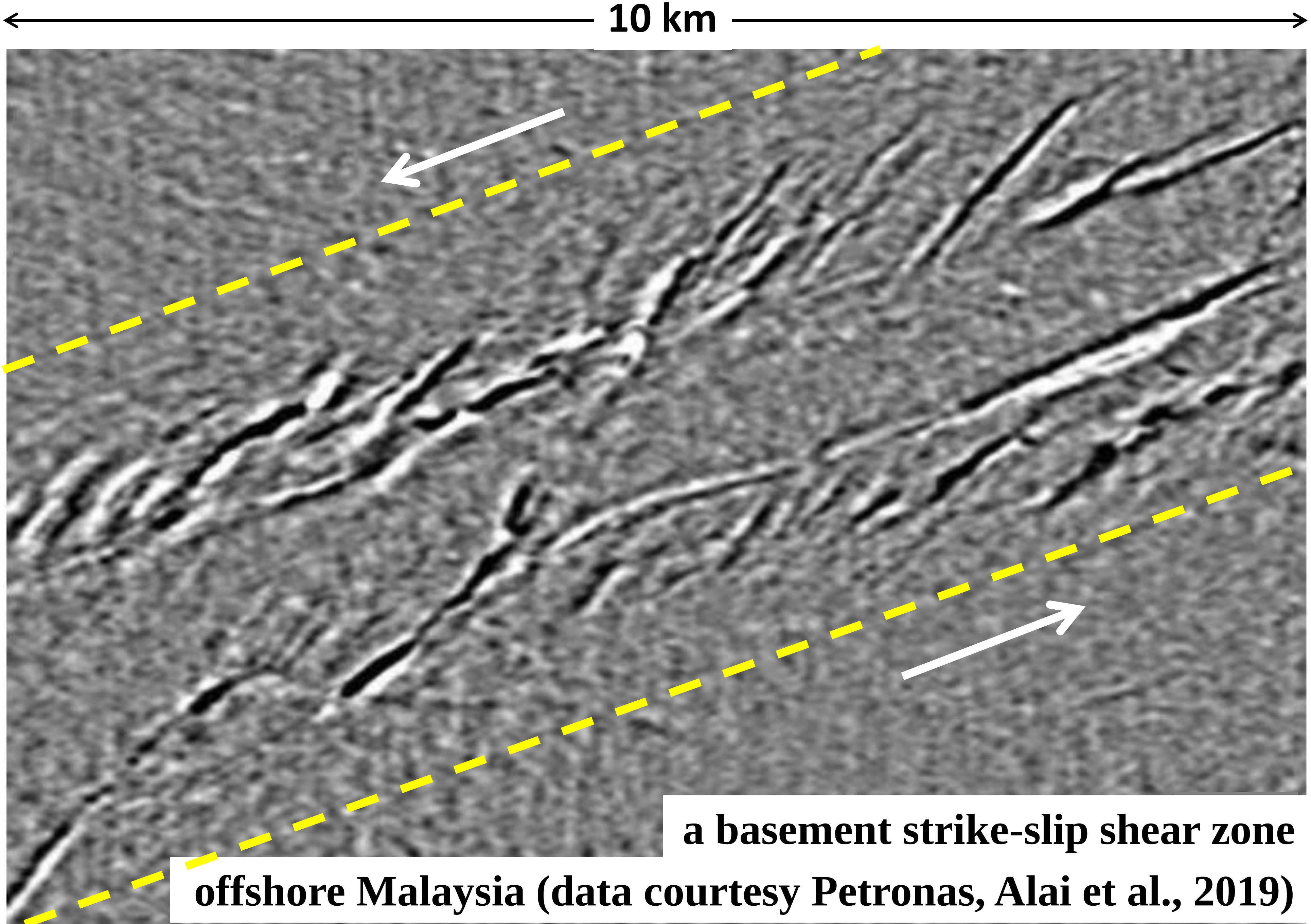
10 km
a basement strike-slip shear zone
offshore Malaysia (data courtesy Petronas, Alai et al., 2019)

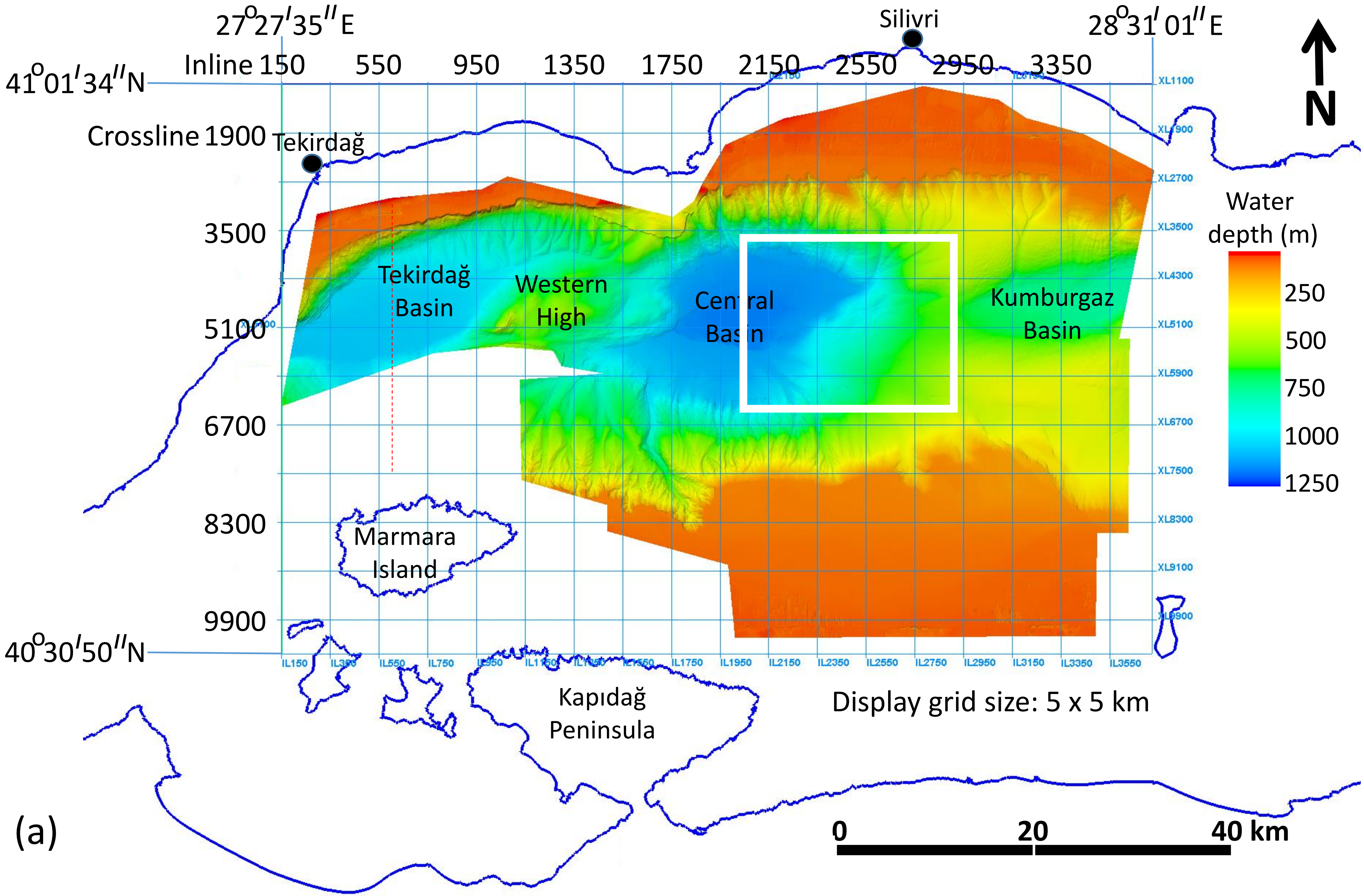

27°27′35″E
Silivri
28°31′01″E
N
41°01′34″N
Inline 150
550
950
1350
1750
2150
2550
2950
3350
Crossline 1900
Tekirdağ
3500
5100
6700
8300
9900
40°30′50″N
Tekirdağ Basin
Western High
Central Basin
Kumburgaz Basin
Marmara Island
Kapıdağ Peninsula
Water depth (m)
250
500
750
1000
1250
Display grid size: 5 x 5 km
0
20
40 km
(a)

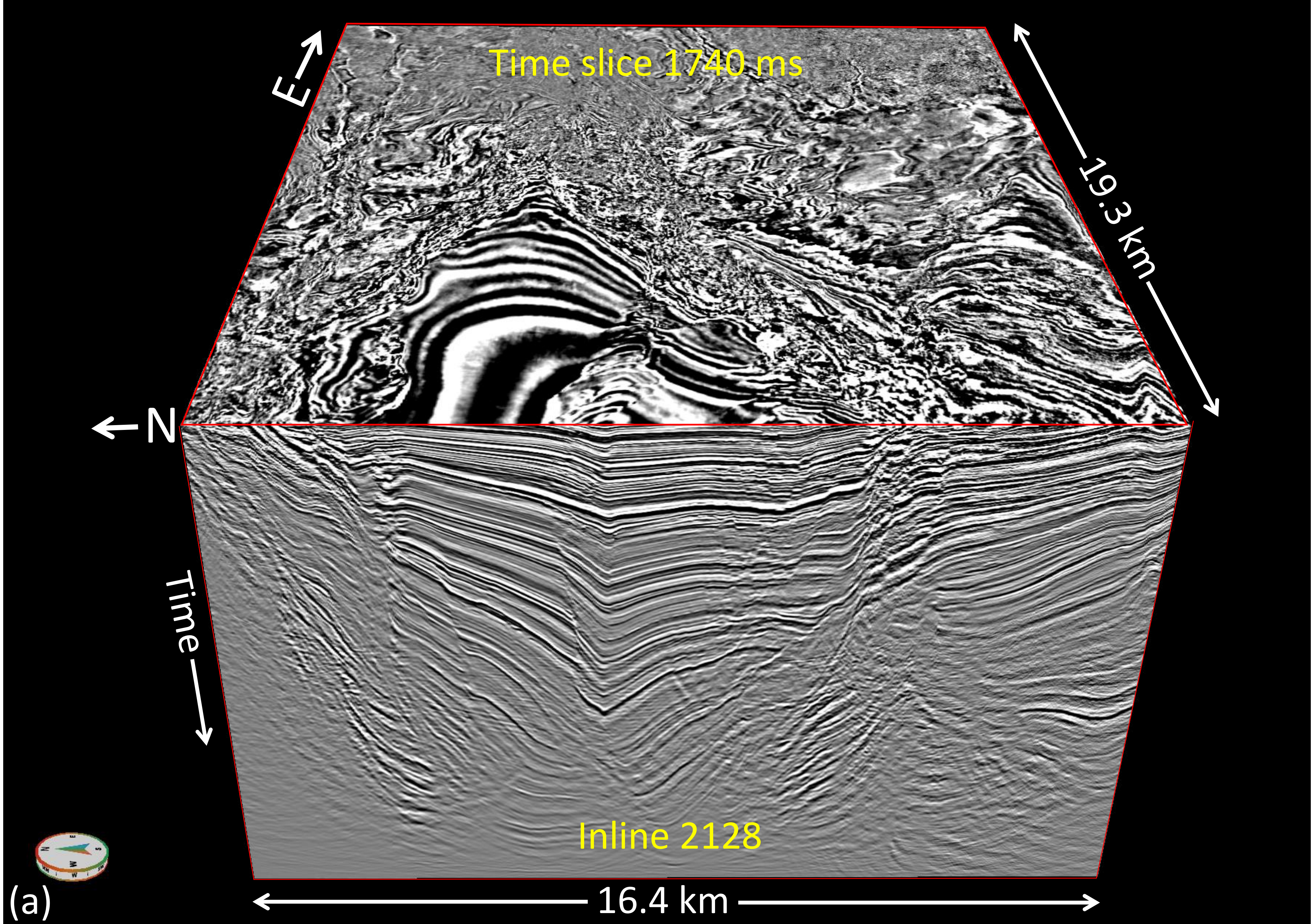
Time slice 1740 ms
E
N
19.3 km
Time
Inline 2128
(a)
16.4 km

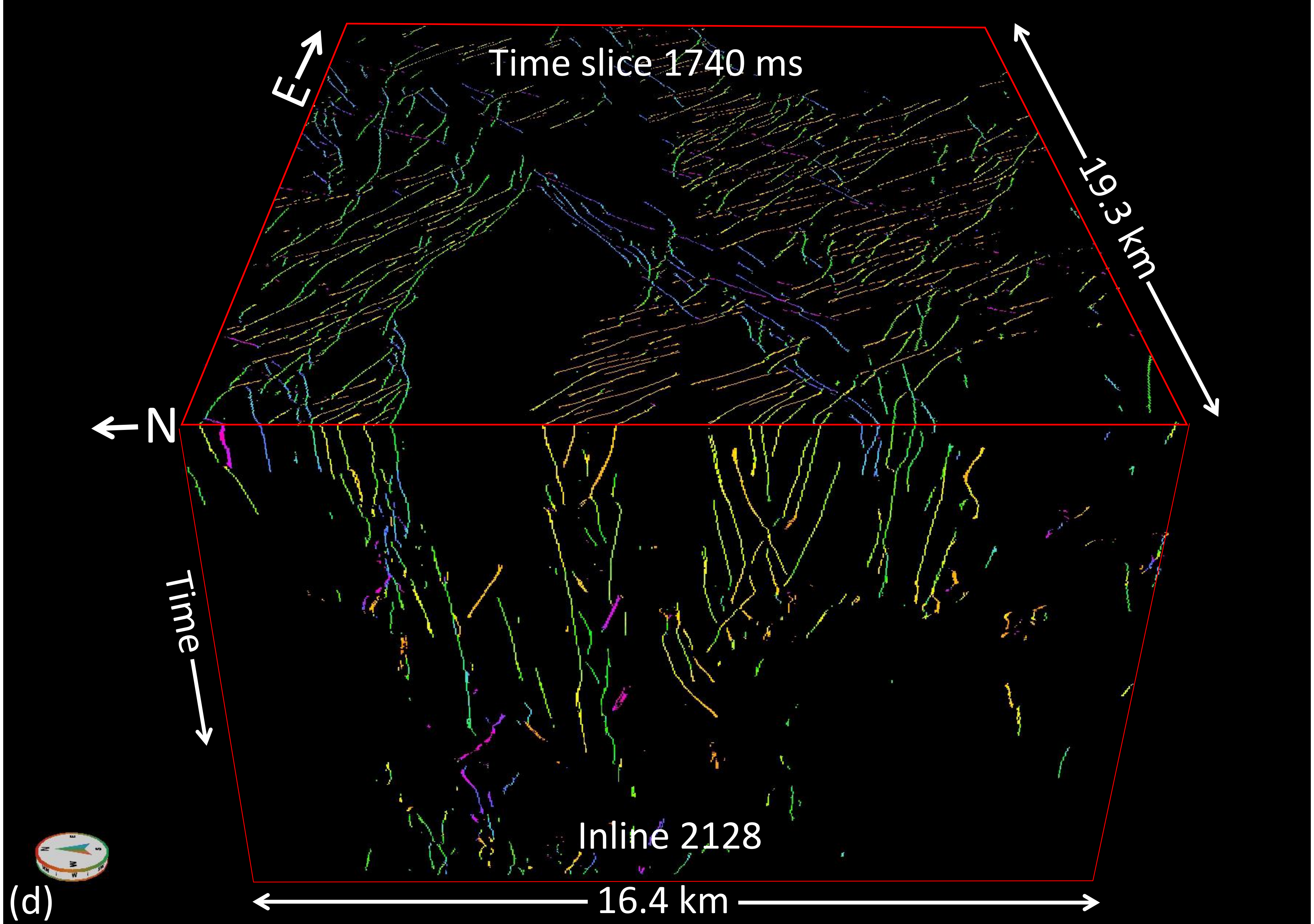
Time slice 1740 ms
E
19.3 km
N
Time
Inline 2128
16.4 km
(d)

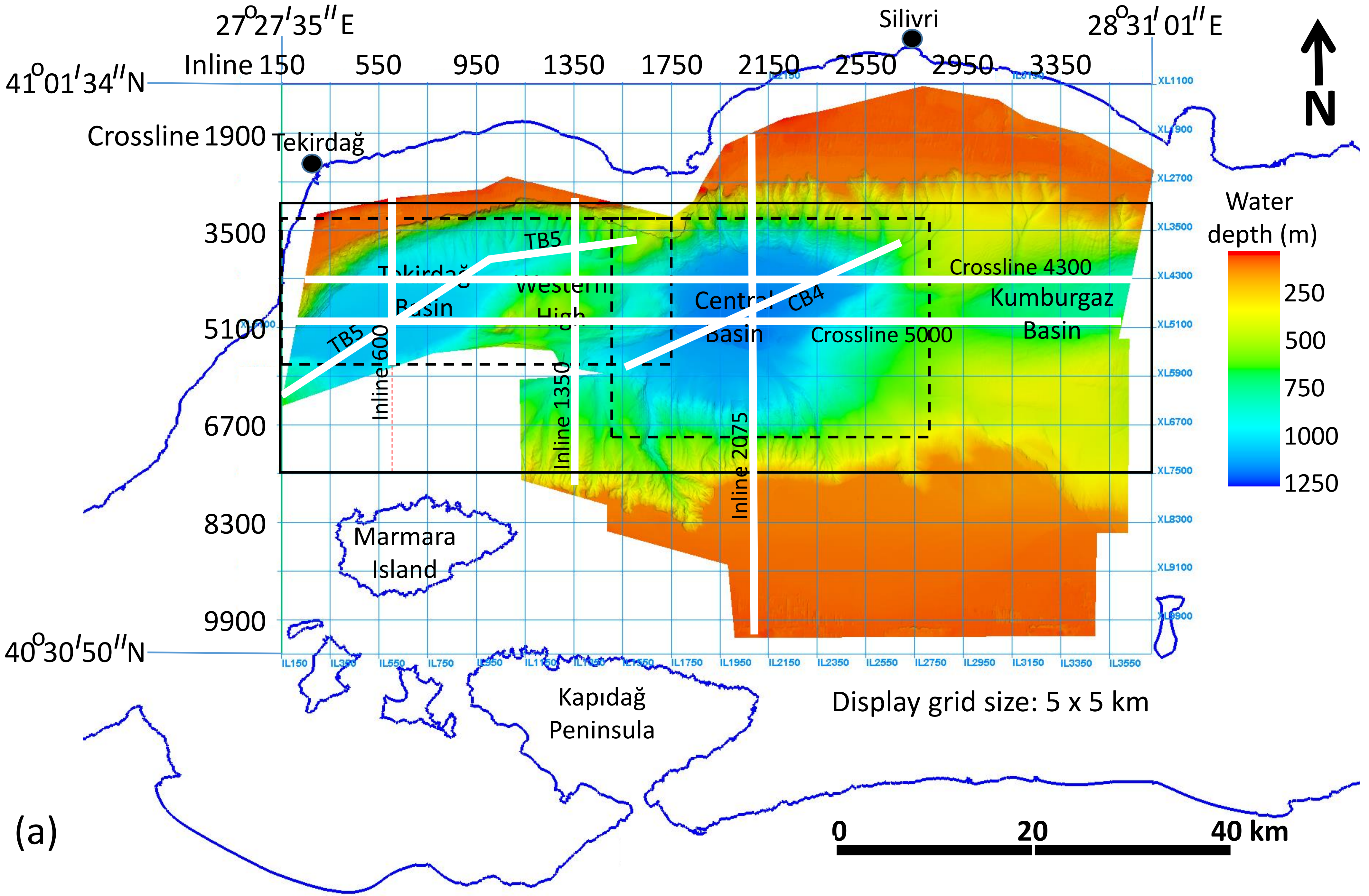

27°27′35″E
Silivri
28°31′01″E
N
Inline 150
550
950
1350
1750
2150
2550
2950
3350
41°01′34″N
Crossline 1900
Tekirdağ
3500
5100
6700
8300
9900
40°30′50″N
TB5
Tekirdağ Basin
Western High
Central Basin
CB4
Crossline 4300
Kumburgaz Basin
Crossline 5000
Inline 600
Inline 1350
Inline 2075
Water depth (m)
250
500
750
1000
1250
Marmara Island
Kapıdağ Peninsula
Display grid size: 5 x 5 km
(a)
0
20
40 km

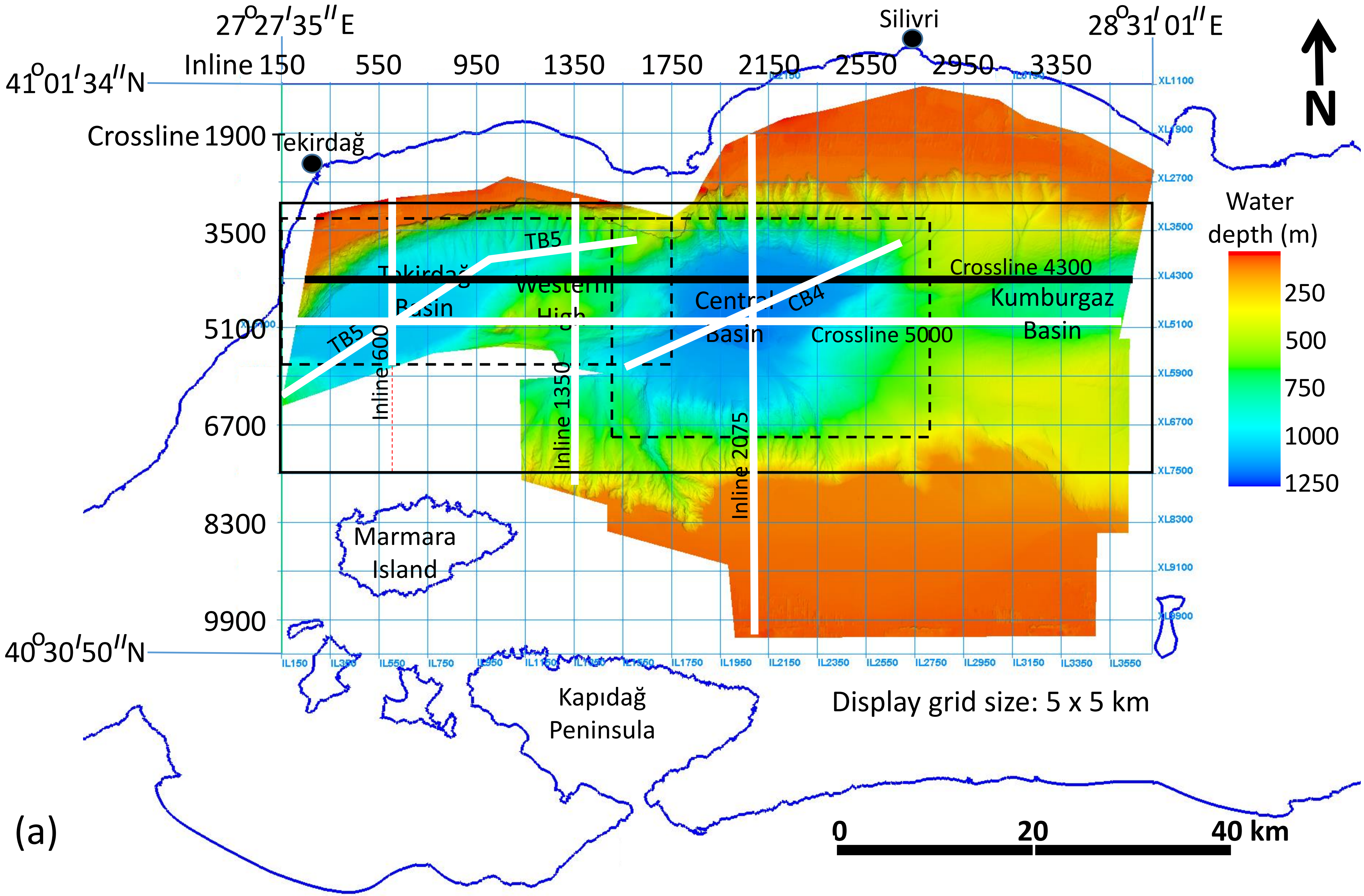
27°27′35″E
Silivri
28°31′01″E
N
Inline 150
550
950
1350
1750
2150
2550
2950
3350
41°01′34″N
Crossline 1900
Tekirdağ
3500
5100
6700
8300
9900
40°30′50″N
TB5
Tekirdağ
Basin
Western
High
Central
Basin
CB4
Crossline 4300
Kumburgaz
Basin
Crossline 5000
Inline 600
Inline 1350
Inline 2075
Water
depth (m)
250
500
750
1000
1250
Marmara
Island
Kapıdağ
Peninsula
Display grid size: 5 x 5 km
0
20
40 km
(a)

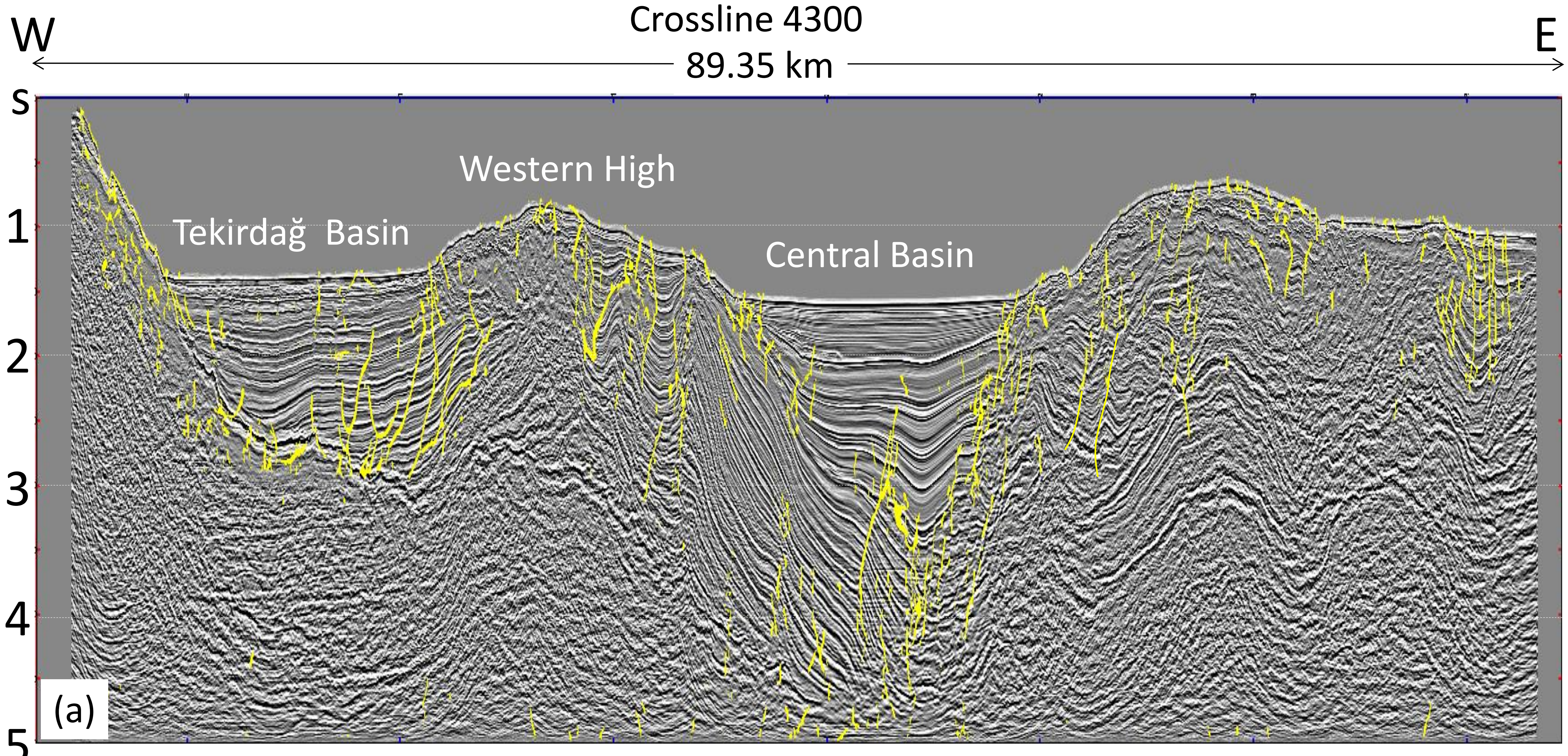

Crossline 4300
W
E
89.35 km
s
1
2
3
4
5
Western High
Tekirdağ Basin
Central Basin
(a)

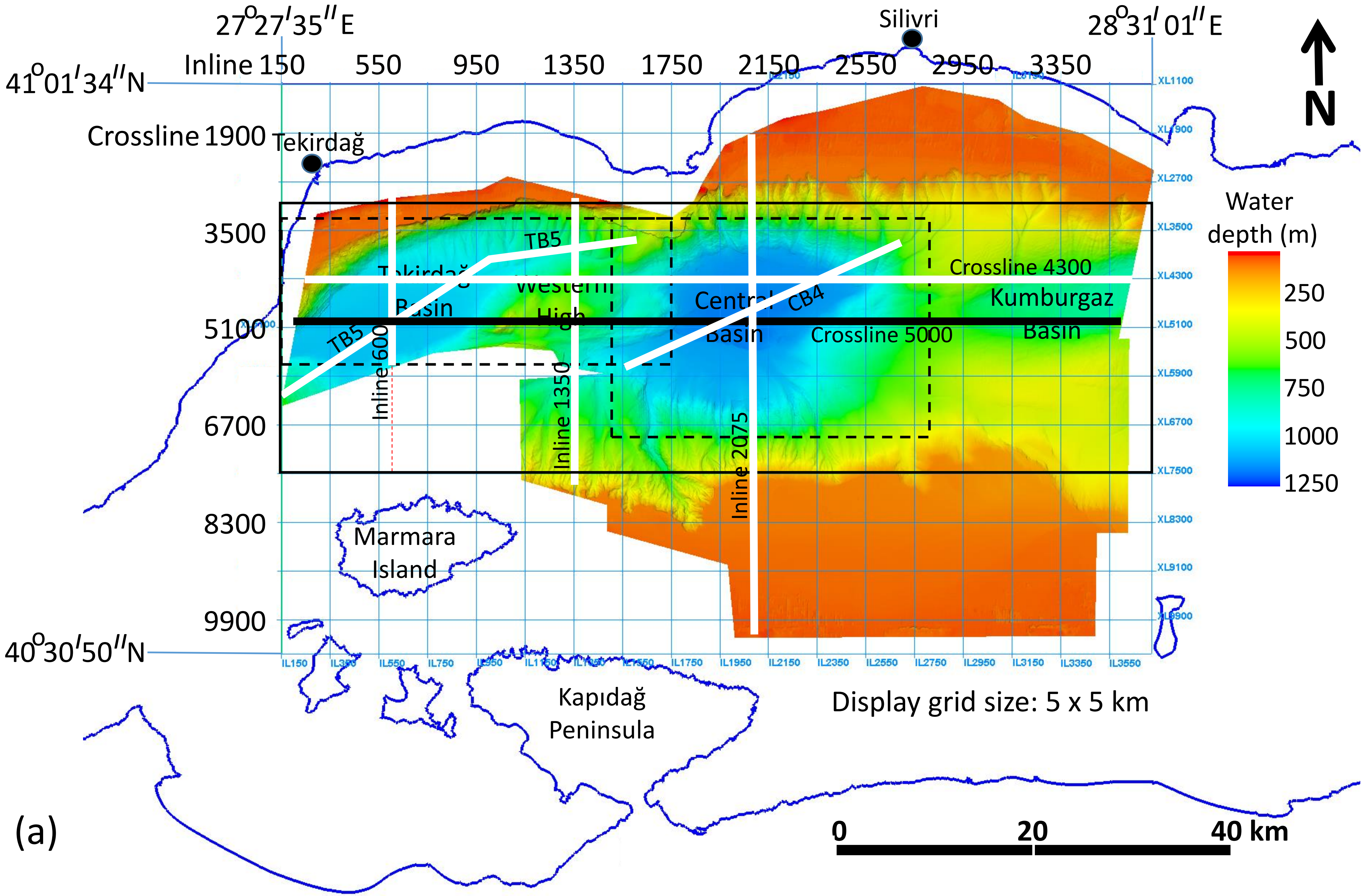

27°27′35″E
Silivri
28°31′01″E
N
41°01′34″N
Inline 150
550
950
1350
1750
2150
2550
2950
3350
Crossline 1900
Tekirdağ
3500
5100
6700
8300
9900
40°30′50″N
TB5
CB4
Crossline 4300
Crossline 5000
Kumburgaz Basin
Central Basin
Western High
Tekirdağ Basin
Inline 600
Inline 1350
Inline 2075
Water depth (m)
250
500
750
1000
1250
Marmara Island
Kapıdağ Peninsula
Display grid size: 5 x 5 km
0
20
40 km
(a)

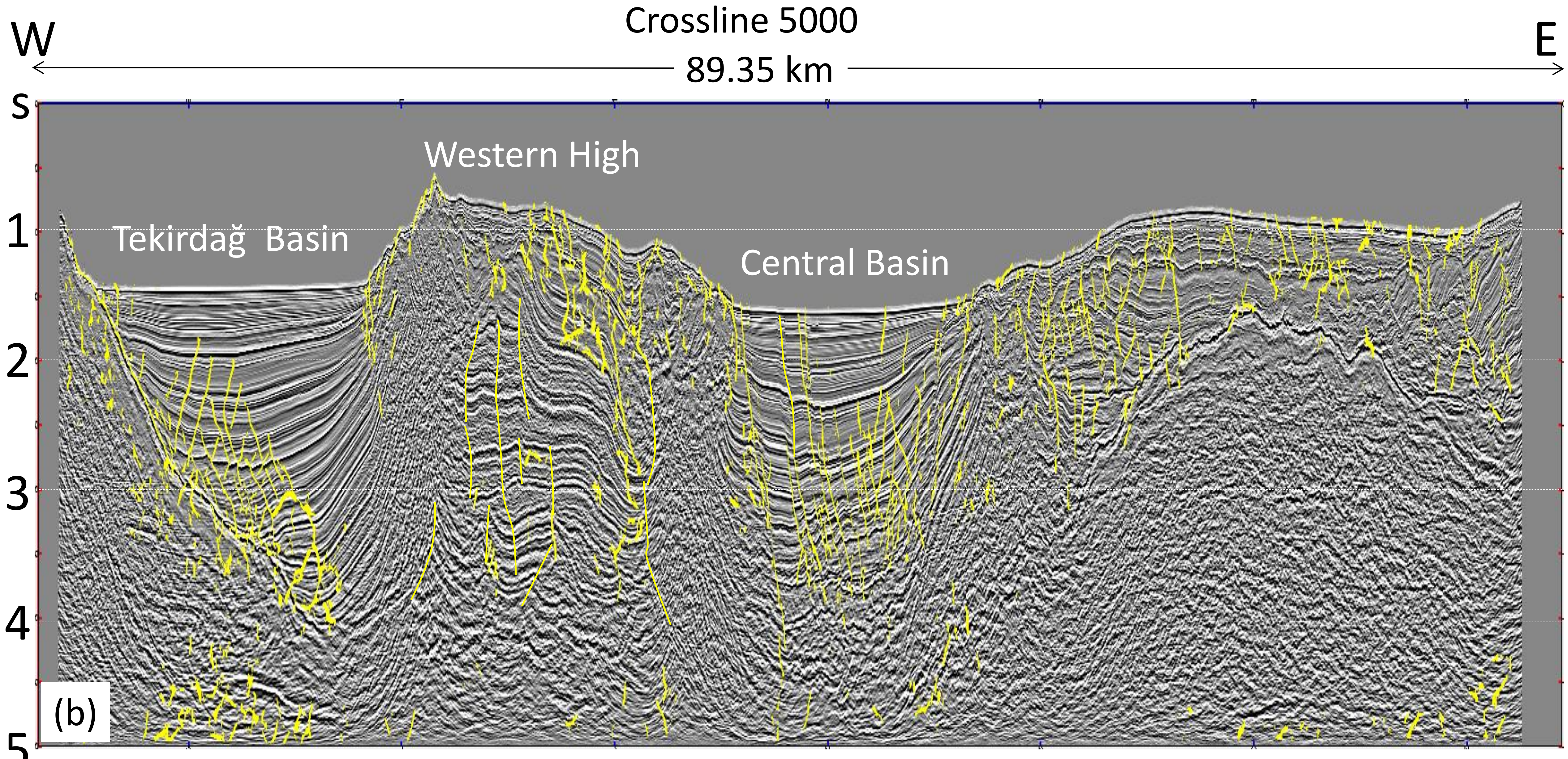
Crossline 5000
W
E
89.35 km
s
1
2
3
4
5
Western High
Tekirdağ Basin
Central Basin
(b)

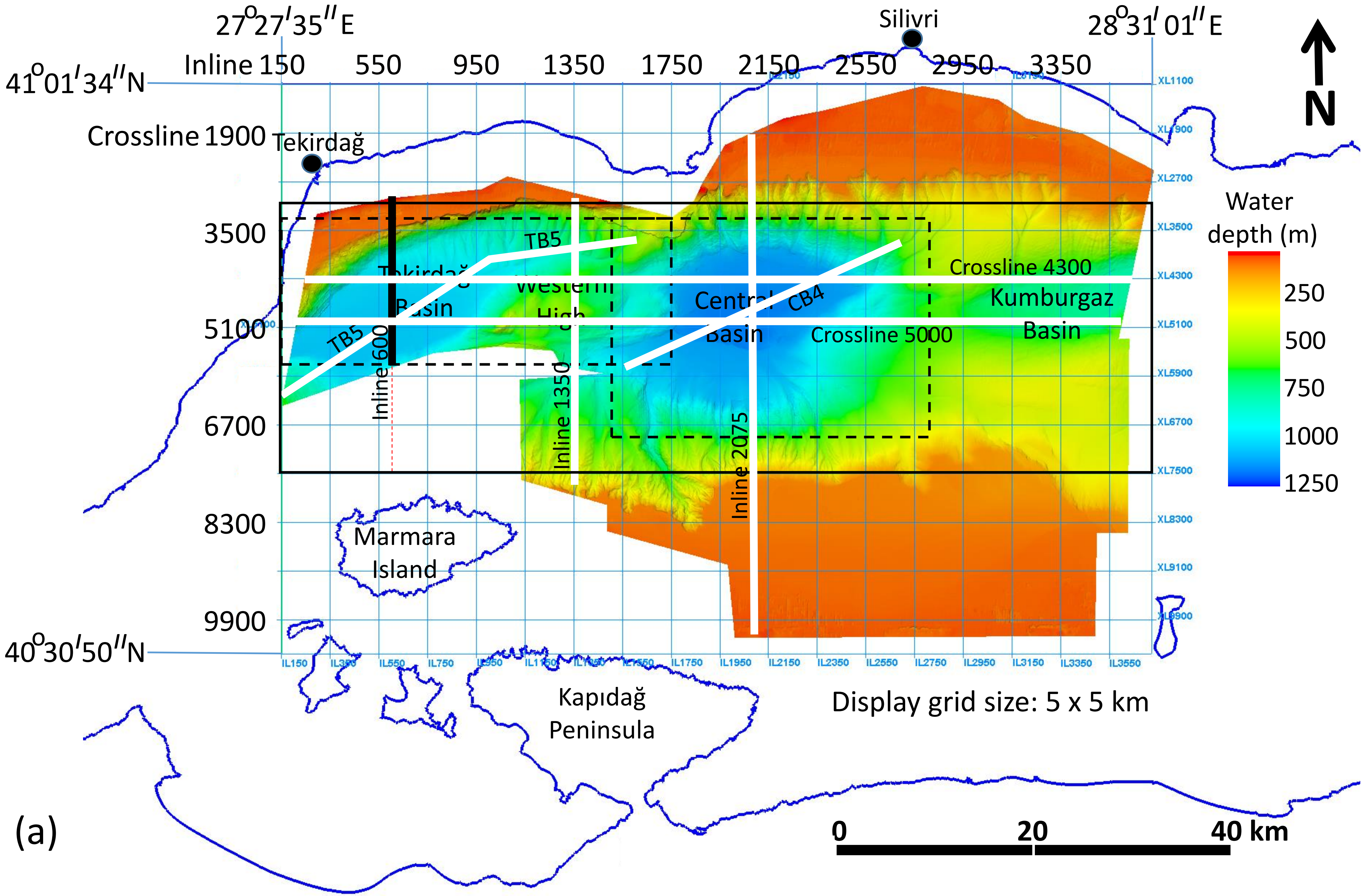

27°27′35″E
Silivri
28°31′01″E
N
Inline 150
550
950
1350
1750
2150
2550
2950
3350
41°01′34″N
Crossline 1900
Tekirdağ
3500
5100
6700
8300
9900
40°30′50″N
TB5
Tekirdağ Basin
Western High
Central Basin
CB4
Crossline 4300
Crossline 5000
Kumburgaz Basin
Inline 600
Inline 1350
Inline 2075
Water depth (m)
250
500
750
1000
1250
Marmara Island
Kapıdağ Peninsula
Display grid size: 5 x 5 km
0
20
40 km
(a)

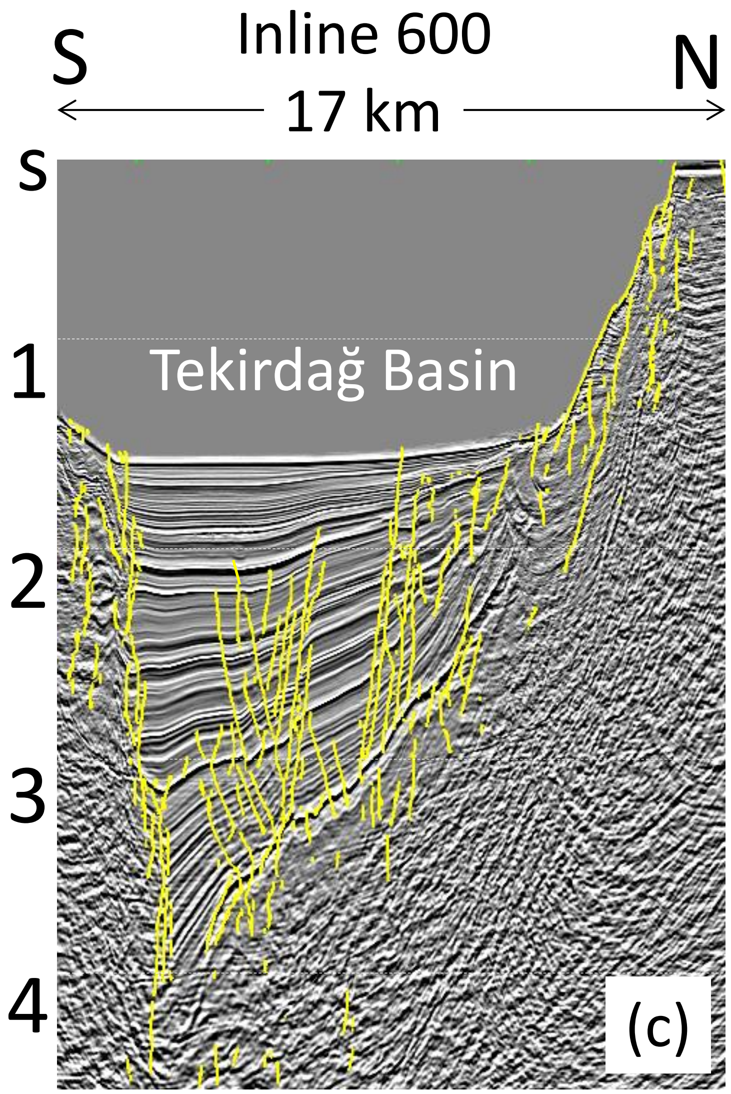
Inline 600
S
N
17 km
s
1
2
3
4
Tekirdağ Basin
(c)

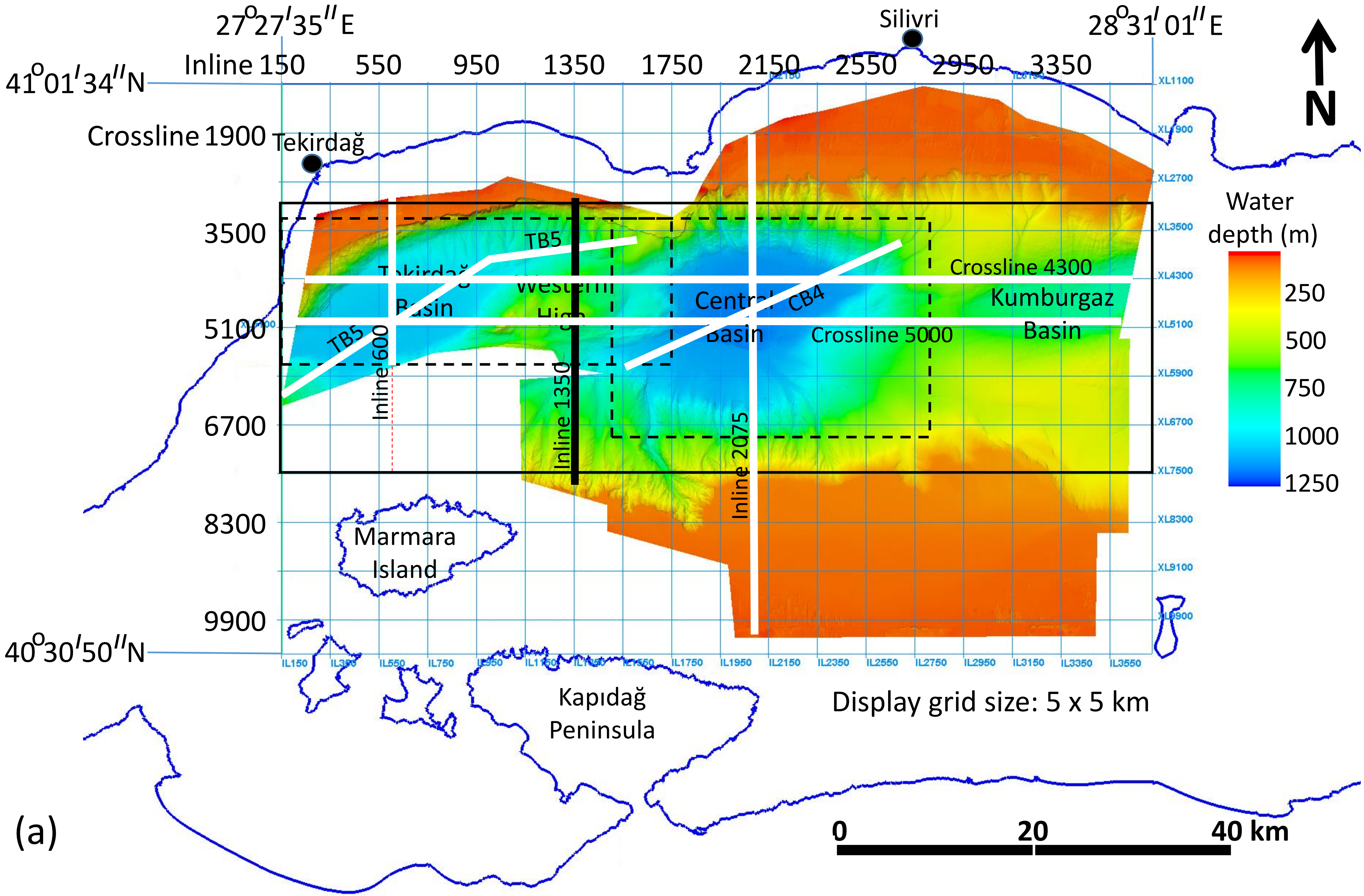

27°27′35″E
Silivri
28°31′01″E
N
Inline 150
550
950
1350
1750
2150
2550
2950
3350
41°01′34″N
Crossline 1900
Tekirdağ
3500
5100
6700
8300
9900
40°30′50″N
TB5
TB5
Western
High
Central
CB4
Basin
Crossline 4300
Kumburgaz
Basin
Crossline 5000
Inline 600
Inline 1350
Inline 2075
Water
depth (m)
250
500
750
1000
1250
Marmara
Island
Kapıdağ
Peninsula
Display grid size: 5 x 5 km
0
20
40 km
(a)

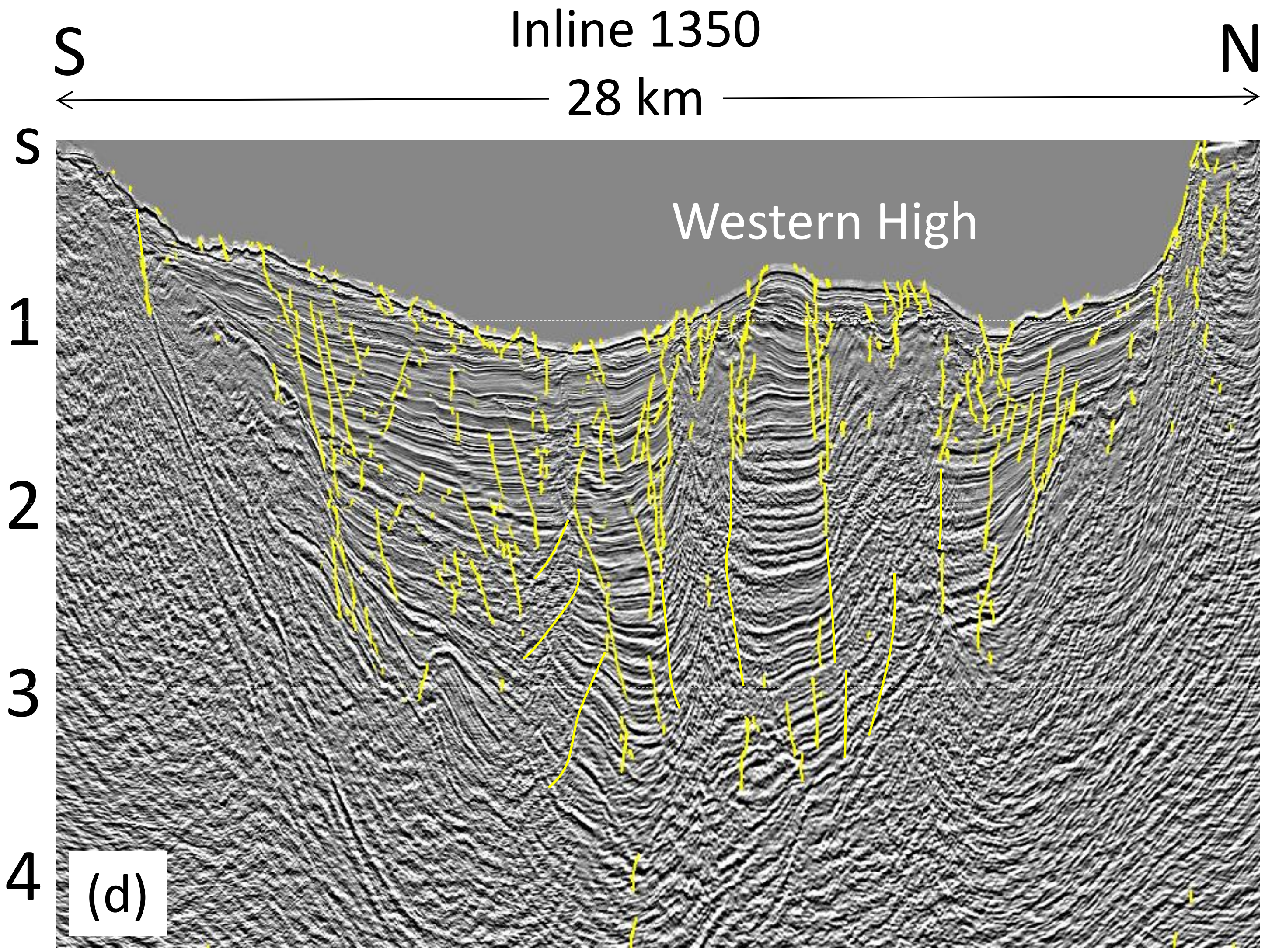
Inline 1350
S
N
28 km
s
1
2
3
4
Western High
(d)

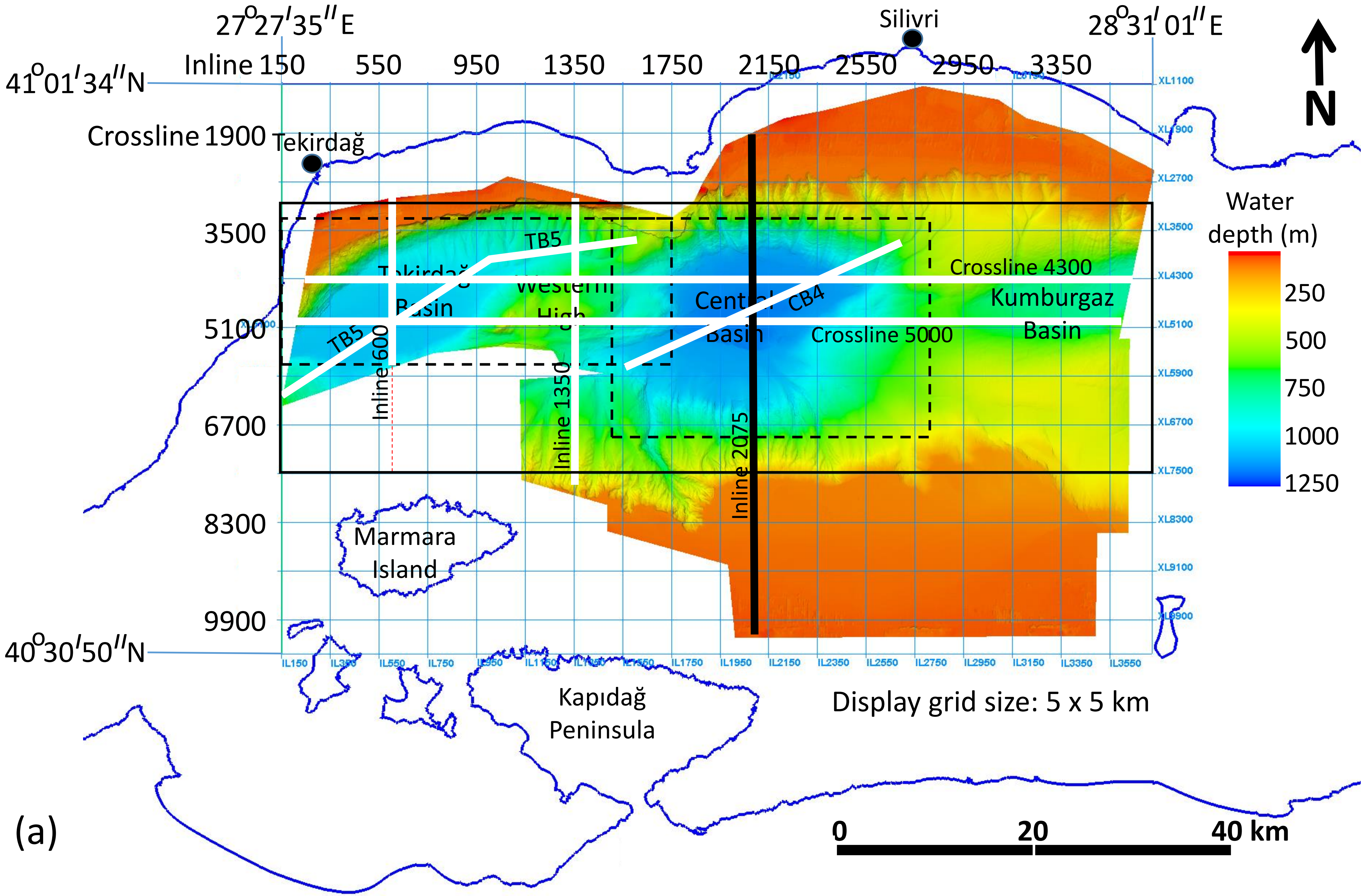

27°27′35″E
Silivri
28°31′01″E
N
41°01′34″N
Inline 150
550
950
1350
1750
2150
2550
2950
3350
Crossline 1900
Tekirdağ
3500
5100
6700
8300
9900
40°30′50″N
TB5
TB5
CB4
Tekirdağ Basin
Western High
Central Basin
Crossline 4300
Crossline 5000
Kumburgaz Basin
Inline 600
Inline 1350
Inline 2075
Water depth (m)
250
500
750
1000
1250
Marmara Island
Kapıdağ Peninsula
Display grid size: 5 x 5 km
0
20
40 km
(a)

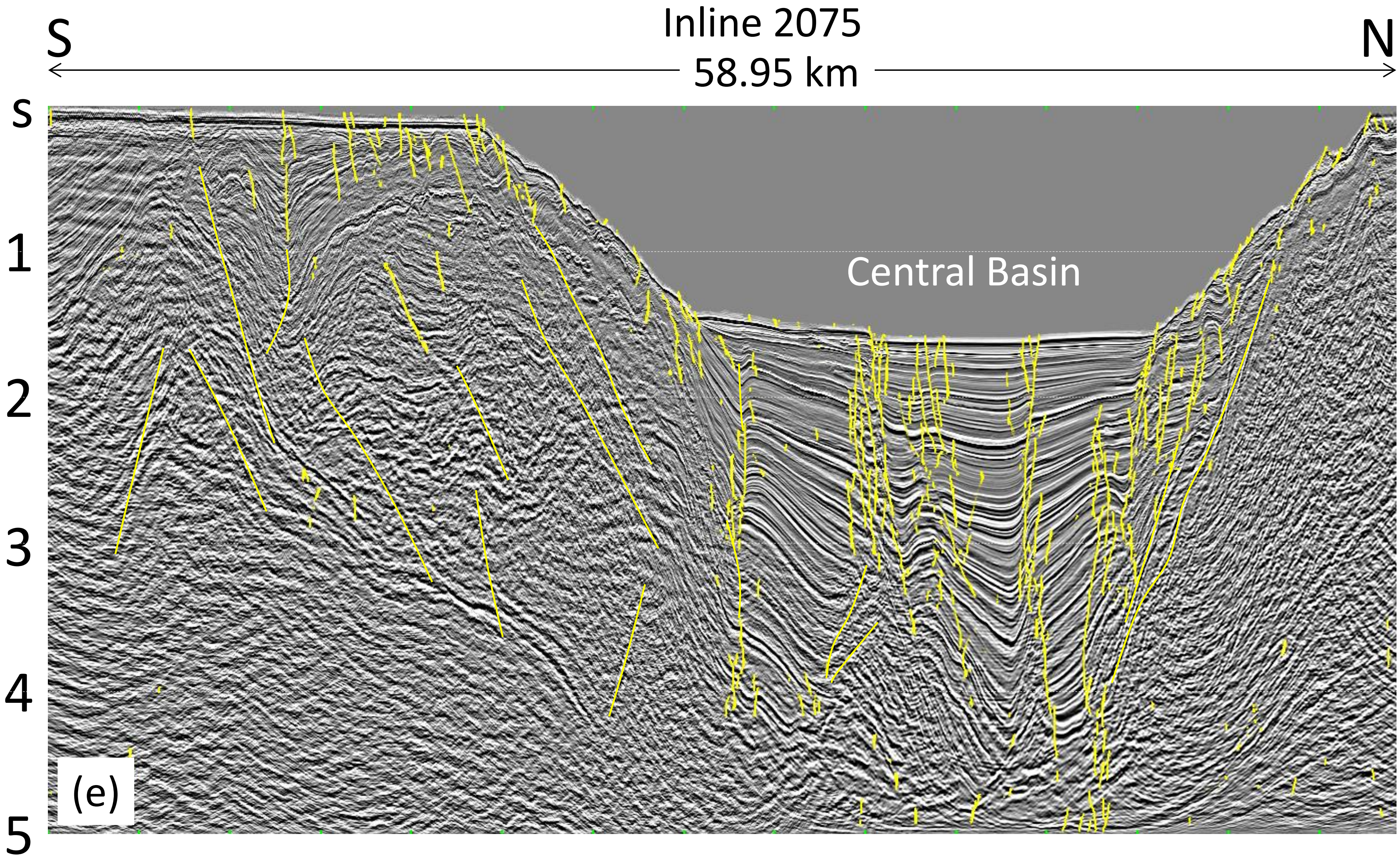
Inline 2075
S
N
58.95 km
s
1
2
3
4
5
Central Basin
(e)

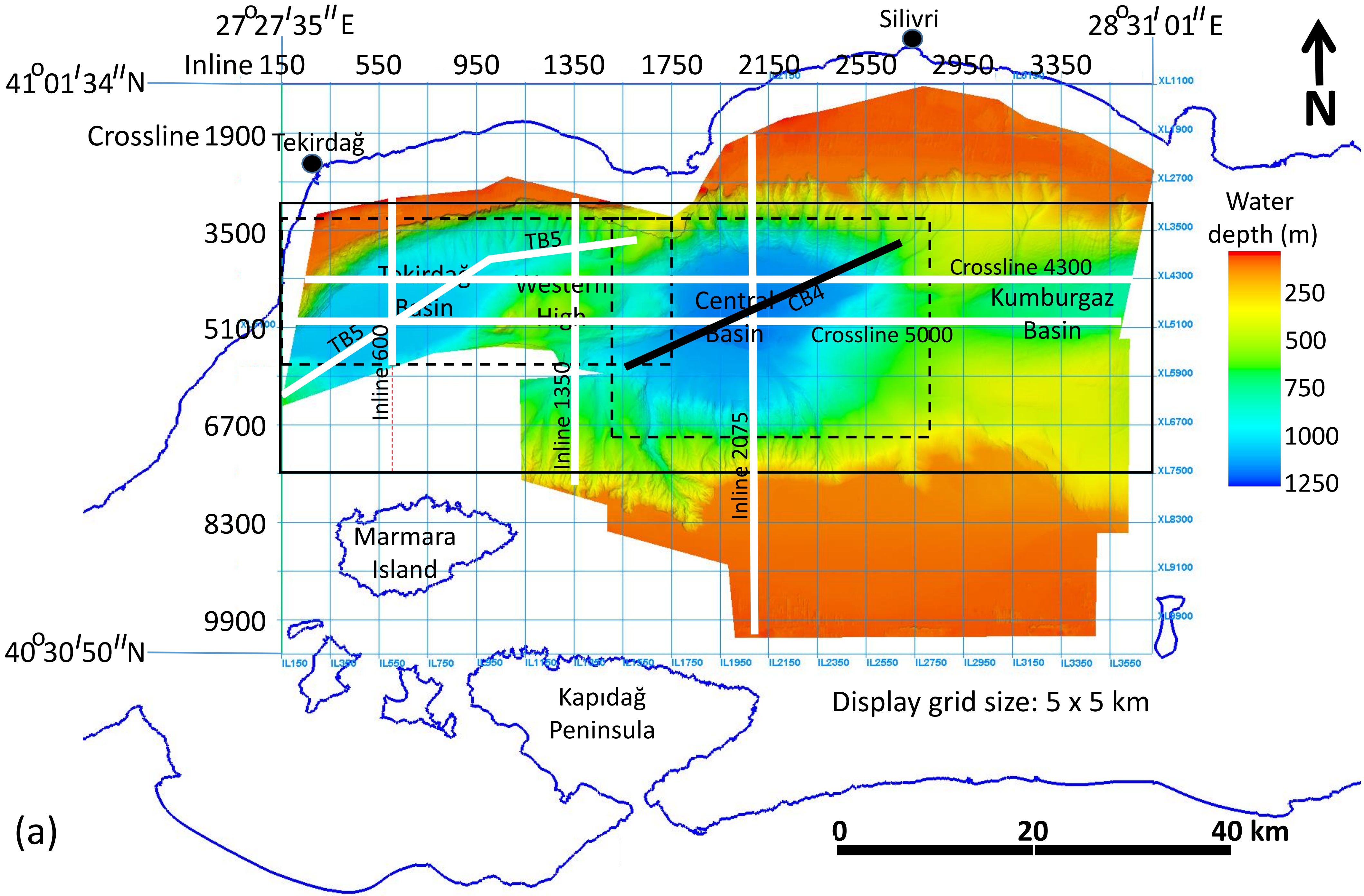
27°27′35″E
Silivri
28°31′01″E
N
41°01′34″N
Inline 150
550
950
1350
1750
2150
2550
2950
3350
Crossline 1900
Tekirdağ
3500
5100
6700
8300
9900
40°30′50″N
TB5
Tekirdağ Basin
Western High
Central Basin
CB4
Crossline 4300
Kumburgaz Basin
Crossline 5000
Inline 600
Inline 1350
Inline 2075
Water depth (m)
250
500
750
1000
1250
Marmara Island
Kapıdağ Peninsula
Display grid size: 5 x 5 km
0
20
40 km
(a)

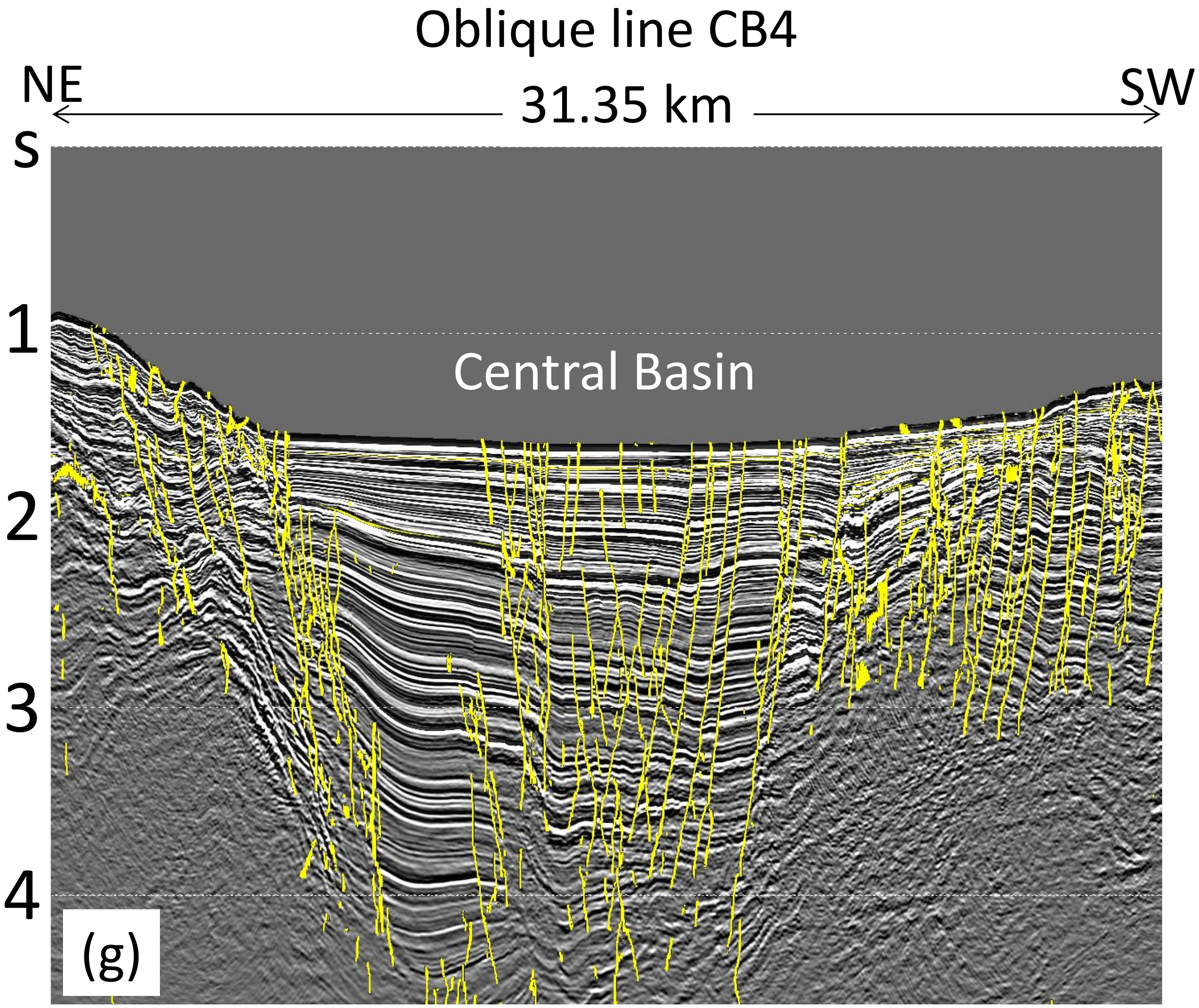

Oblique line CB4
NE
31.35 km
SW
s
1
2
3
4
Central Basin
(g)

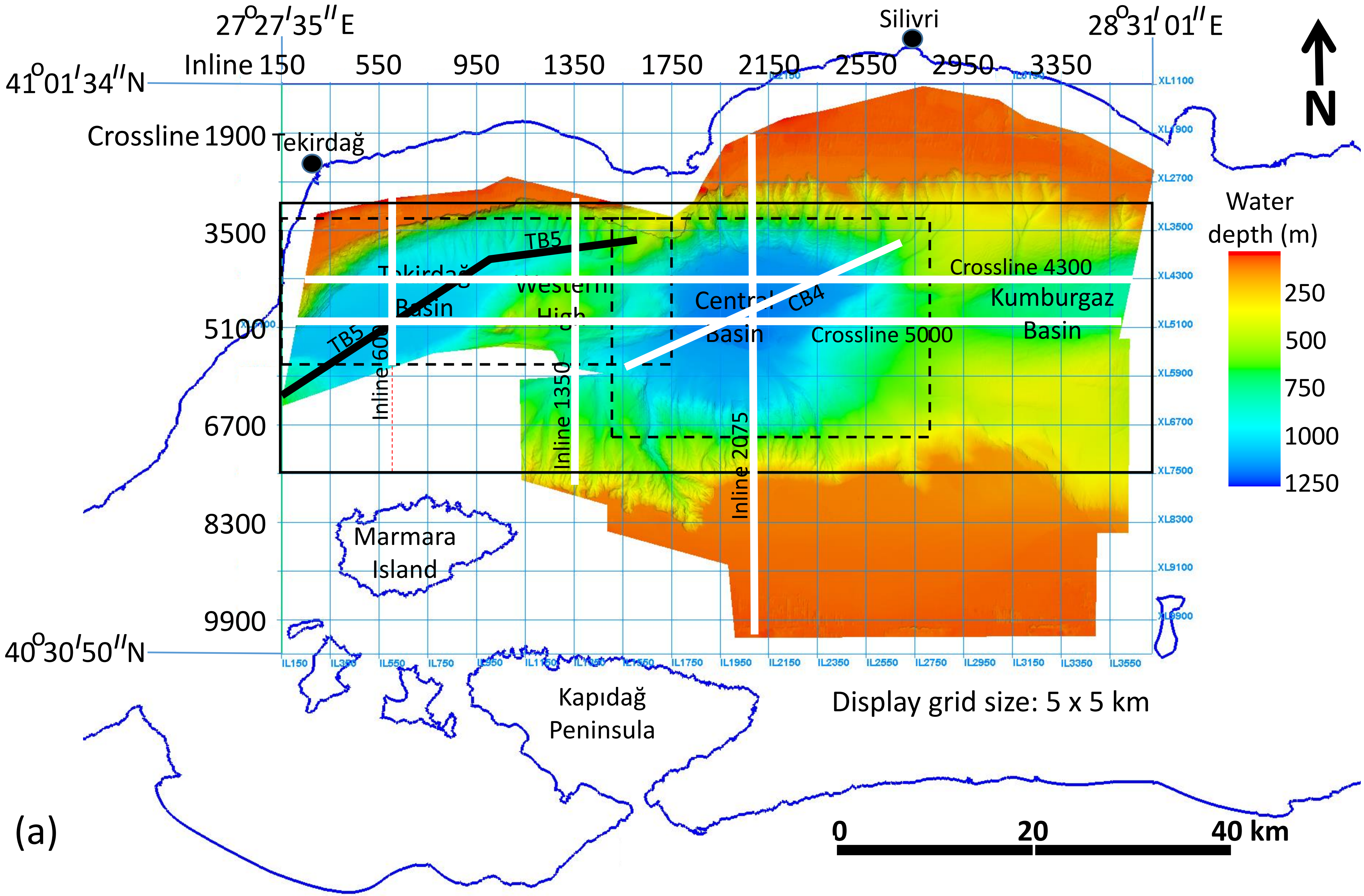

27°27′35″E
Silivri
28°31′01″E
N
Inline 150
550
950
1350
1750
2150
2550
2950
3350
41°01′34″N
Crossline 1900
Tekirdağ
3500
5100
6700
8300
9900
40°30′50″N
TB5
Tekirdağ Basin
Western High
Central Basin
CB4
Crossline 4300
Kumburgaz Basin
Crossline 5000
Inline 600
Inline 1350
Inline 2075
Water depth (m)
250
500
750
1000
1250
Marmara Island
Kapıdağ Peninsula
Display grid size: 5 x 5 km
0
20
40 km
(a)

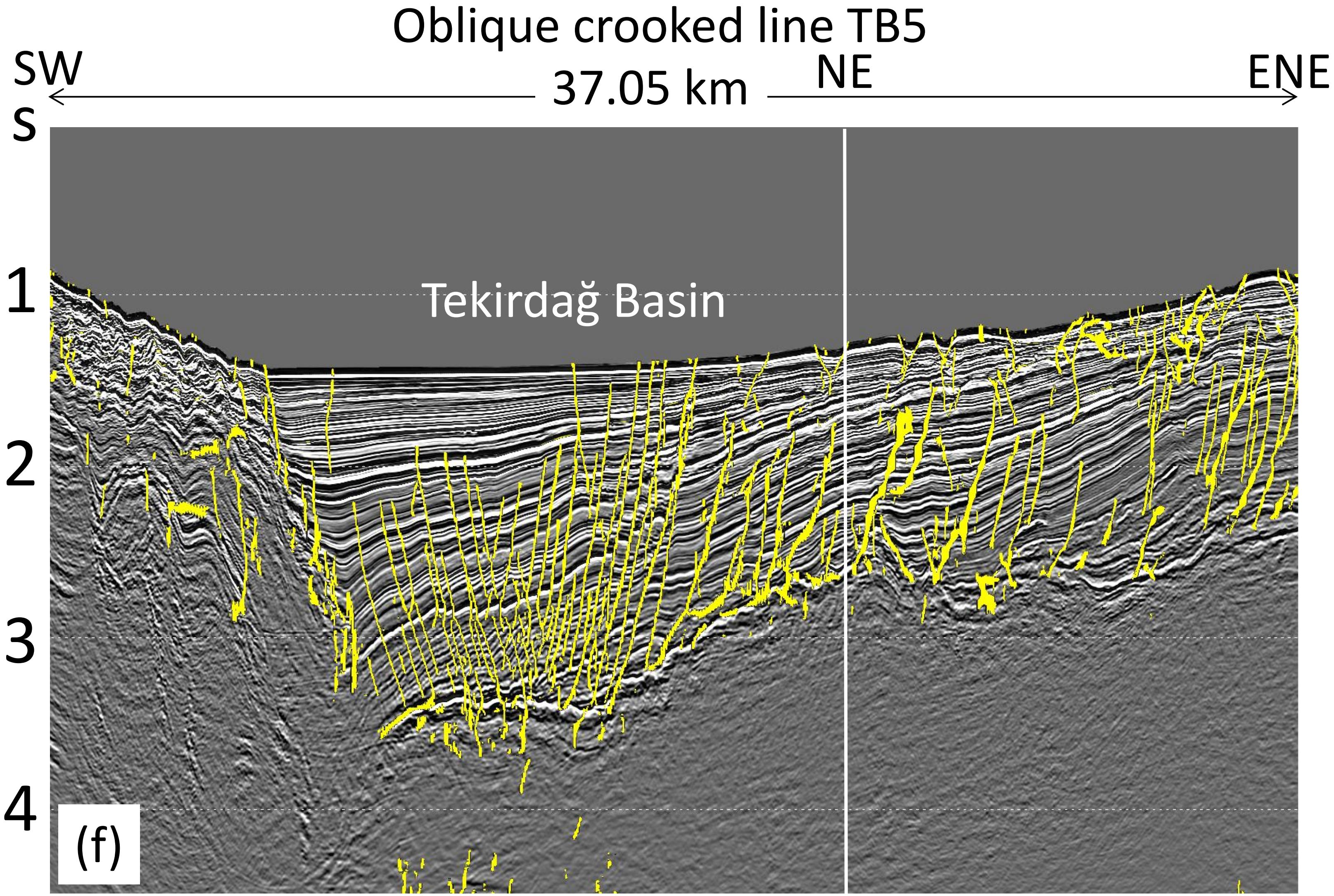
Oblique crooked line TB5
SW
S
37.05 km
NE
ENE
1
2
3
4
Tekirdağ Basin
(f)

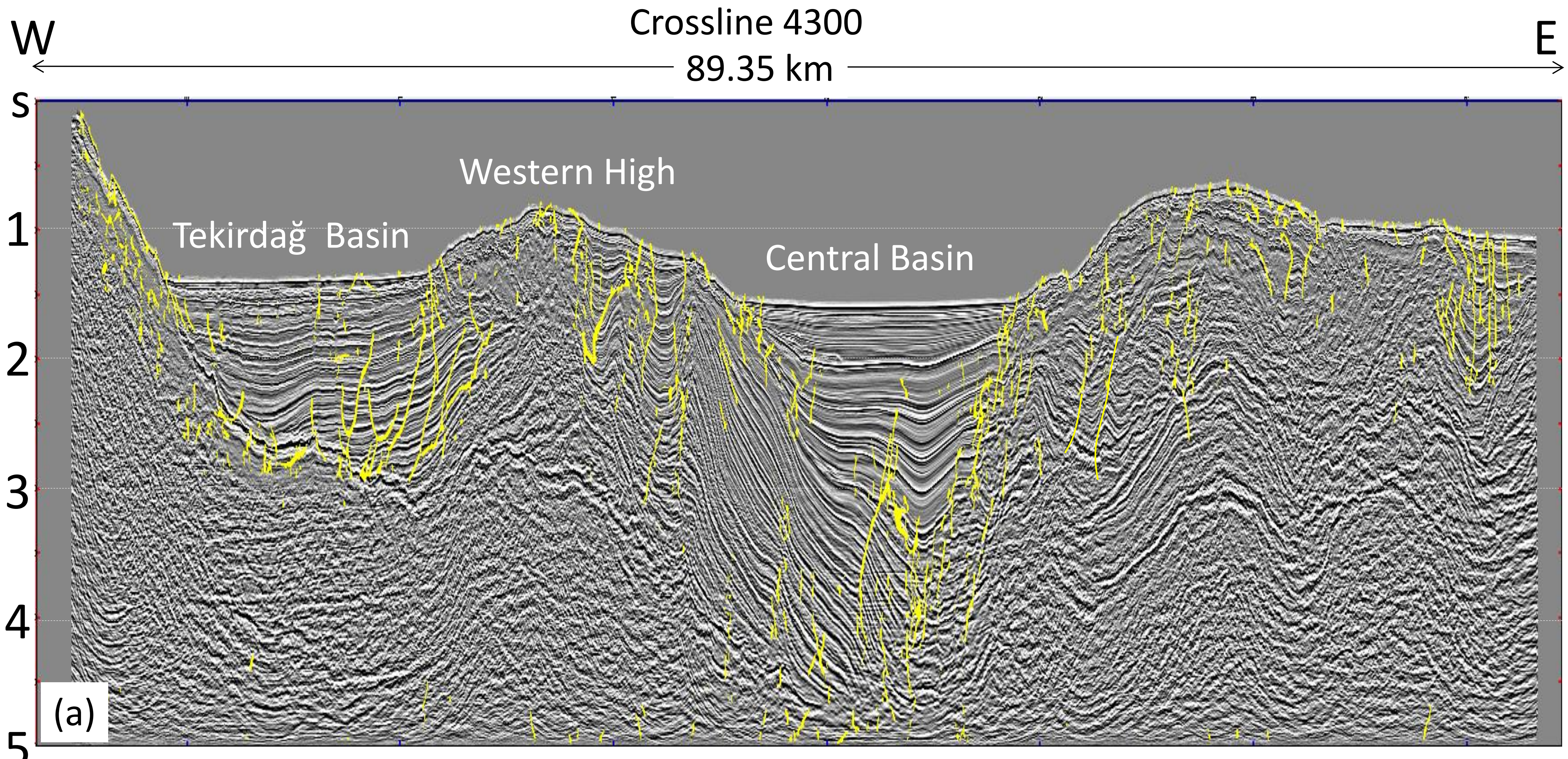

Crossline 4300
W
E
89.35 km
s
1
2
3
4
5
Western High
Tekirdağ Basin
Central Basin
(a)

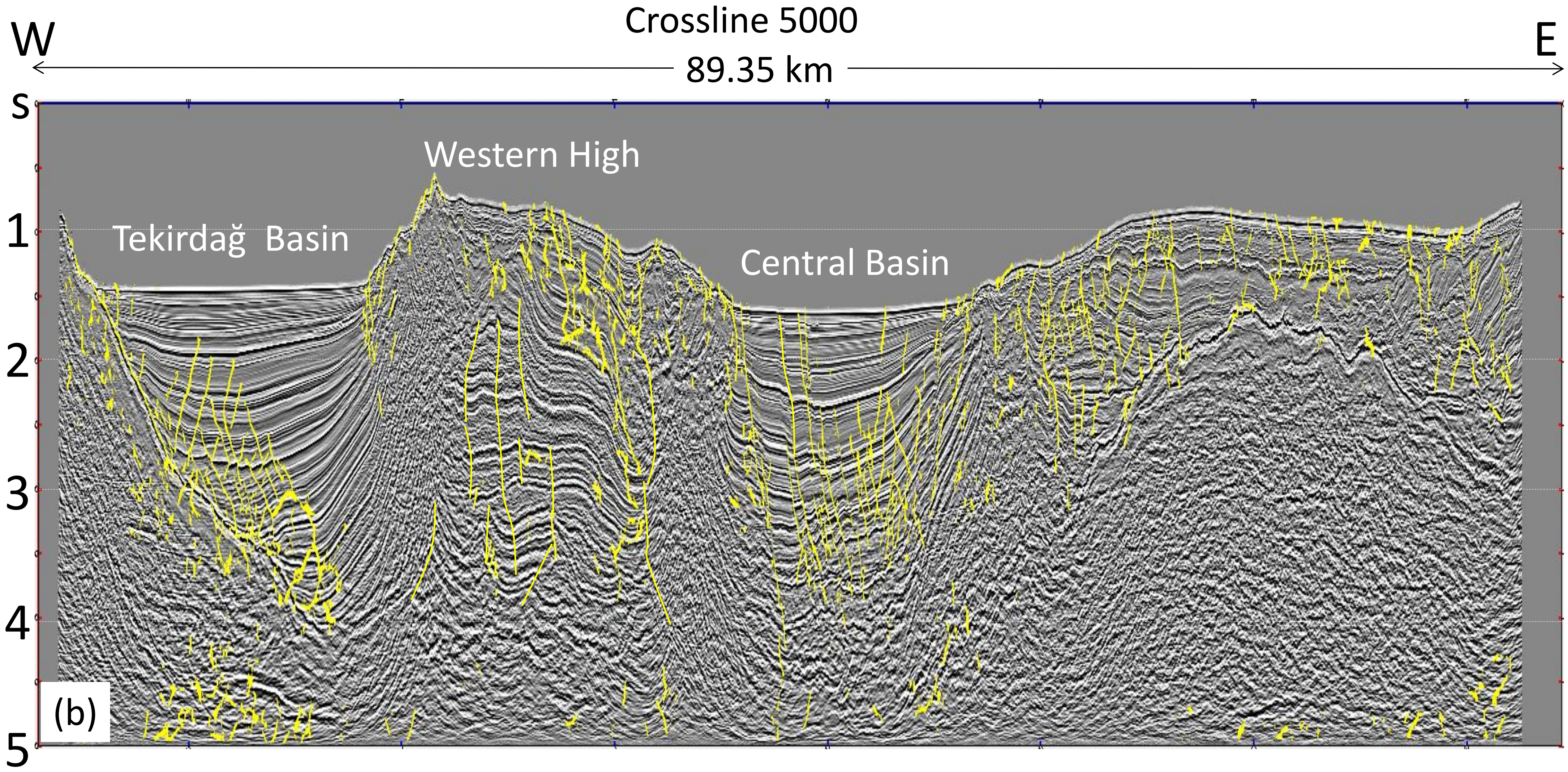

Crossline 5000
W
E
89.35 km
s
1
2
3
4
5
Western High
Tekirdağ Basin
Central Basin
(b)

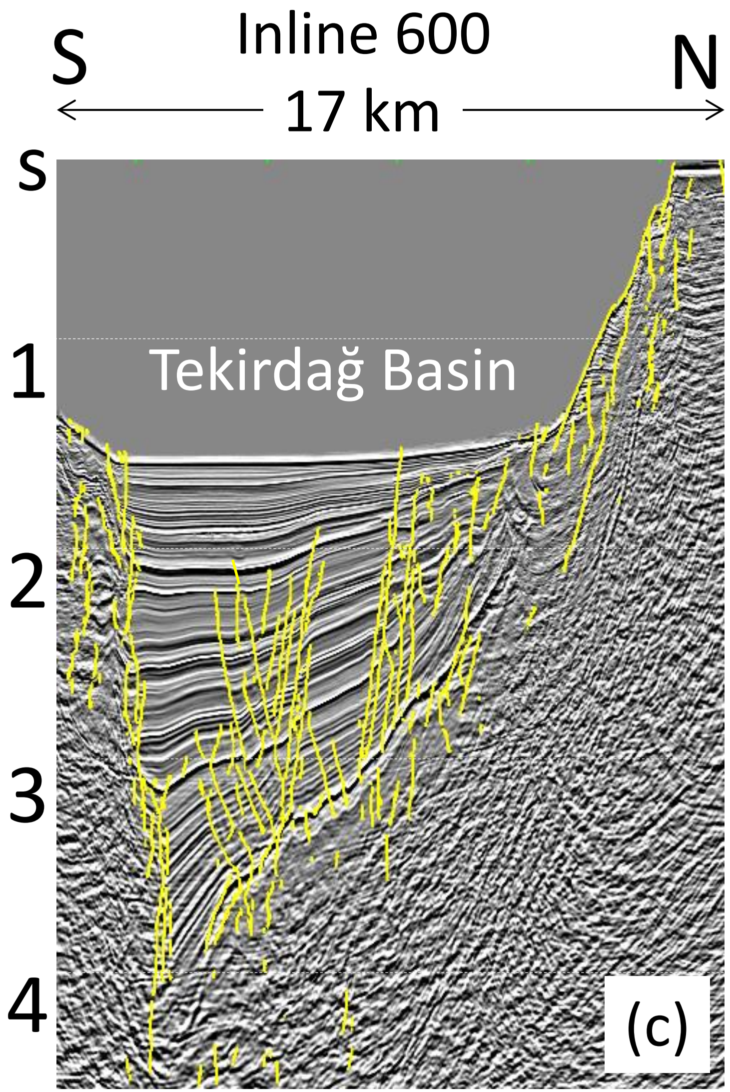

Inline 600
S
N
17 km
s
1
2
3
4
Tekirdağ Basin
(c)

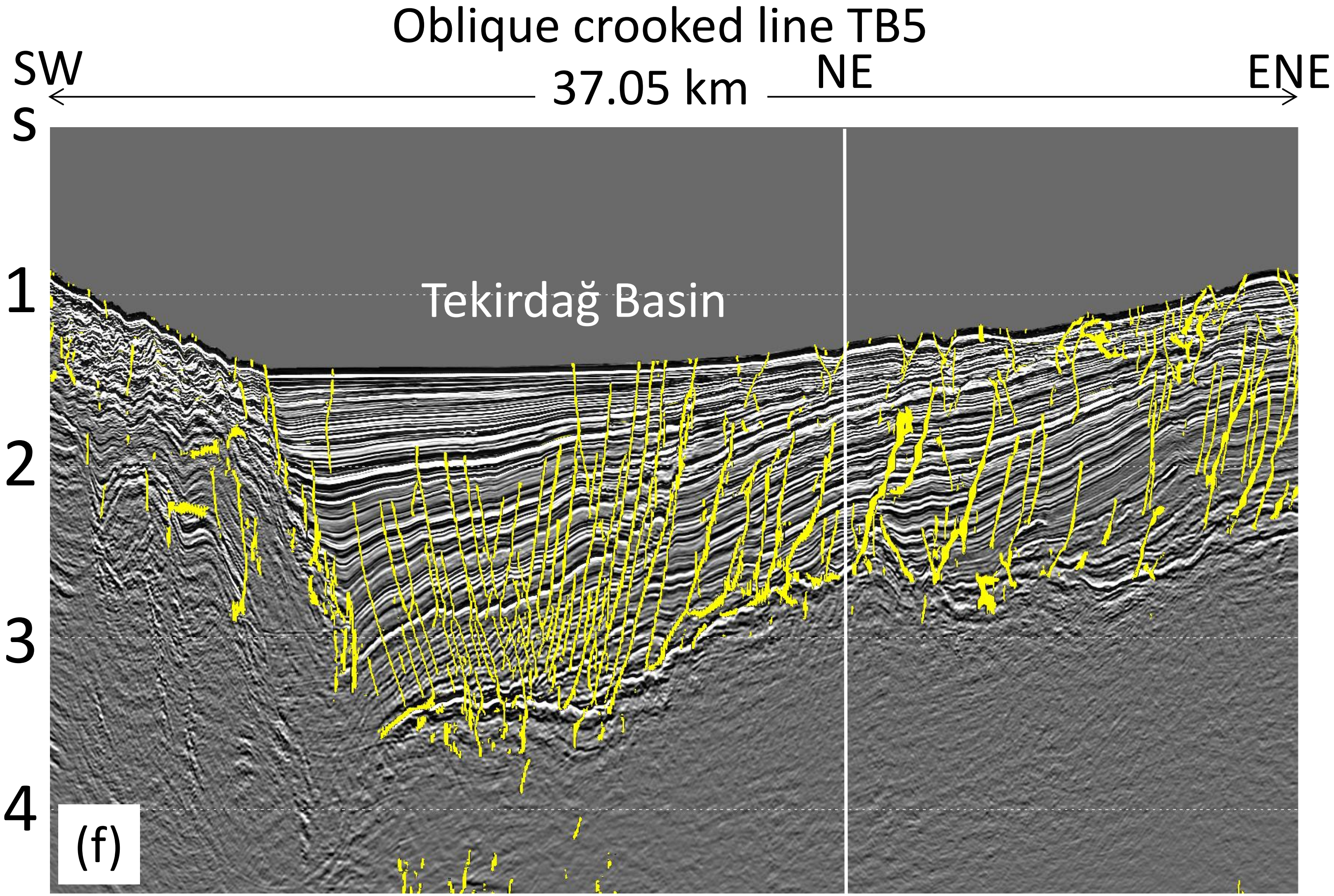
Oblique crooked line TB5
SW
37.05 km
NE
ENE
S
1
2
3
4
Tekirdağ Basin
(f)

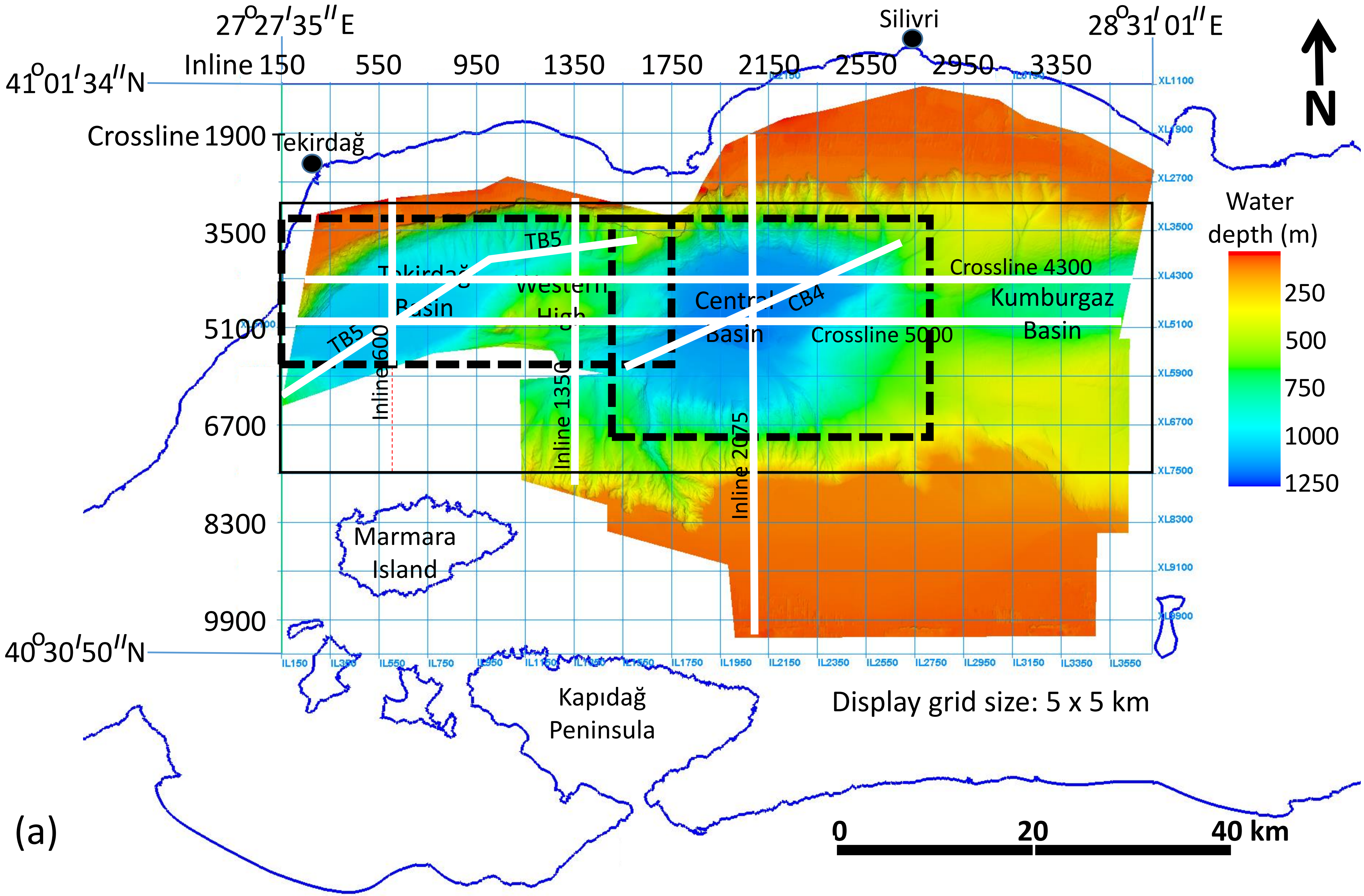
27°27′35″E
Silivri
28°31′01″E
N
Inline 150
550
950
1350
1750
2150
2550
2950
3350
41°01′34″N
Crossline 1900
Tekirdağ
3500
5100
6700
8300
9900
40°30′50″N
TB5
Tekirdağ Basin
Western High
Central Basin
CB4
Crossline 4300
Kumburgaz Basin
Crossline 5000
Inline 600
Inline 1350
Inline 2075
Water depth (m)
250
500
750
1000
1250
Marmara Island
Kapıdağ Peninsula
Display grid size: 5 x 5 km
0
20
40 km
(a)

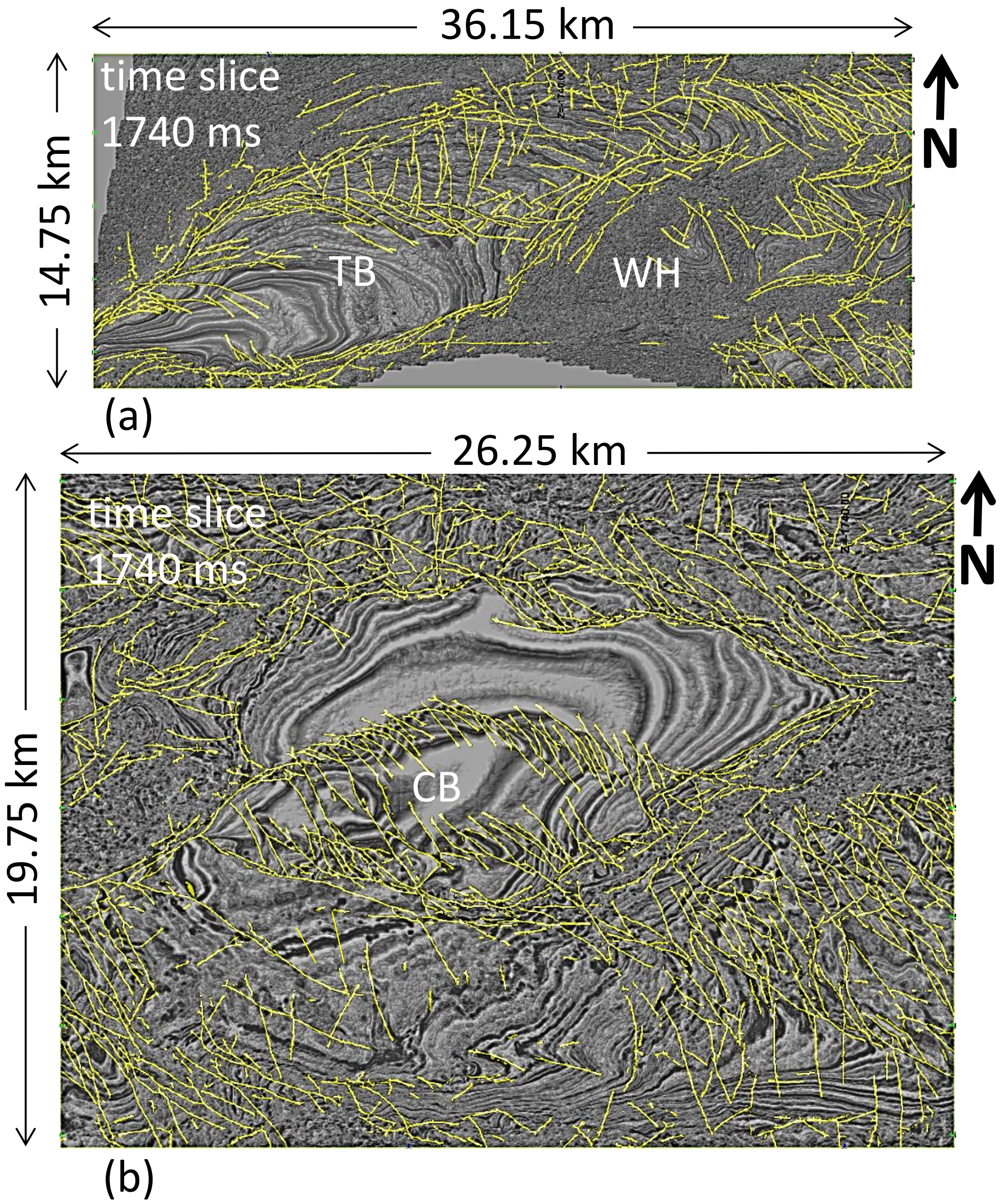
36.15 km
14.75 km
time slice
1740 ms
N
TB
WH
(a)
26.25 km
19.75 km
time slice
1740 ms
N
CB
(b)

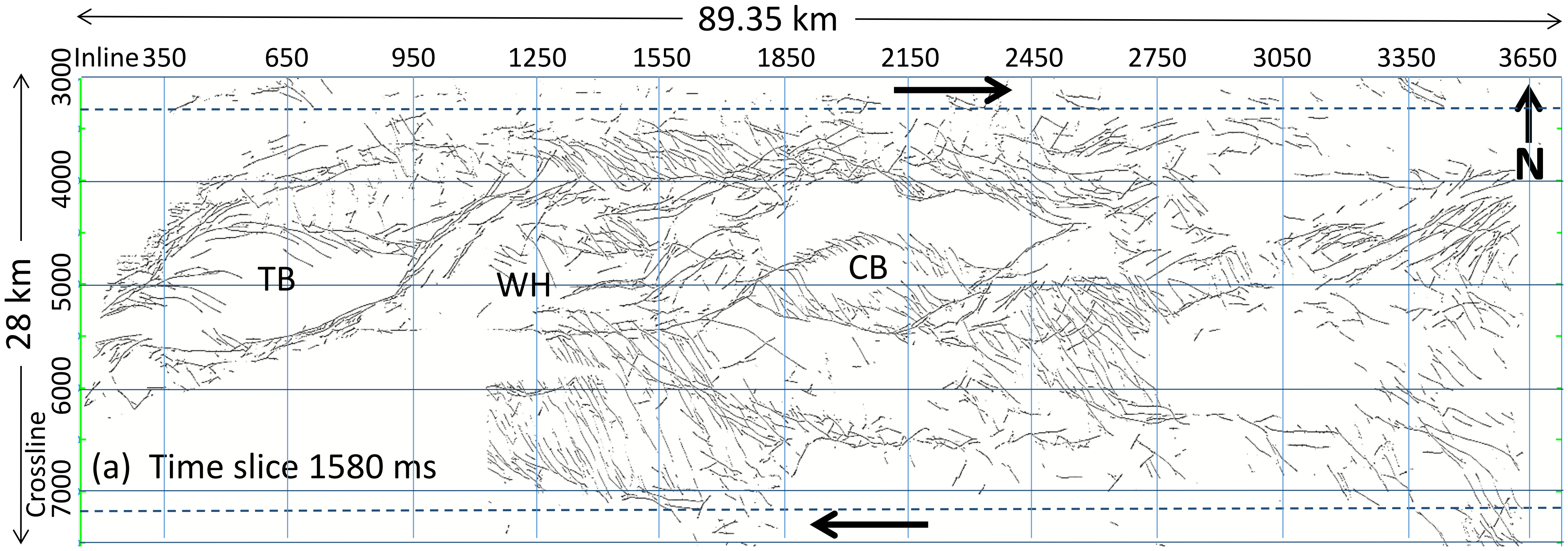
89.35 km
Inline 350
650
950
1250
1550
1850
2150
2450
2750
3050
3350
3650
N
28 km
Crossline
3000
4000
5000
6000
7000
TB
WH
CB
(a) Time slice 1580 ms

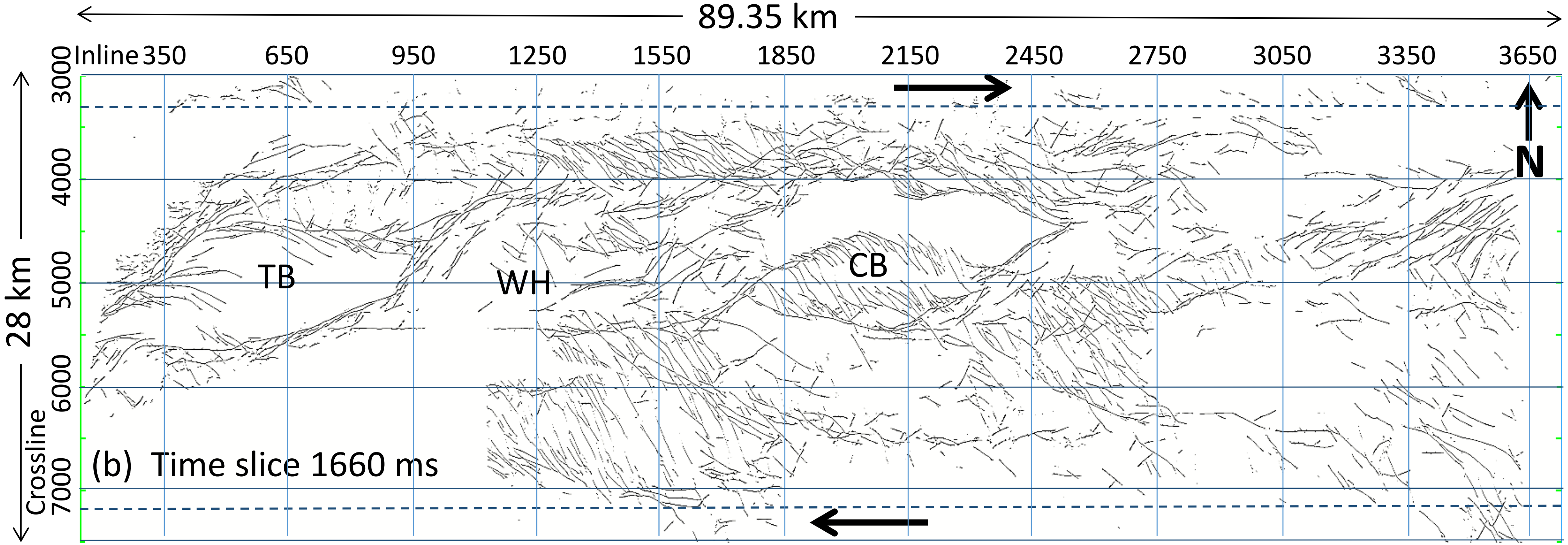
89.35 km
Inline 350
650
950
1250
1550
1850
2150
2450
2750
3050
3350
3650
3000
4000
5000
6000
7000
Crossline
28 km
N
TB
WH
CB
(b) Time slice 1660 ms

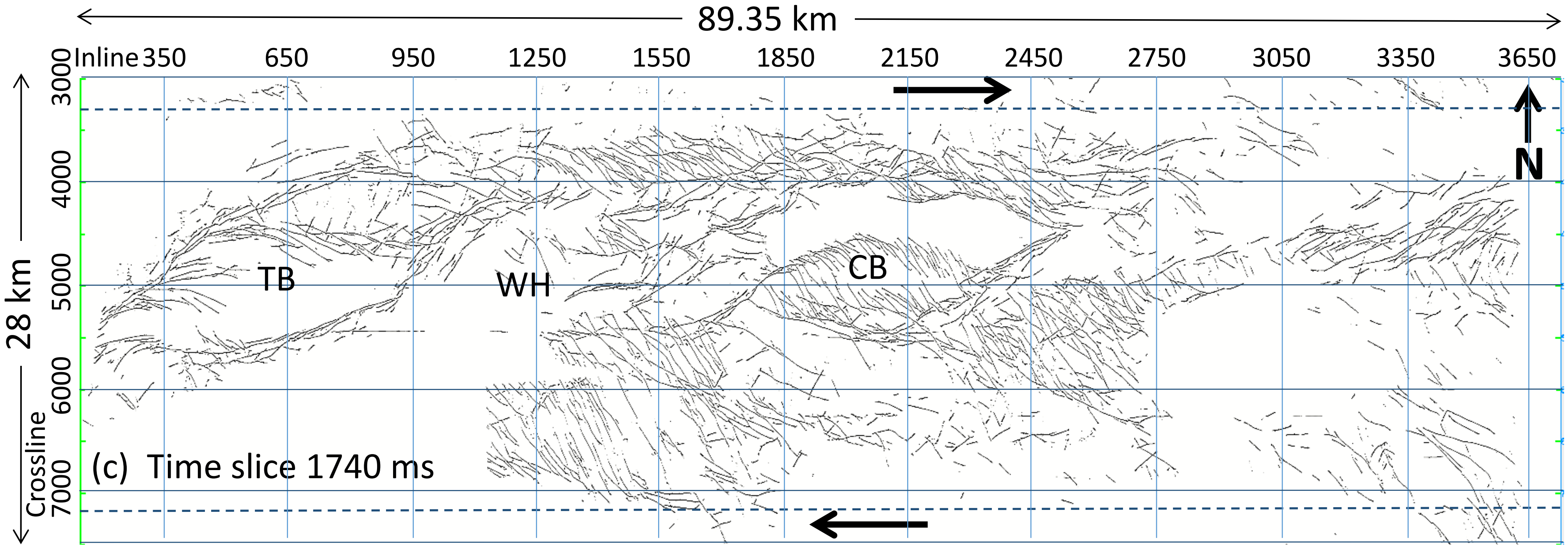
89.35 km
Inline 350
650
950
1250
1550
1850
2150
2450
2750
3050
3350
3650
3000
4000
5000
6000
7000
Crossline
28 km
N
TB
WH
CB
(c) Time slice 1740 ms

sandbox modeling of releasing stepovers in basement strike-slip faults that lead to the formation of pull-apart basins

30-degree releasing stepover

early stage

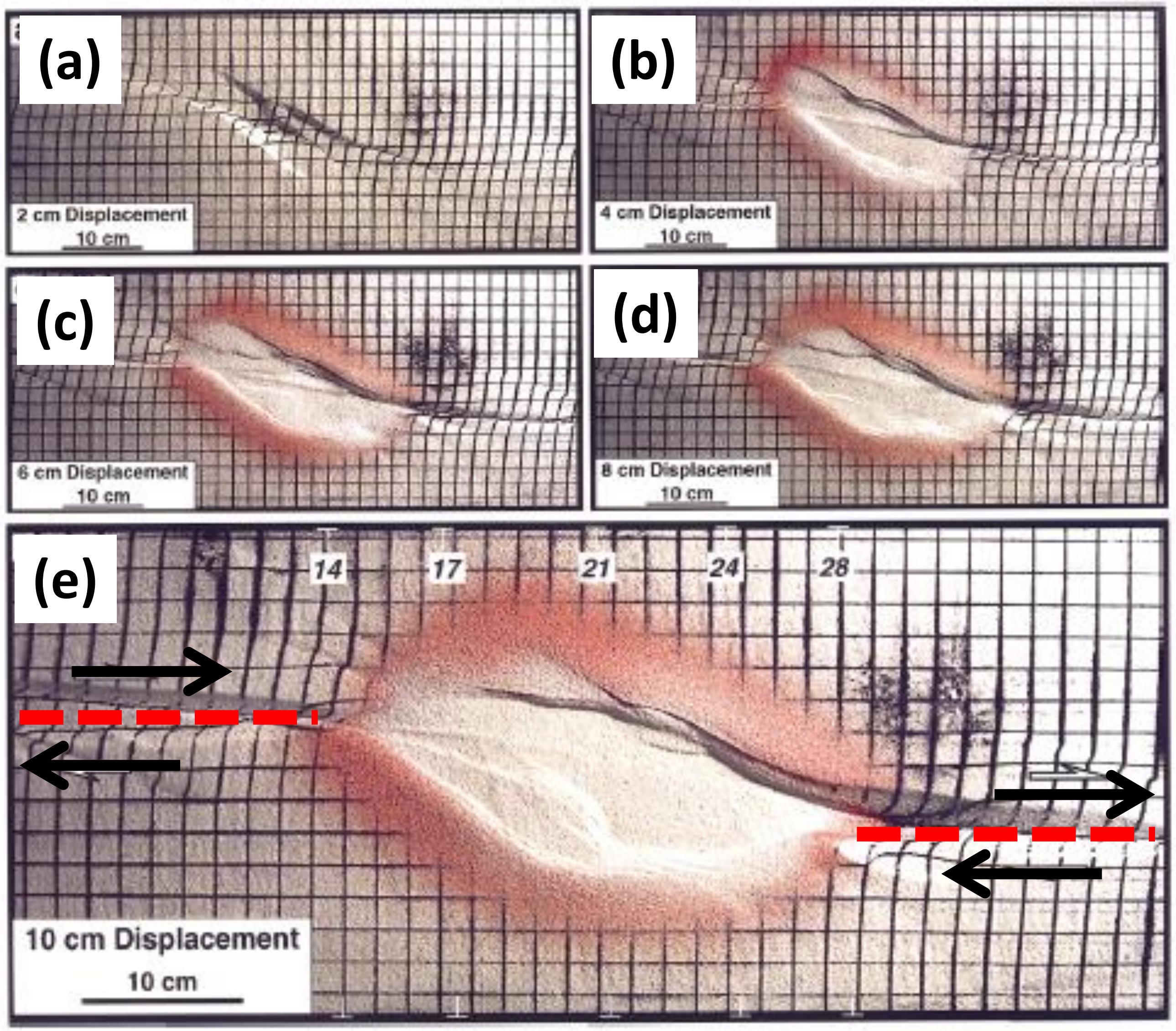


final stage

Basement strike-slip fault pair

(Dooley and McClay, 1997)

# Scaled sandbox modeling of restraining stepovers in basement strike-slip faults that lead to the formation of pop-up structures

## No sedimentation 30-deg underlapping restraining stepover

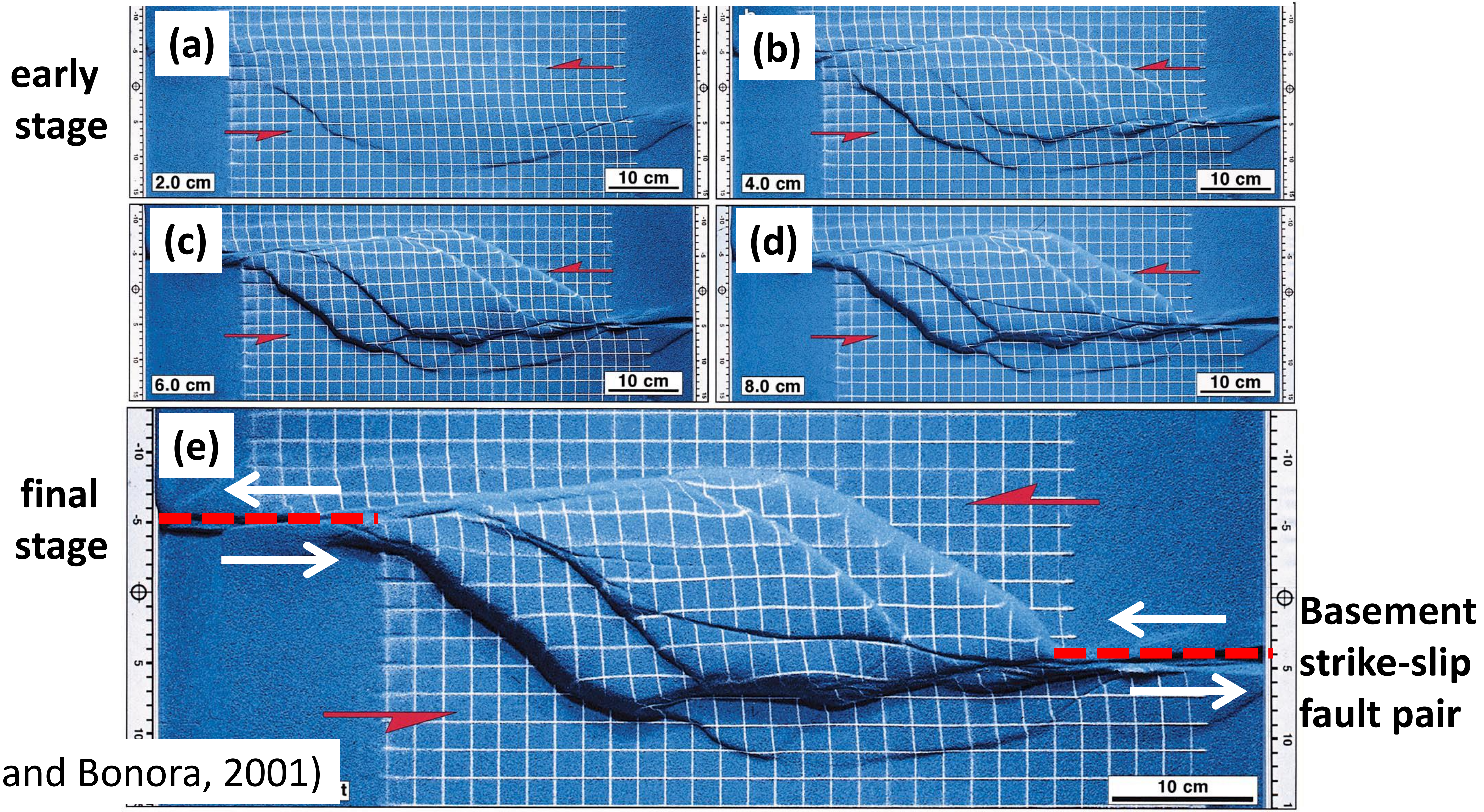


(McClay and Bonora, 2001)

transtensional pull-apart basin formed by the basement strike-slip fault pair A and B

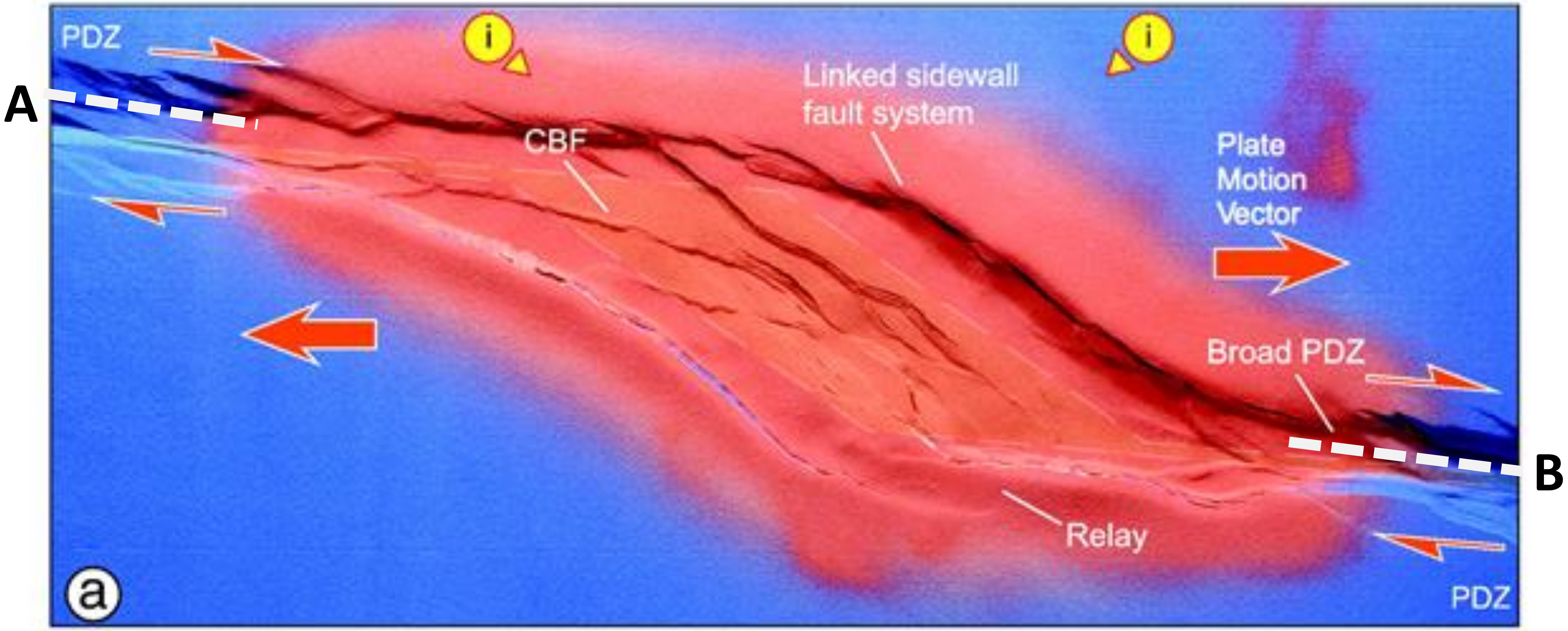


(Dooley and Schreurs, 2012)

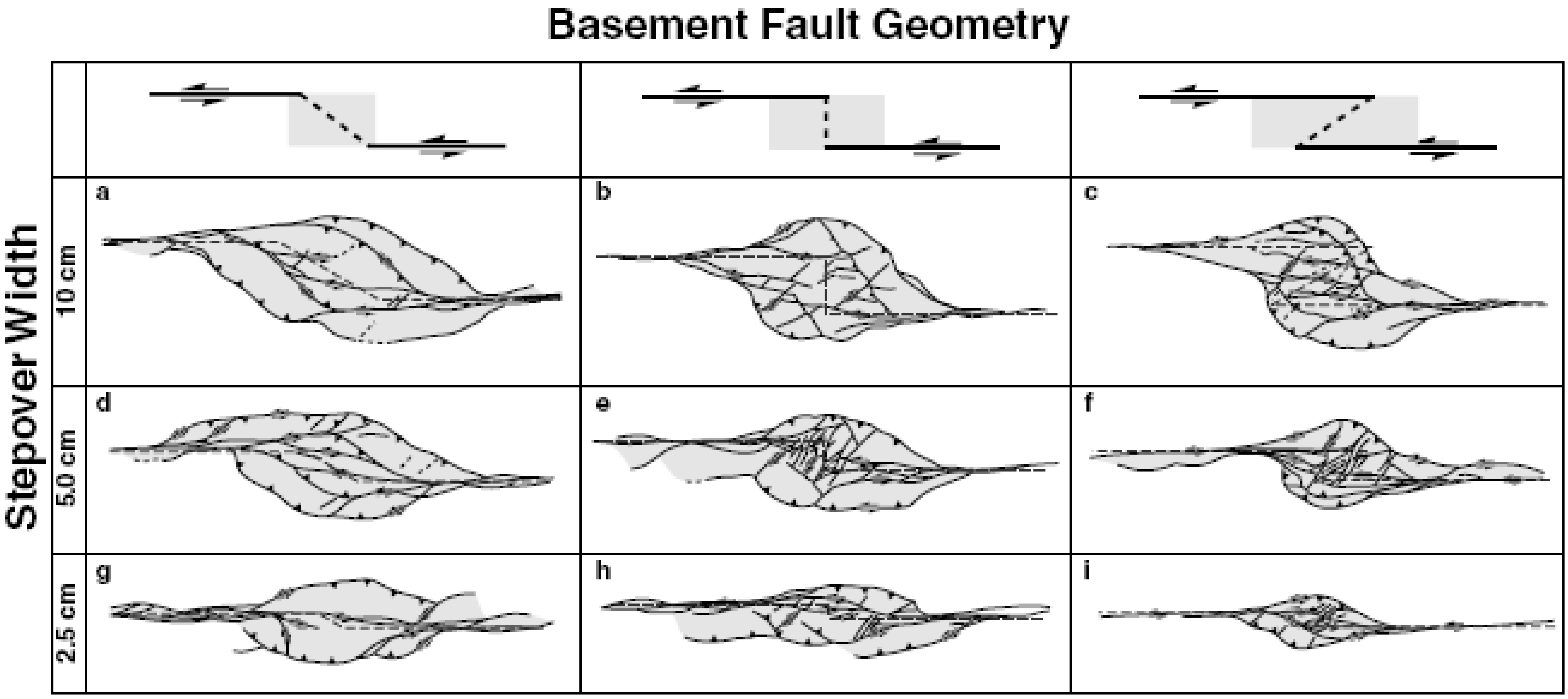


**(McClay and Bonora, 2001)**

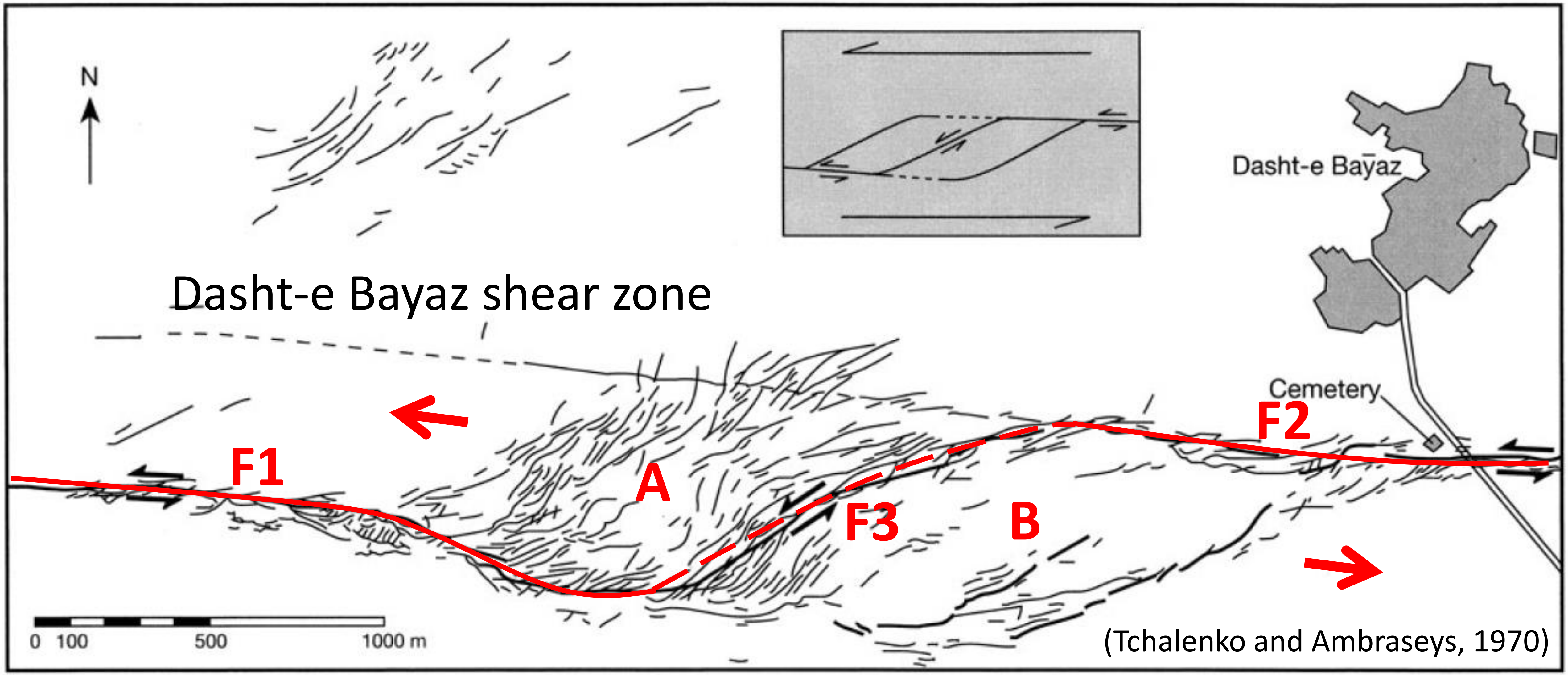

N
Dasht-e Bayaz shear zone
Dasht-e Bayaz
Cemetery
F1
F2
F3
A
B
0 100 500 1000 m
(Tchalenko and Ambraseys, 1970)

**A pair of sinistral strike-slip basement fault segments along the EAFZ with contractional stepover that gave rise to the formation of Bingöl pop-up structure**

**(Courtesy Nuretdin Kaymakçı, 2025)**

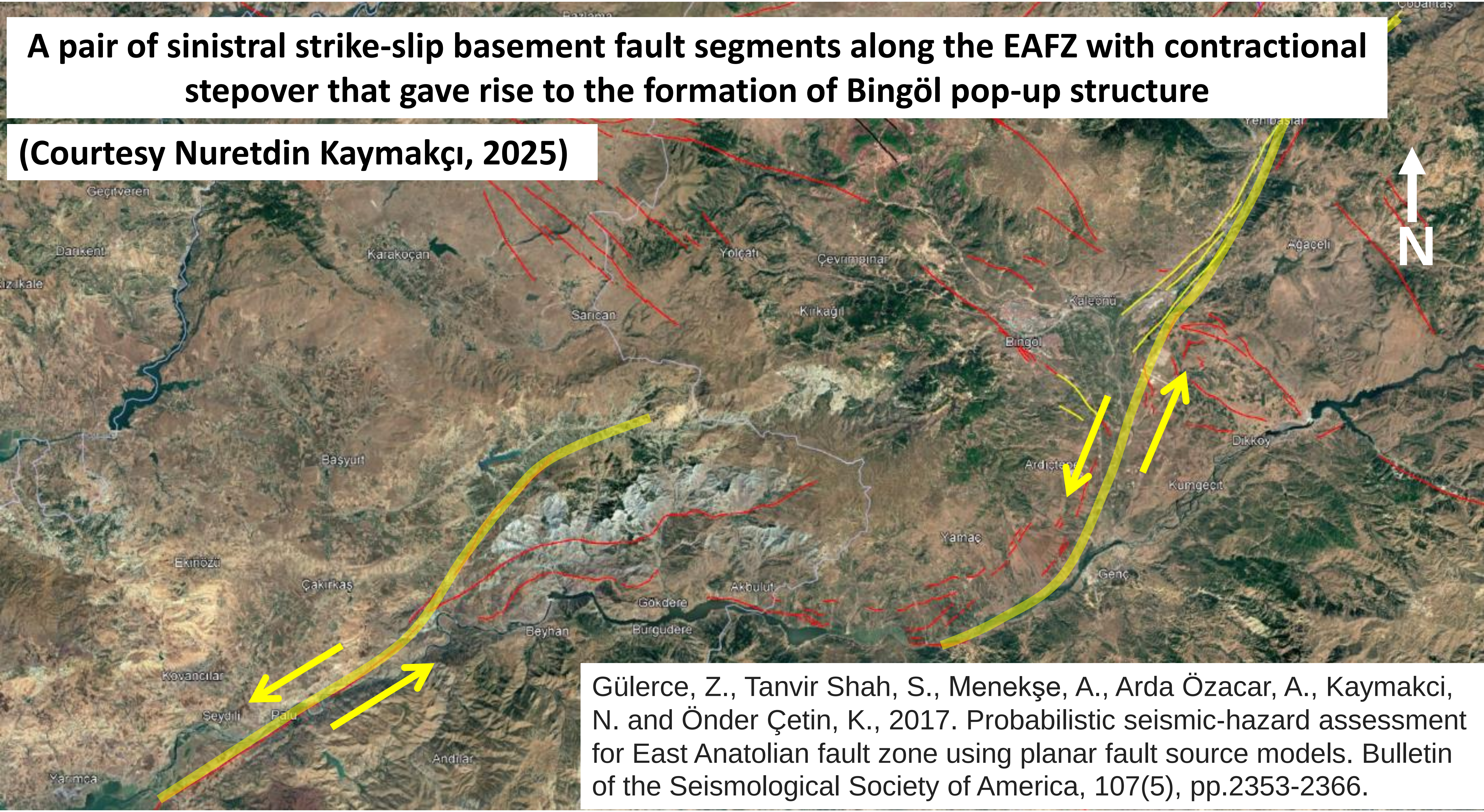


Gülerce, Z., Tanvir Shah, S., Menekşe, A., Arda Özacar, A., Kaymakci, N. and Önder Çetin, K., 2017. Probabilistic seismic-hazard assessment for East Anatolian fault zone using planar fault source models. Bulletin of the Seismological Society of America, 107(5), pp.2353-2366.

# A pair of dextral strike-slip basement fault segments along the NAFZ with extensional stepover that gave rise to the formation of Niksar Basin

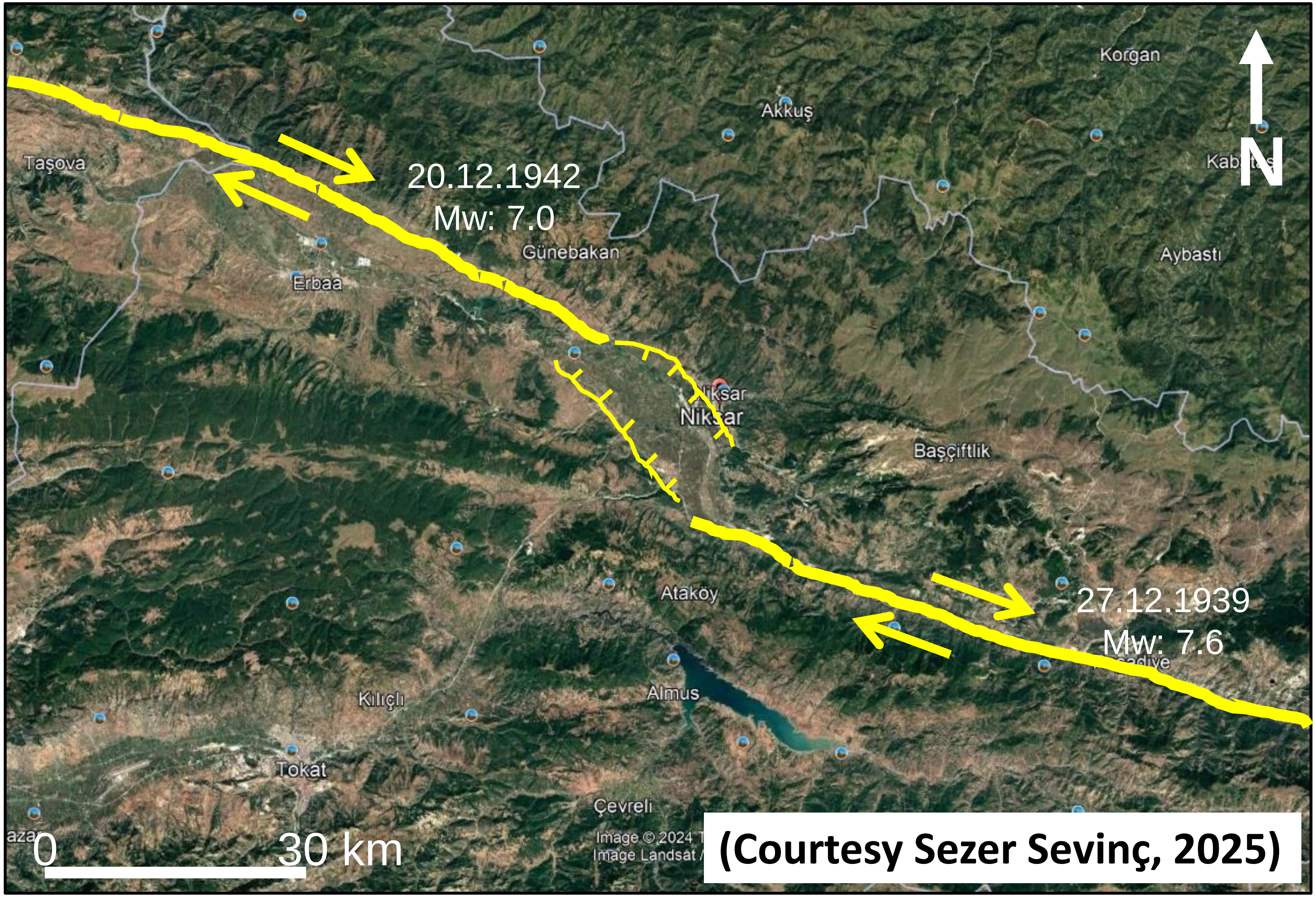

# A pair of dextral strike-slip basement fault segments along the NAFZ with extensional stepover that gave rise to the formation of Mudurnu Basin

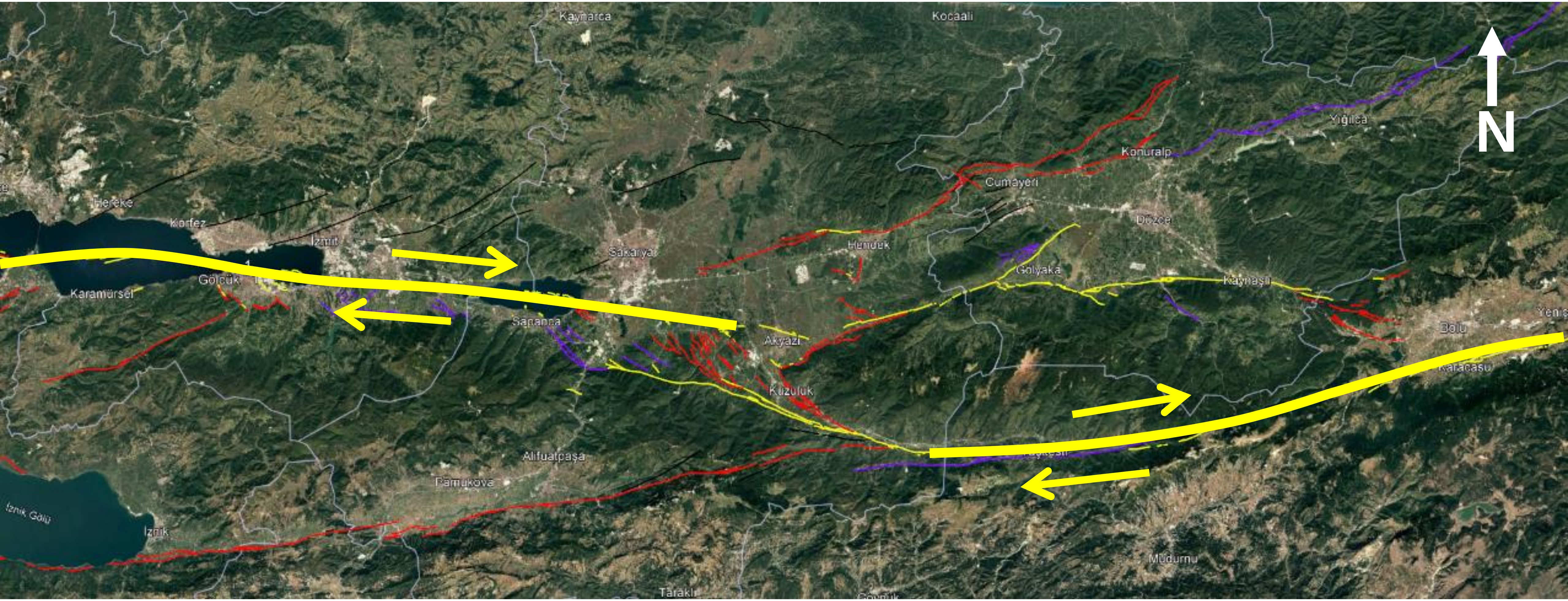


Emre, Ö., Duman, T.Y., Özalp, S., Şaroğlu, F., Olgun, Ş., Elmacı, H. and Çan, T., 2018. Active fault database of Turkey. Bulletin of Earthquake Engineering, 16(8), pp.3229-3275.

**(Courtesy Nuretdin Kaymakçı, 2025)**

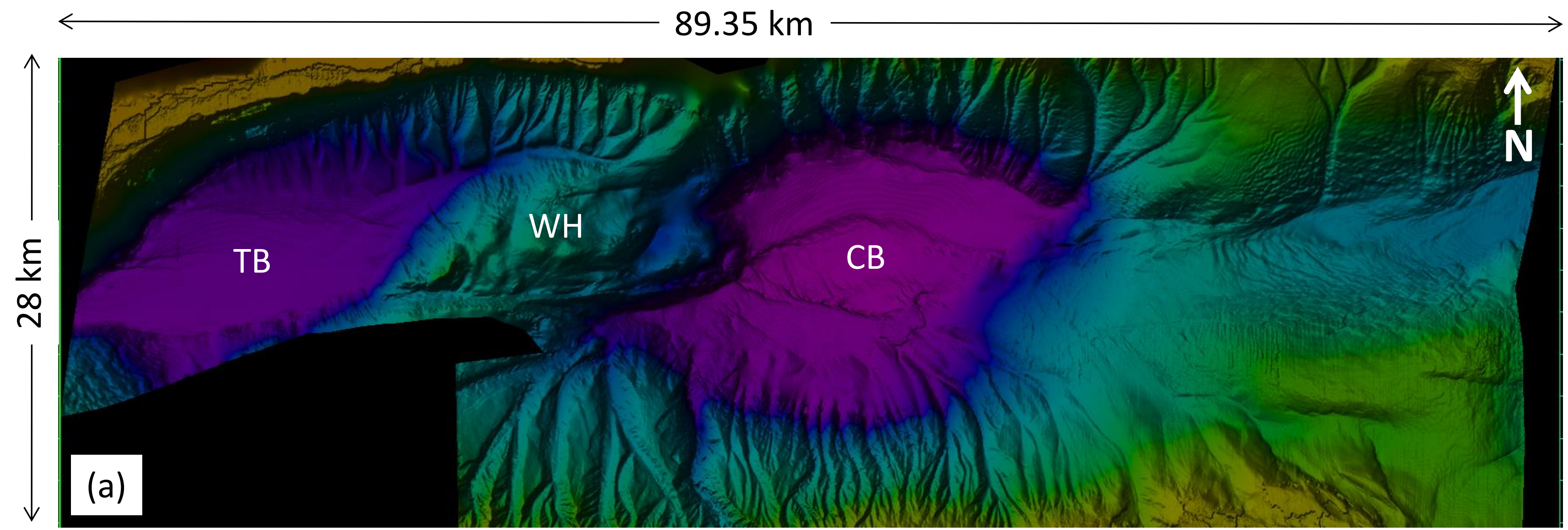


Structural template for a transtensional basin

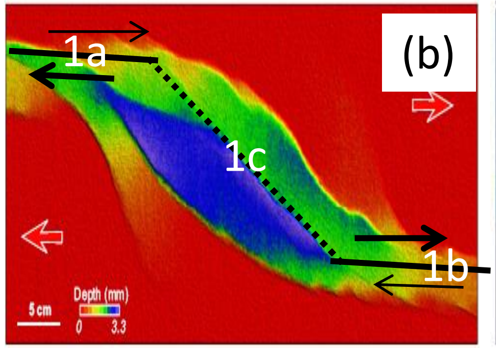


(Wu et al., 2009)

Structural template for a pop-up structure

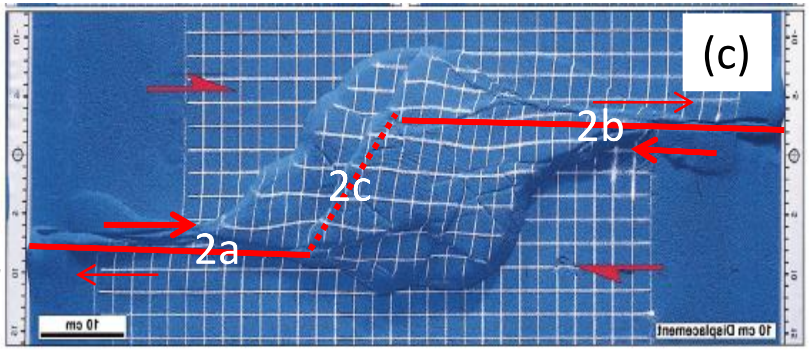


(McClay and Bonora, 2001)

Structural template for a pull-apart basin

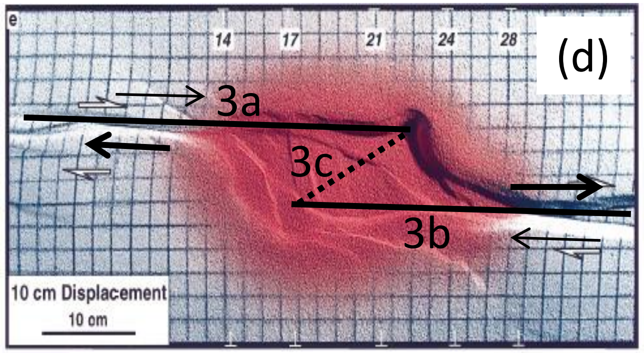


(Dooley and McClay, 1997)

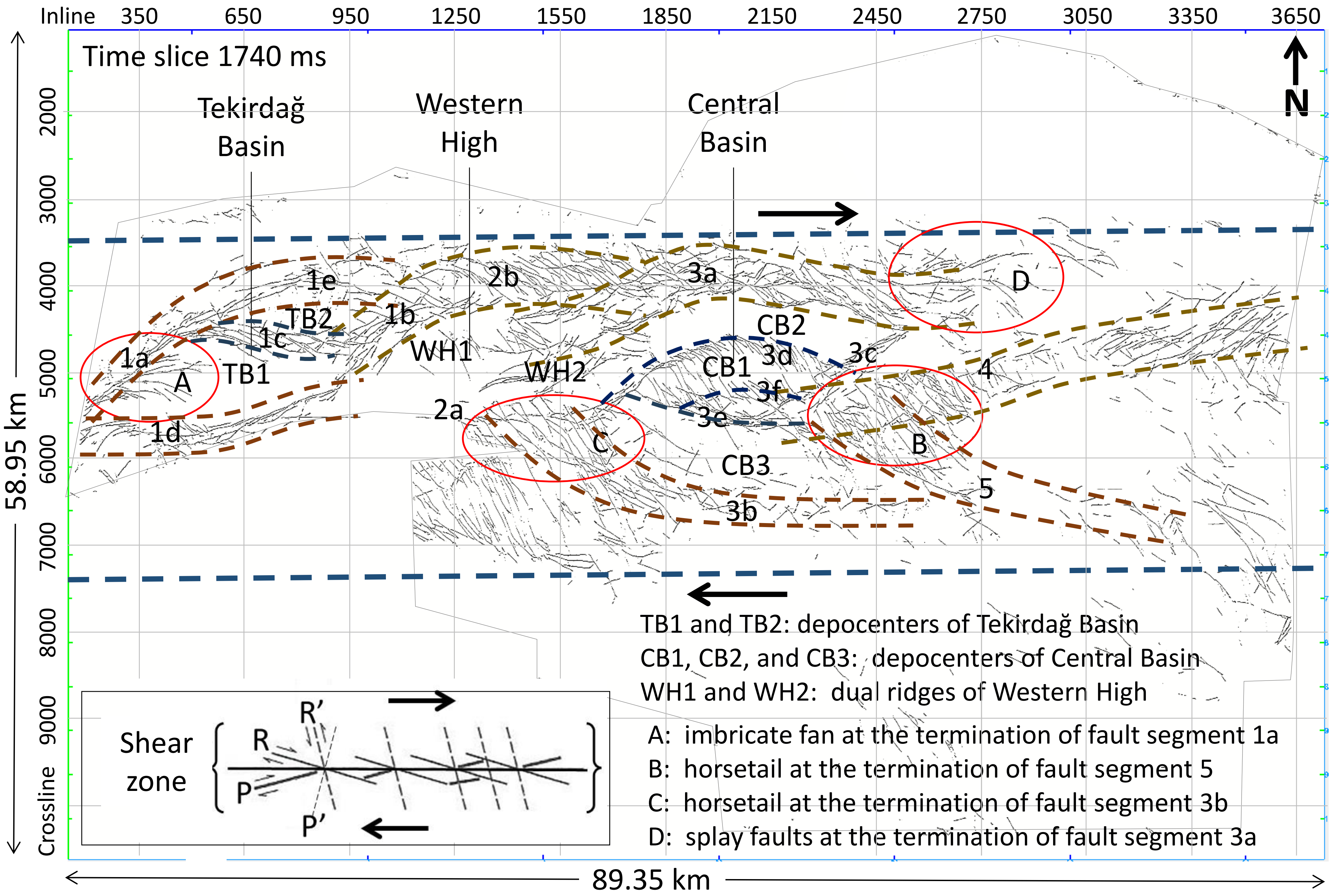

Inline 350 650 950 1250 1550 1850 2150 2450 2750 3050 3350 3650
Time slice 1740 ms
N
Tekirdağ Basin
Western High
Central Basin
2000 3000 4000 5000 6000 7000 8000 9000 Crossline
58.95 km
89.35 km
1a 1b 1c 1d 1e TB1 TB2 2a 2b WH1 WH2 3a 3b 3c 3d 3e 3f CB1 CB2 CB3 4 5
A B C D
Shear zone
R R' P P'
TB1 and TB2: depocenters of Tekirdağ Basin
CB1, CB2, and CB3: depocenters of Central Basin
WH1 and WH2: dual ridges of Western High
A: imbricate fan at the termination of fault segment 1a
B: horsetail at the termination of fault segment 5
C: horsetail at the termination of fault segment 3b
D: splay faults at the termination of fault segment 3a

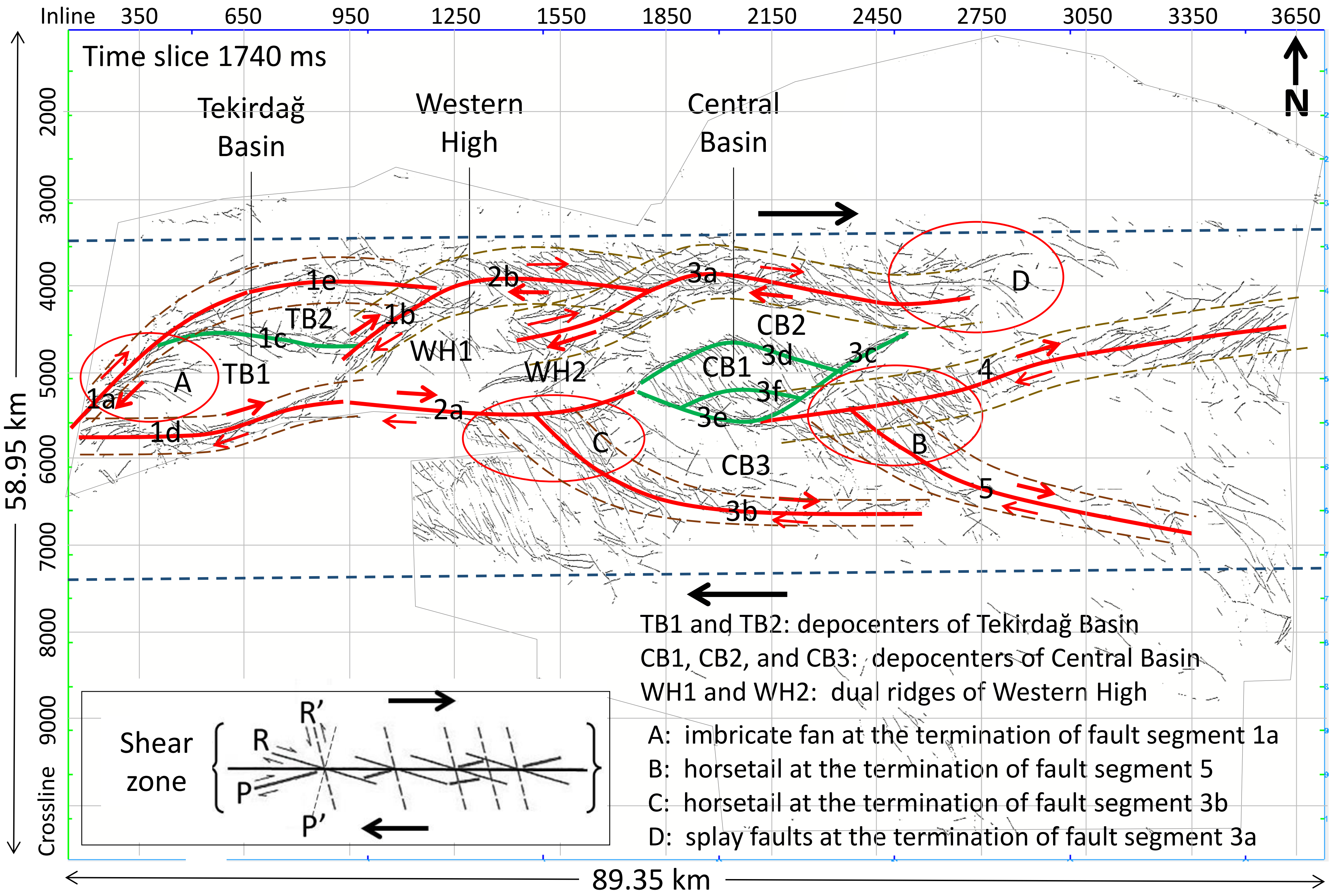

Inline
350
650
950
1250
1550
1850
2150
2450
2750
3050
3350
3650
Time slice 1740 ms
N
Tekirdağ Basin
Western High
Central Basin
2000
3000
4000
5000
6000
7000
8000
9000
Crossline
58.95 km
89.35 km
1a
1b
1c
1d
1e
2a
2b
3a
3b
3c
3d
3e
3f
4
5
TB1
TB2
WH1
WH2
CB1
CB2
CB3
A
B
C
D
Shear zone
R
R'
P
P'
TB1 and TB2: depocenters of Tekirdağ Basin
CB1, CB2, and CB3: depocenters of Central Basin
WH1 and WH2: dual ridges of Western High
A: imbricate fan at the termination of fault segment 1a
B: horsetail at the termination of fault segment 5
C: horsetail at the termination of fault segment 3b
D: splay faults at the termination of fault segment 3a

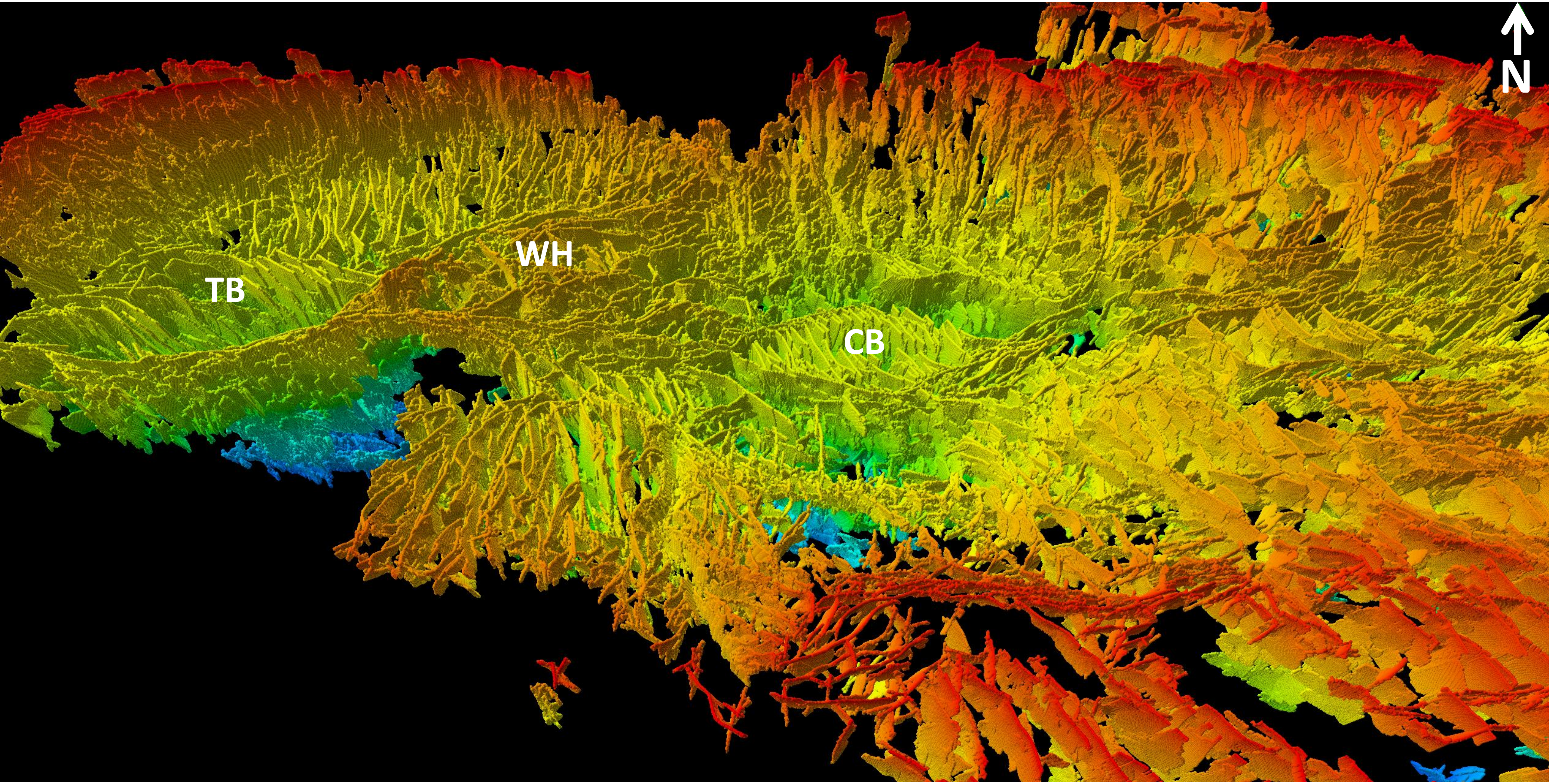

N
WH
TB
CB

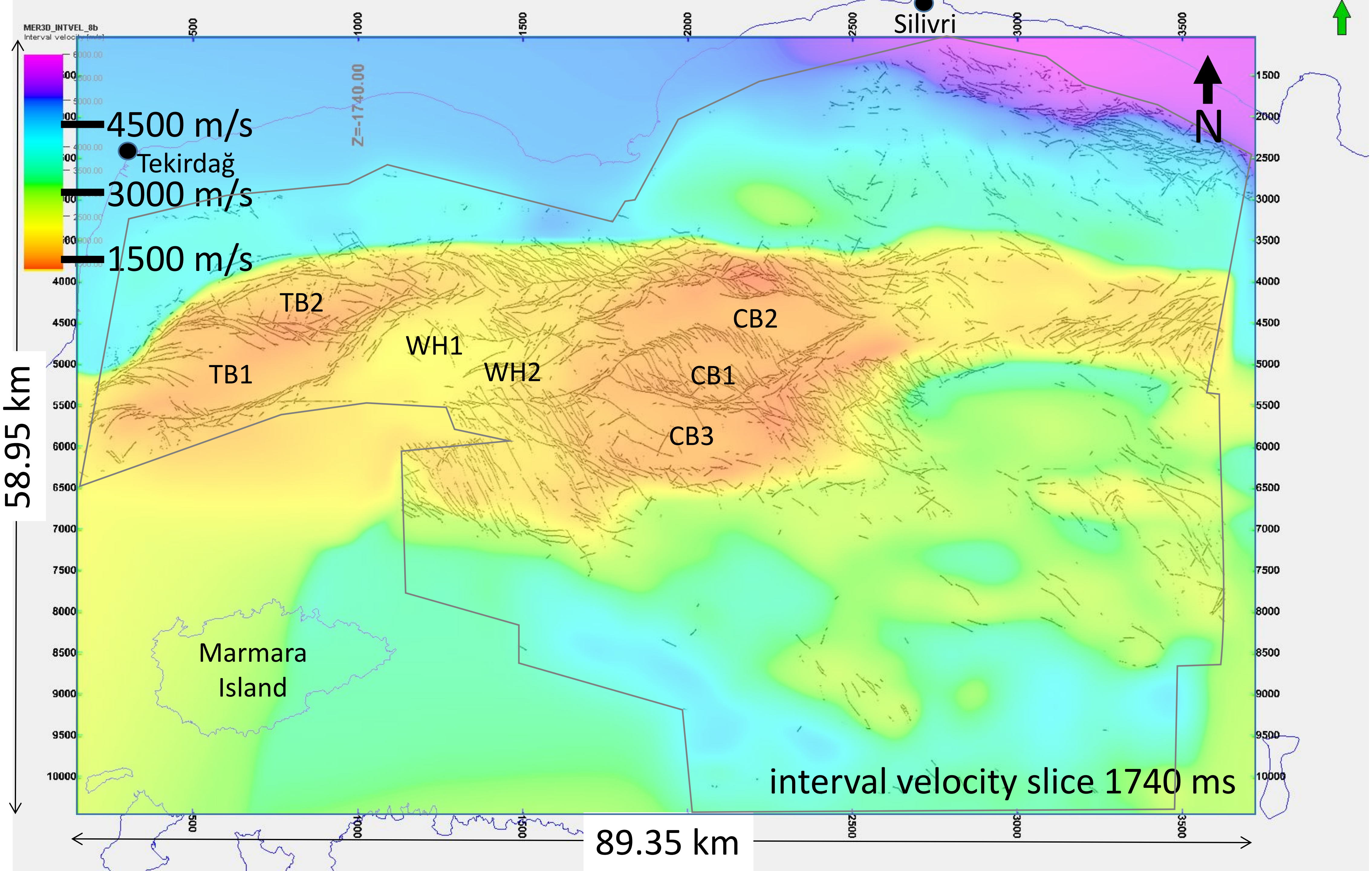

MER3D_INTVEL_8b
Interval velocity [m/s]
4500 m/s
3000 m/s
1500 m/s
Z=-1740.00
Tekirdağ
Silivri
N
TB1
TB2
WH1
WH2
CB1
CB2
CB3
Marmara
Island
58.95 km
89.35 km
interval velocity slice 1740 ms

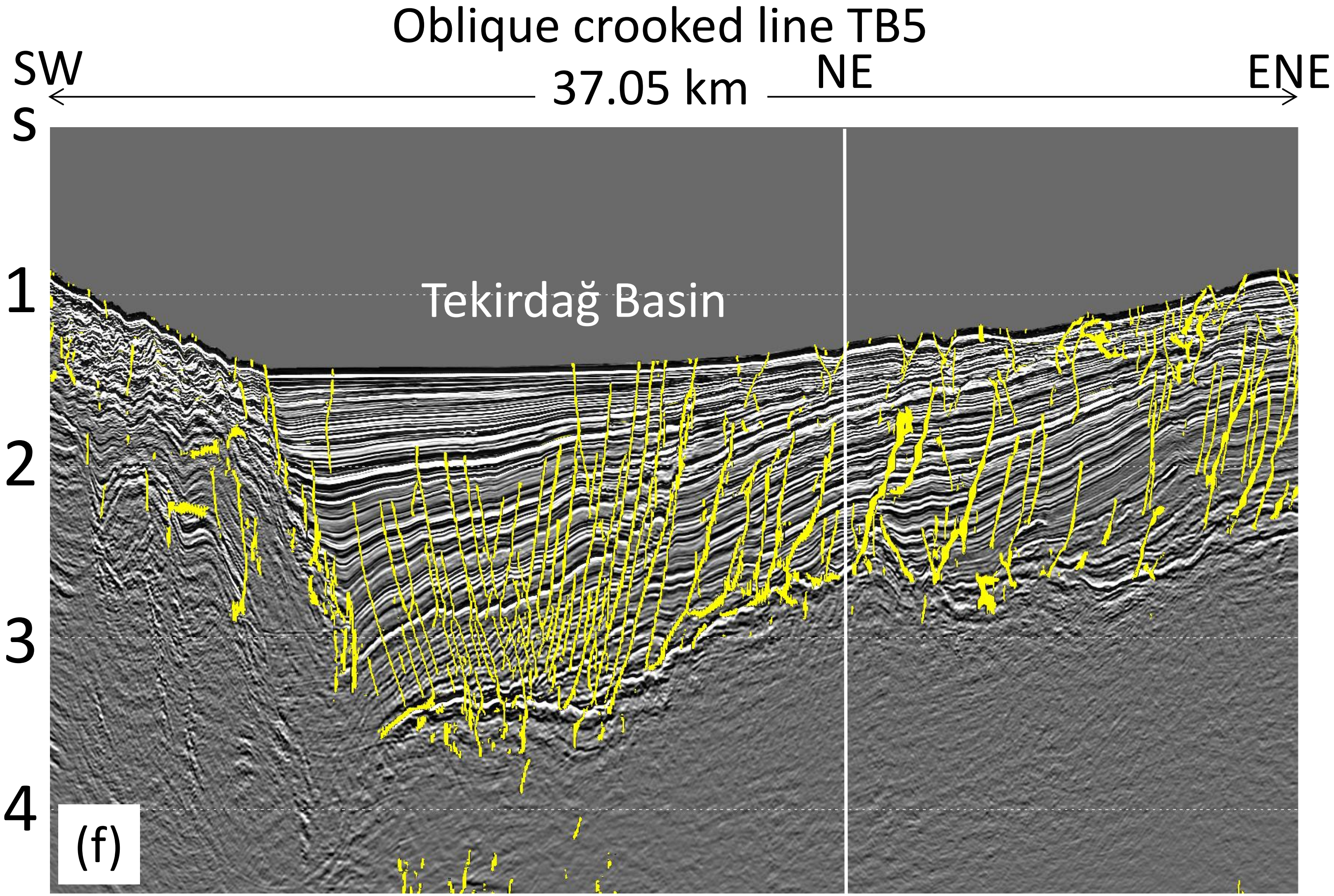
Oblique crooked line TB5
SW
S
37.05 km
NE
ENE
Tekirdağ Basin
1
2
3
4
(f)

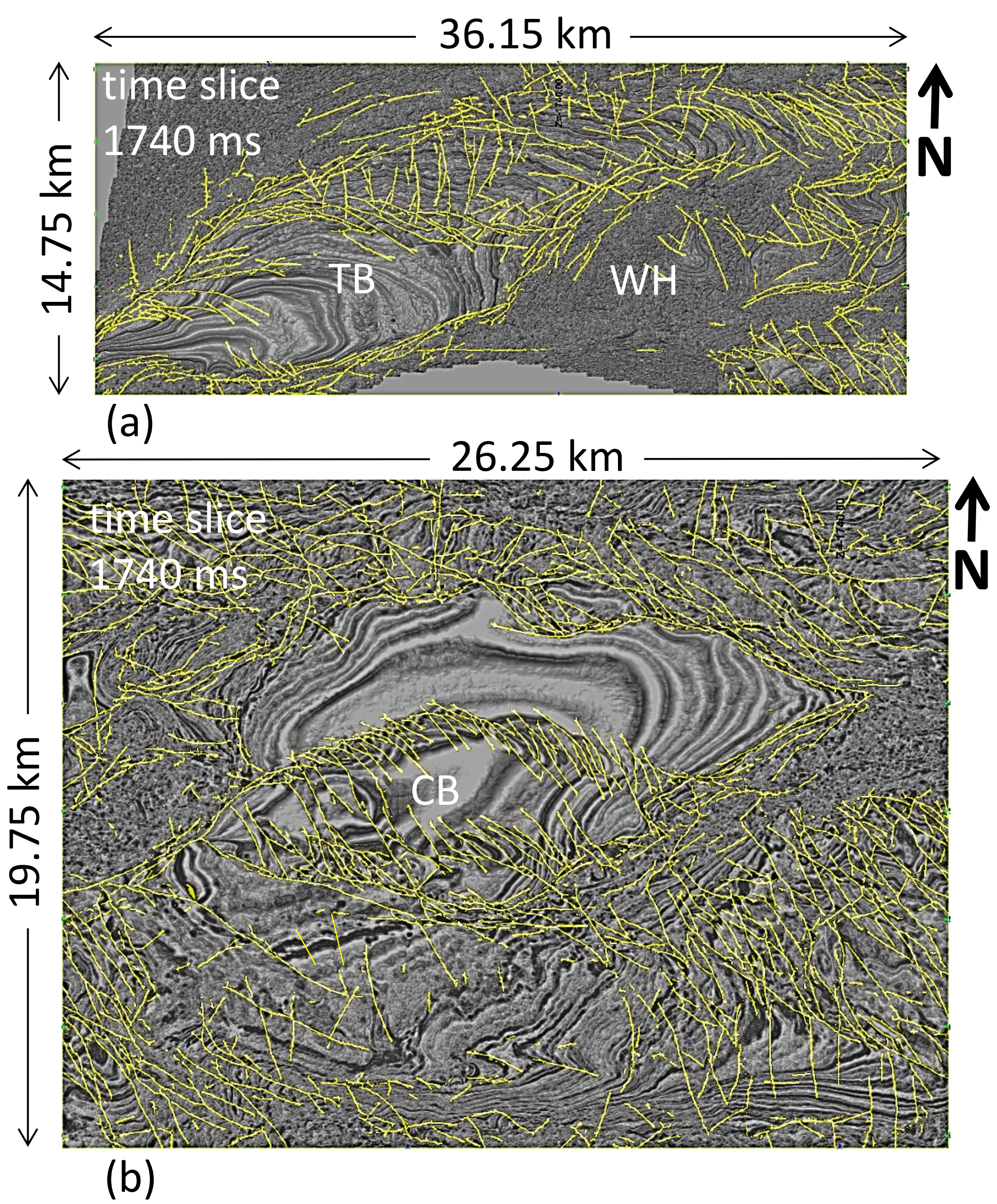
36.15 km
14.75 km
time slice
1740 ms
TB
WH
N
(a)
26.25 km
19.75 km
time slice
1740 ms
CB
N
(b)

A pair of dextral strike-slip basement fault segments along the NAFZ with extensional stepover that gave rise to the formation of Mudurnu Basin

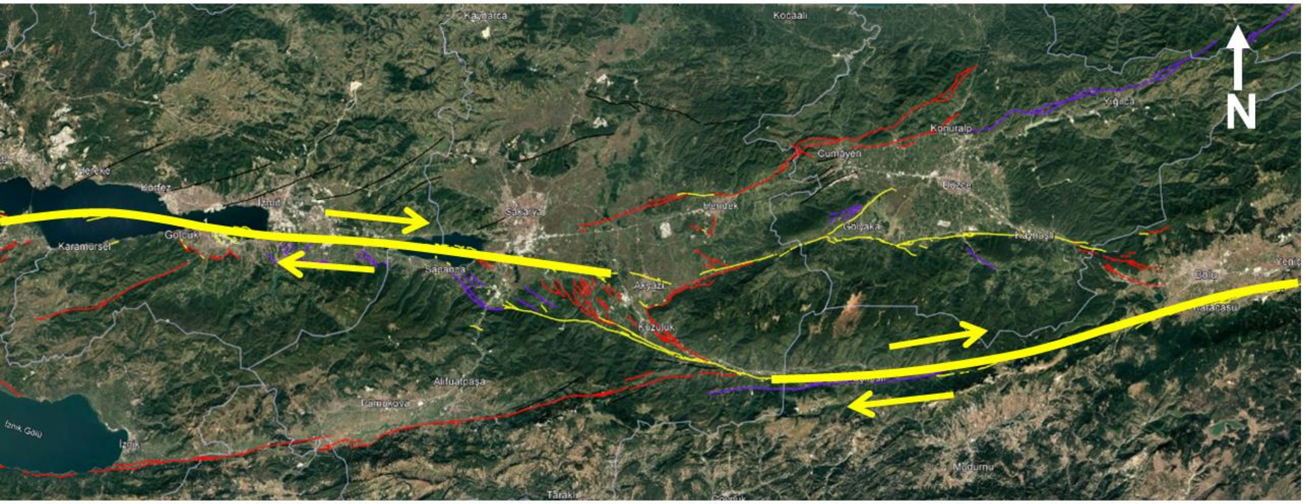


Emre, Ö., Duman, T.Y., Özalp, S., Şaroğlu, F., Olgun, Ş., Elmacı, H. and Çan, T., 2018. Active fault database of Turkey. Bulletin of Earthquake Engineering, 16(8), pp.3229-3275.

**(Courtesy Nuretdin Kaymakçı, 2025)**

A pair of dextral strike-slip basement fault segments along the NAFZ with extensional stepover that gave rise to the formation of Niksar Basin

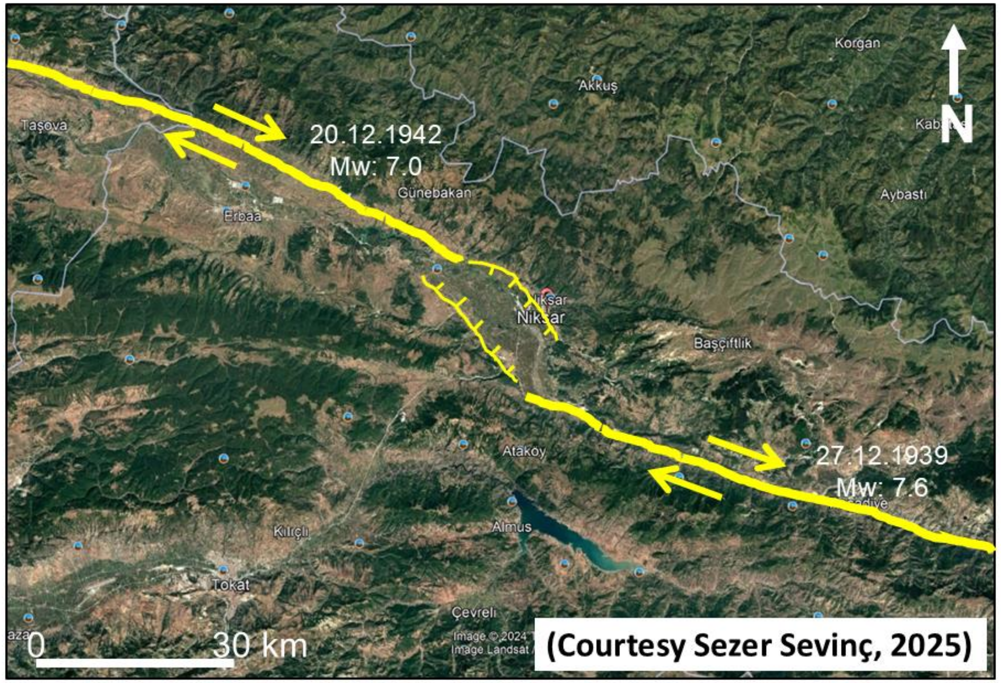


**(Courtesy Sezer Sevinç, 2025)**

# Fault segmentation that gave rise to the formation of Mudurnu Basin (left) and Niksar Basin (right)

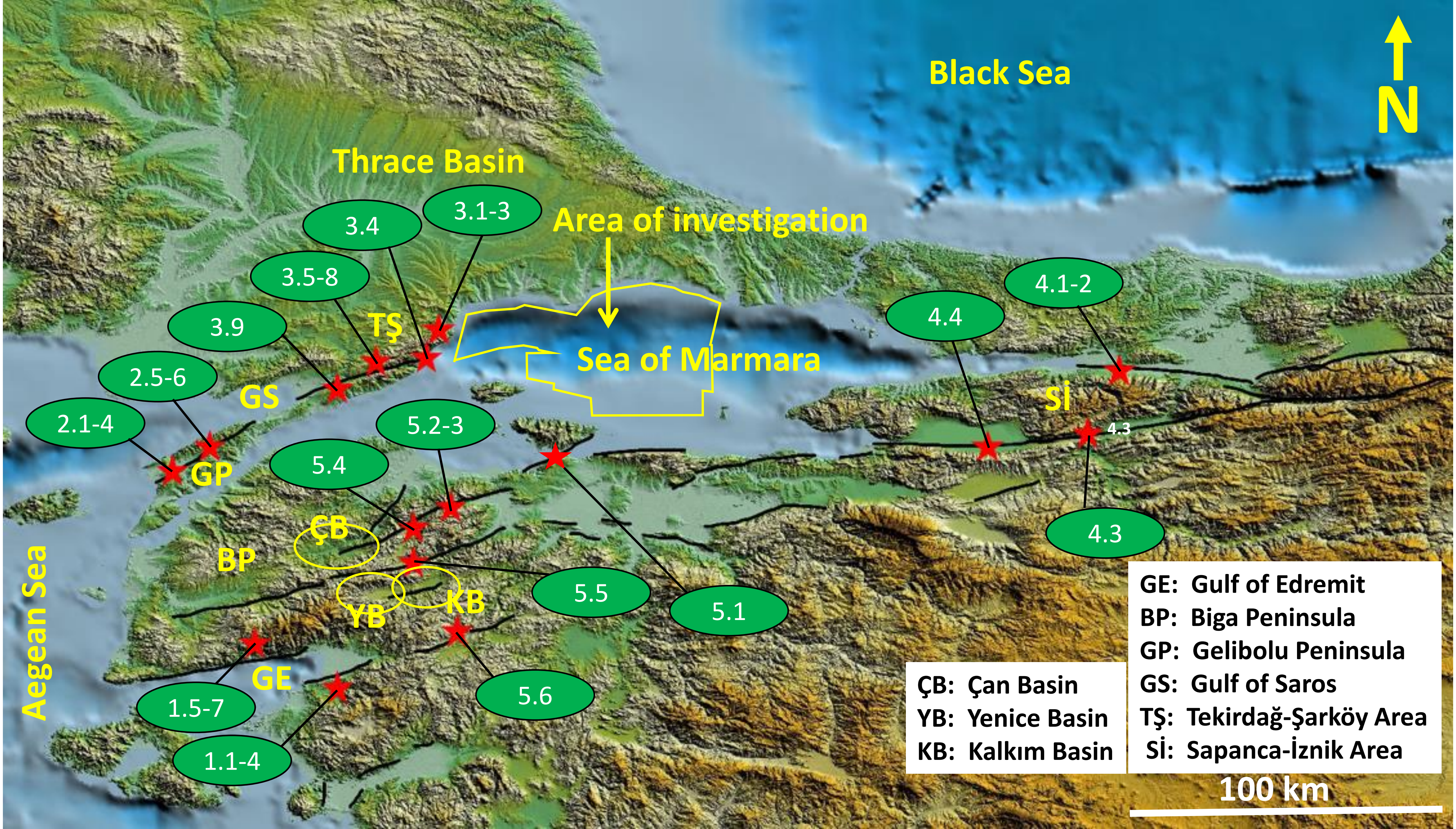
Black Sea
N
Thrace Basin
Area of investigation
Sea of Marmara
3.4
3.1-3
3.5-8
TŞ
3.9
2.5-6
GS
2.1-4
GP
5.2-3
5.4
ÇB
BP
YB
KB
5.5
5.1
Aegean Sea
GE
1.5-7
1.1-4
5.6
4.4
4.1-2
Sİ
4.3
4.3
GE: Gulf of Edremit
BP: Biga Peninsula
GP: Gelibolu Peninsula
GS: Gulf of Saros
TŞ: Tekirdağ-Şarköy Area
Sİ: Sapanca-İznik Area
ÇB: Çan Basin
YB: Yenice Basin
KB: Kalkım Basin
100 km

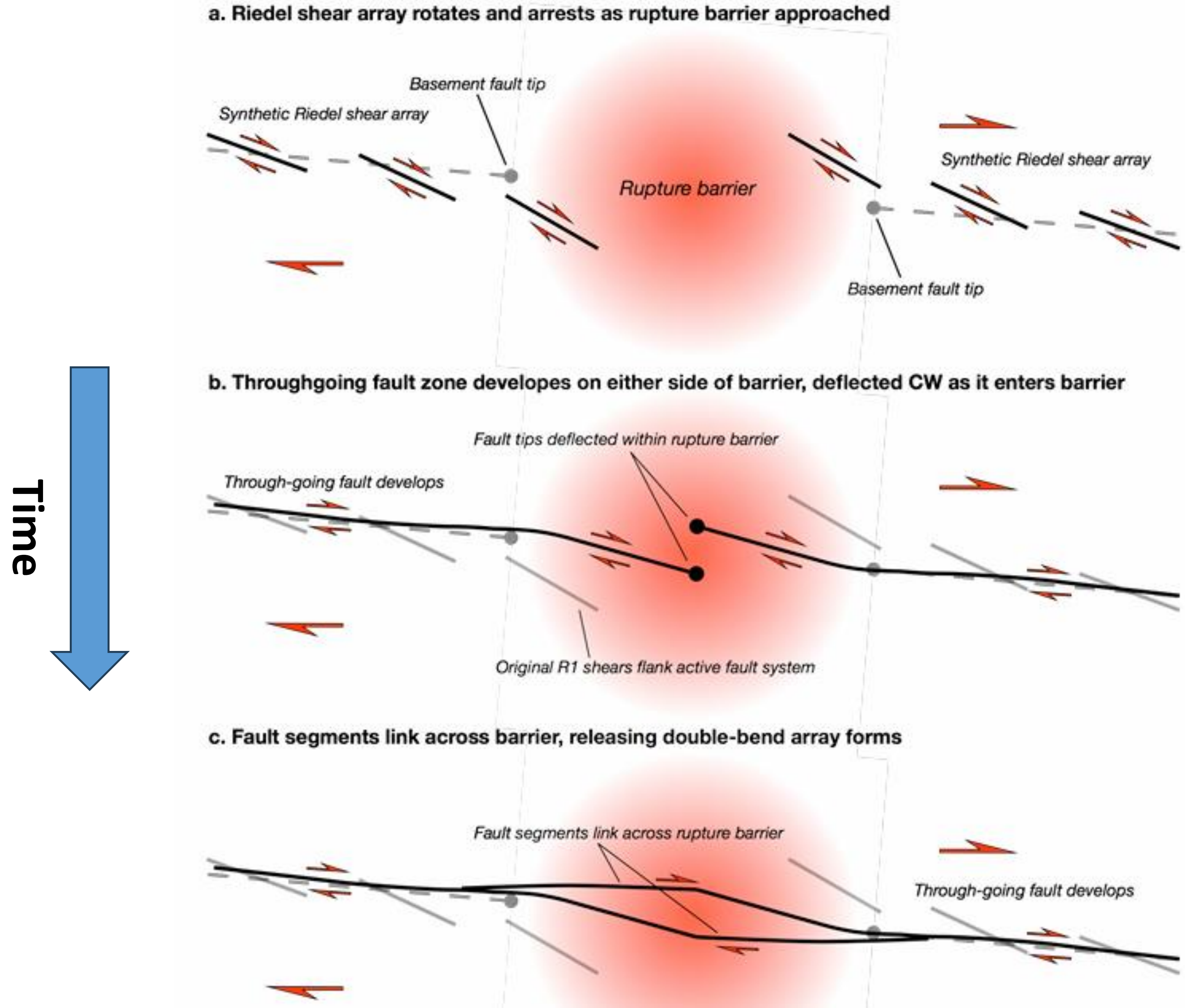
a. Riedel shear array rotates and arrests as rupture barrier approached
Basement fault tip
Synthetic Riedel shear array
Rupture barrier
Synthetic Riedel shear array
Basement fault tip
b. Throughgoing fault zone developes on either side of barrier, deflected CW as it enters barrier
Fault tips deflected within rupture barrier
Through-going fault develops
Original R1 shears flank active fault system
c. Fault segments link across barrier, releasing double-bend array forms
Fault segments link across rupture barrier
Through-going fault develops
Time

(Dooley, 2008)

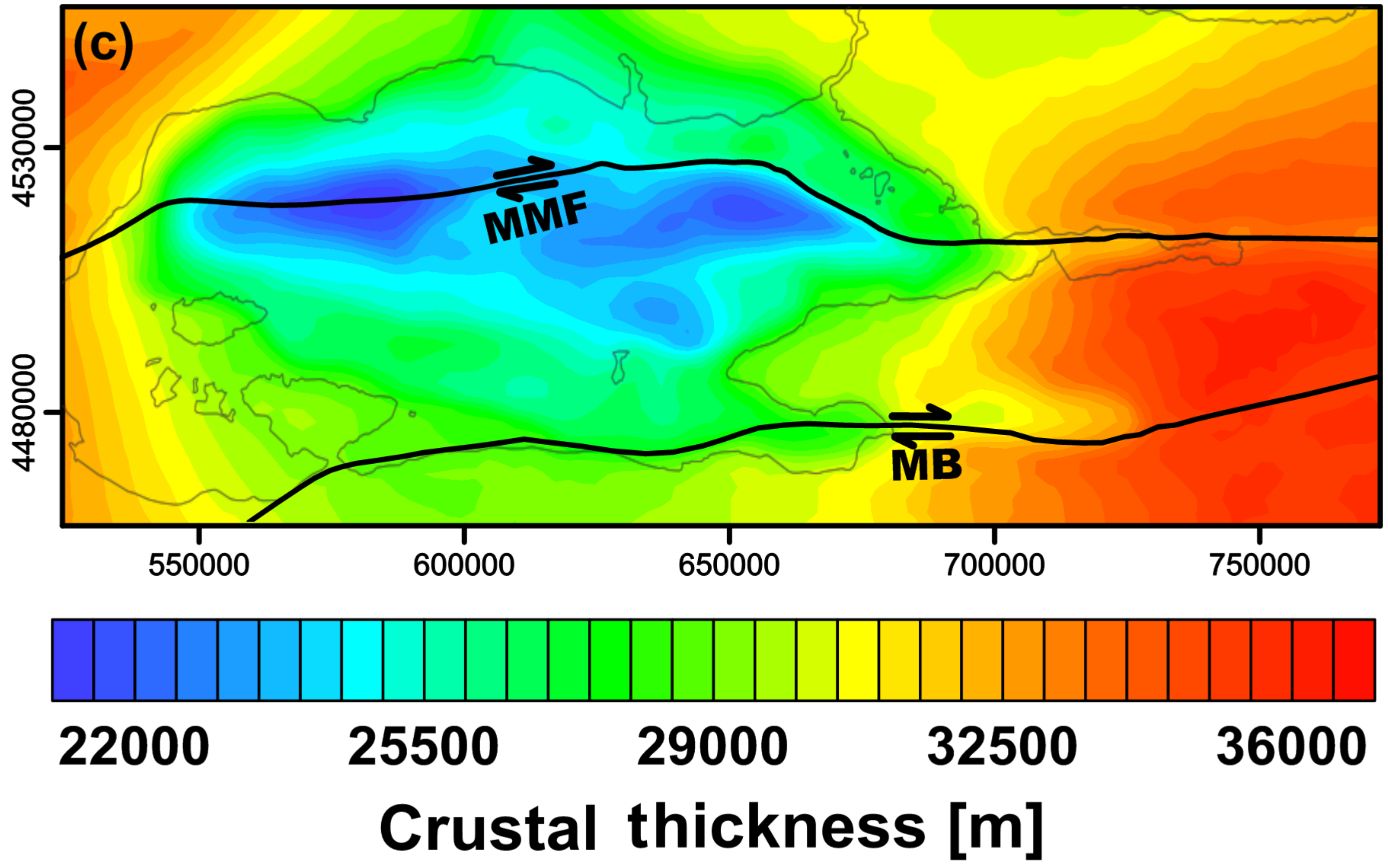


**3-D forward gravity modeling suggesting that significant crustal heterogeneities may have influenced the basement fault segmentation below the Sea of Marmara**

(Gholamrezaie et al., 2019)

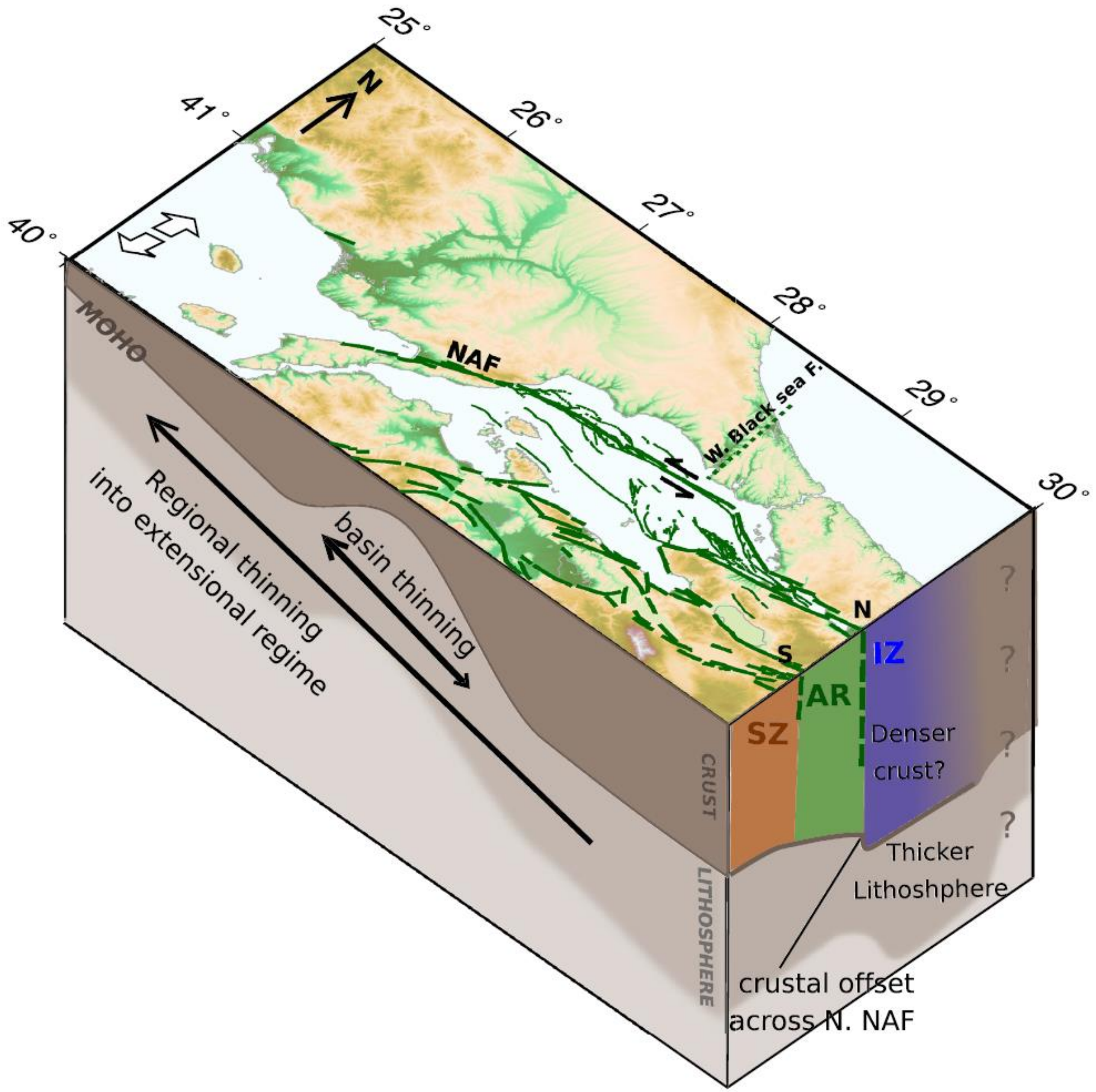


**P-to-S converted arrival times and receiver-function analysis of selected earthquake seismograms to create a map of 3-D crustal thickness variation in Marmara Basin**

**(Jenkins et al., 2020)**

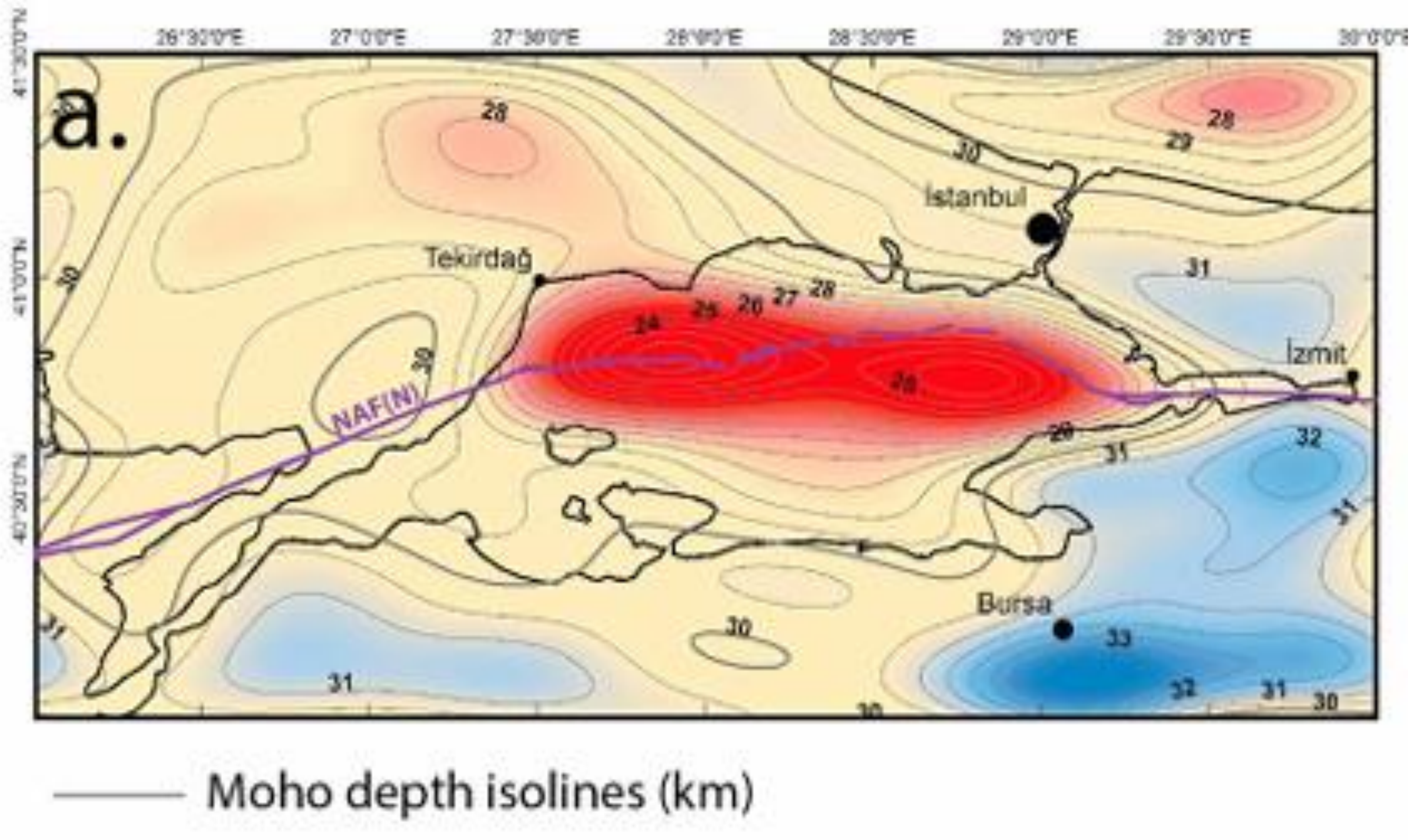


**3-D gravity inversion to estimate the Moho depth**

**(Kende et al., 2017)**

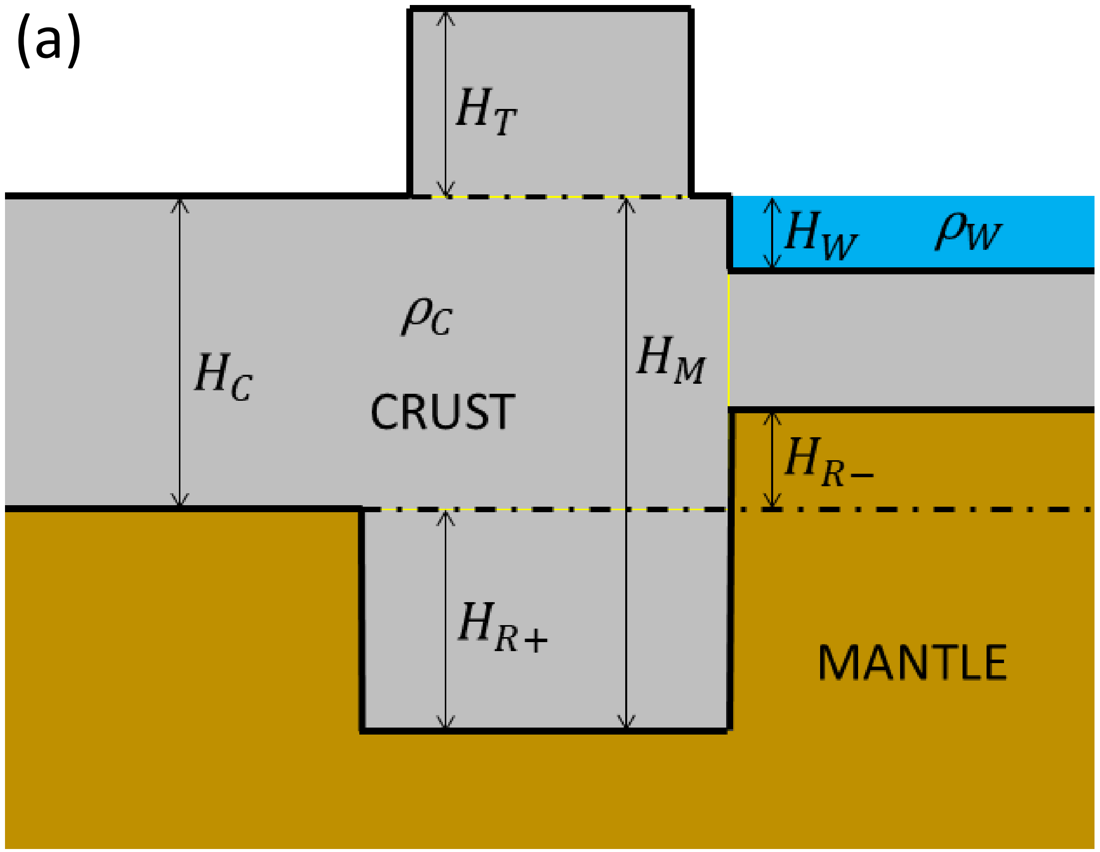


$$H_{R+} = \frac{H_T * \rho_C}{\Delta\rho_{ML}} \quad (1)$$

$$H_{R-} = \frac{H_W * (\rho_C - \rho_W)}{\Delta\rho_{MS}} \quad (2)$$

at sea: $H_M = H_C + H_{R+}$ (3)

on land: $H_M = H_C - H_{R-}$ (4)

$\rho_C = 2.67\ \mathrm{g/cm^3}$
$\rho_W = 1.03\ \mathrm{g/cm^3}$
$\Delta\rho_{ML} = 0.33\ \mathrm{g/cm^3}$
$\Delta\rho_{MS} = 0.35\ \mathrm{g/cm^3}$
$H_C = 30\ \mathrm{km}$

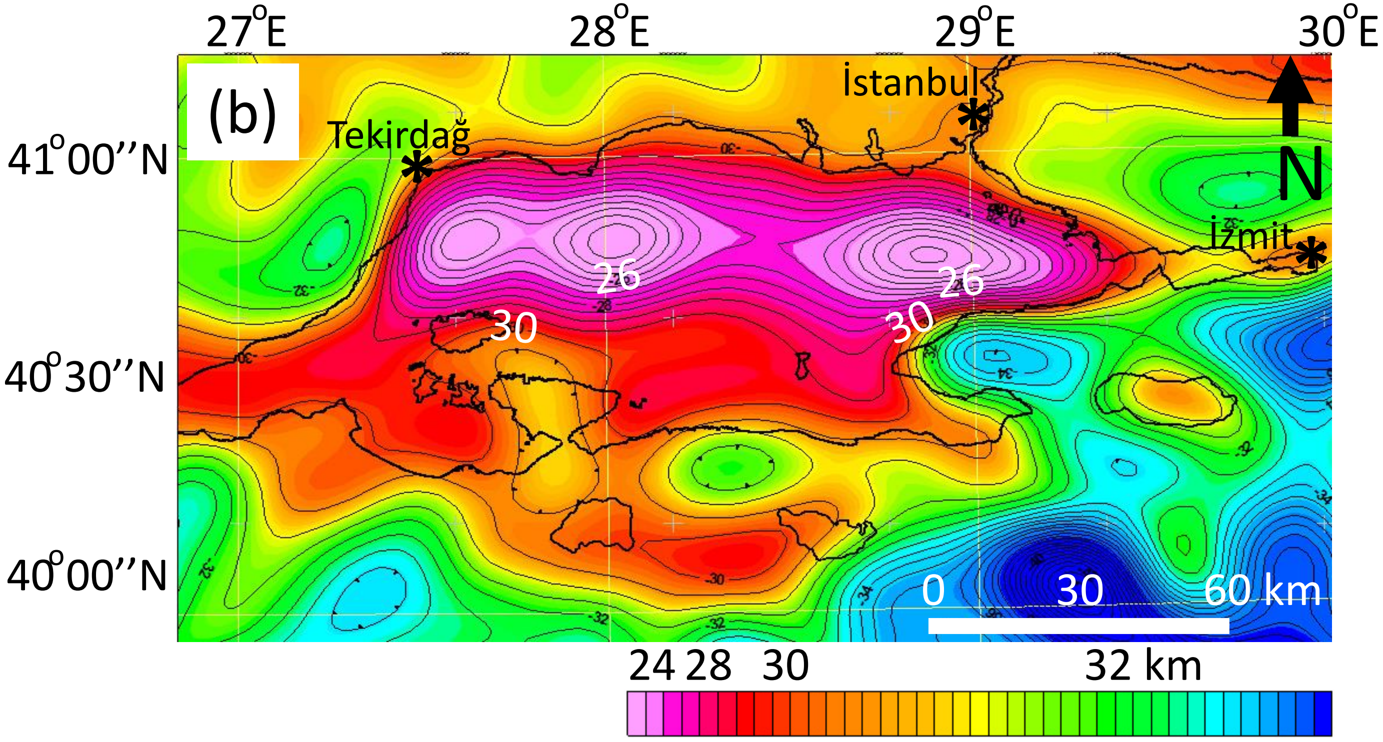


**Moho depth map constructed by the Airy isostasy method**

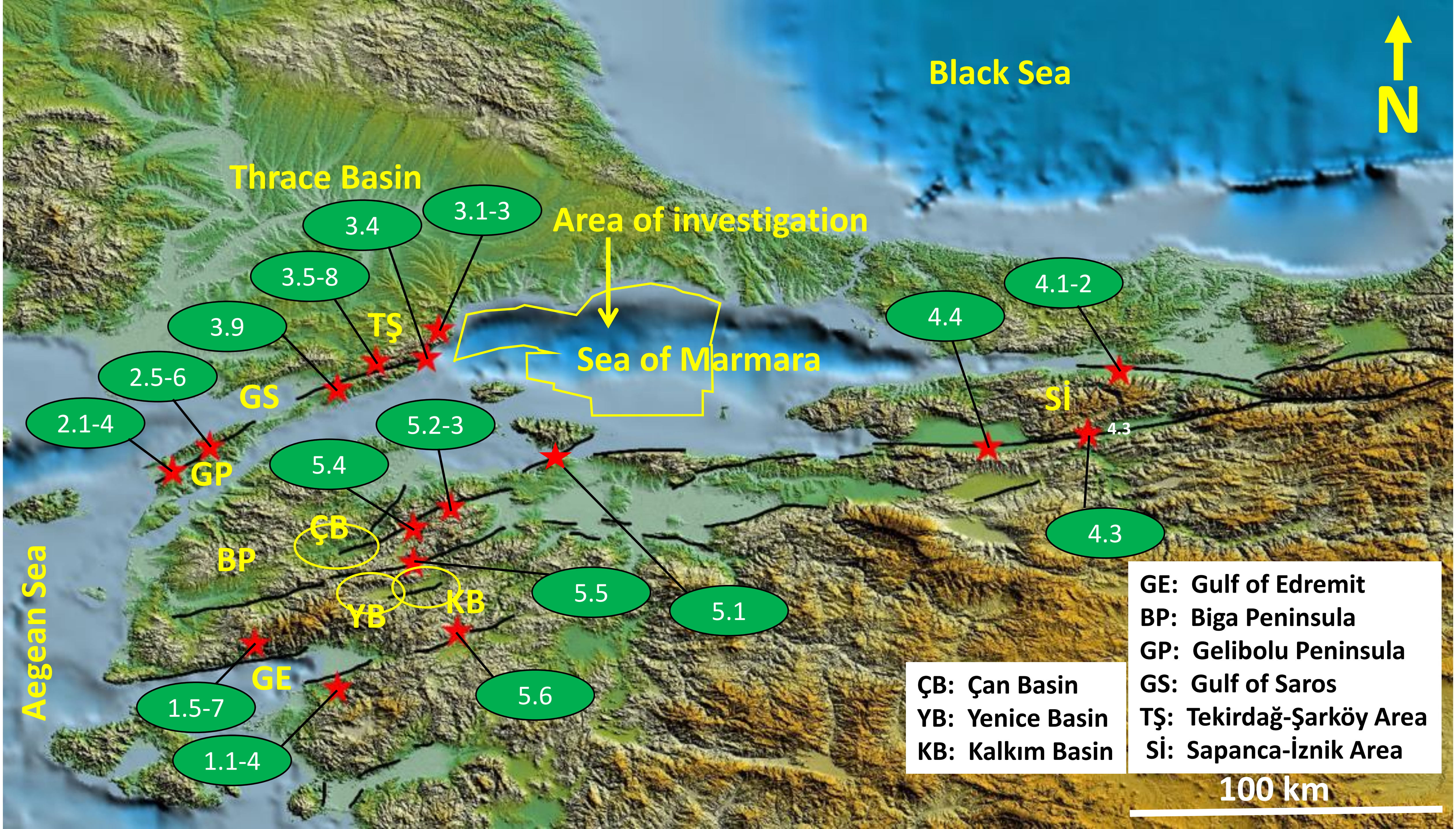

Black Sea
N
Thrace Basin
Area of investigation
Sea of Marmara
Aegean Sea
3.4
3.1-3
3.5-8
3.9
2.5-6
2.1-4
TŞ
GS
GP
5.2-3
5.4
ÇB
BP
YB
KB
5.5
5.1
5.6
GE
1.5-7
1.1-4
4.1-2
4.4
Sİ
4.3
4.3
ÇB: Çan Basin
YB: Yenice Basin
KB: Kalkım Basin
GE: Gulf of Edremit
BP: Biga Peninsula
GP: Gelibolu Peninsula
GS: Gulf of Saros
TŞ: Tekirdağ-Şarköy Area
Sİ: Sapanca-İznik Area
100 km

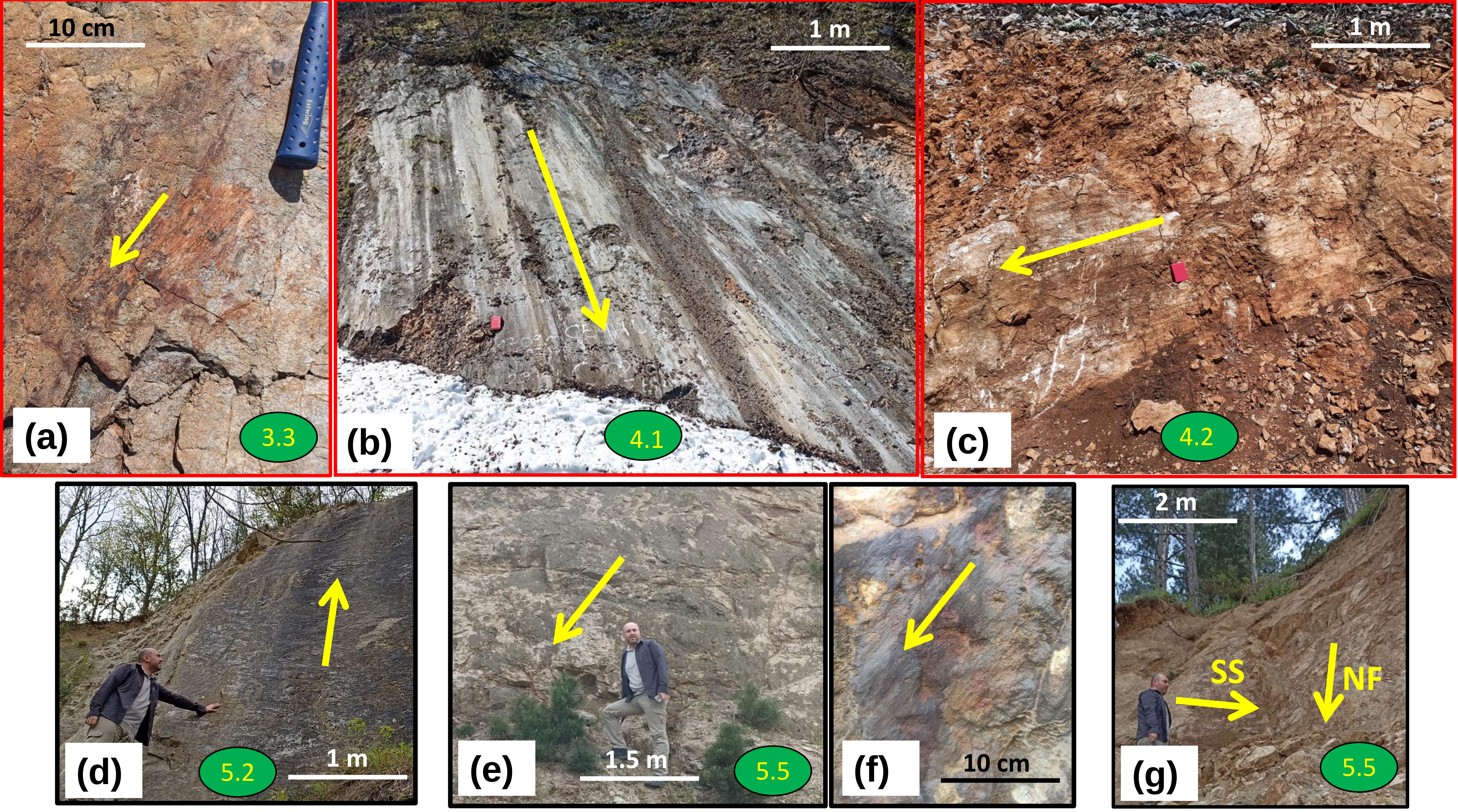

10 cm
(a)
3.3
1 m
(b)
4.1
1 m
(c)
4.2
(d)
5.2
1 m
(e)
1.5 m
5.5
(f)
10 cm
2 m
SS
NF
(g)
5.5

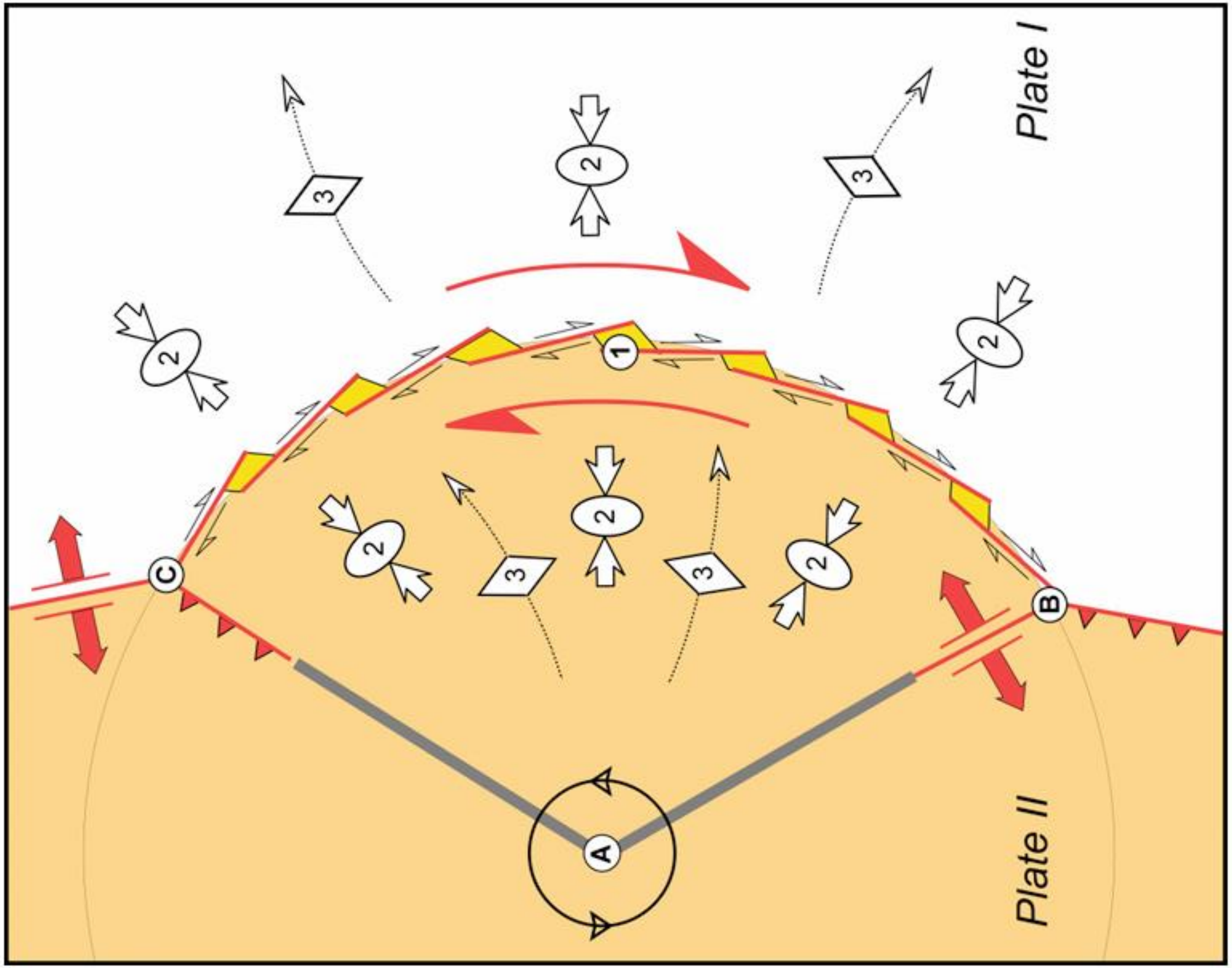


(Dooley, 2008)

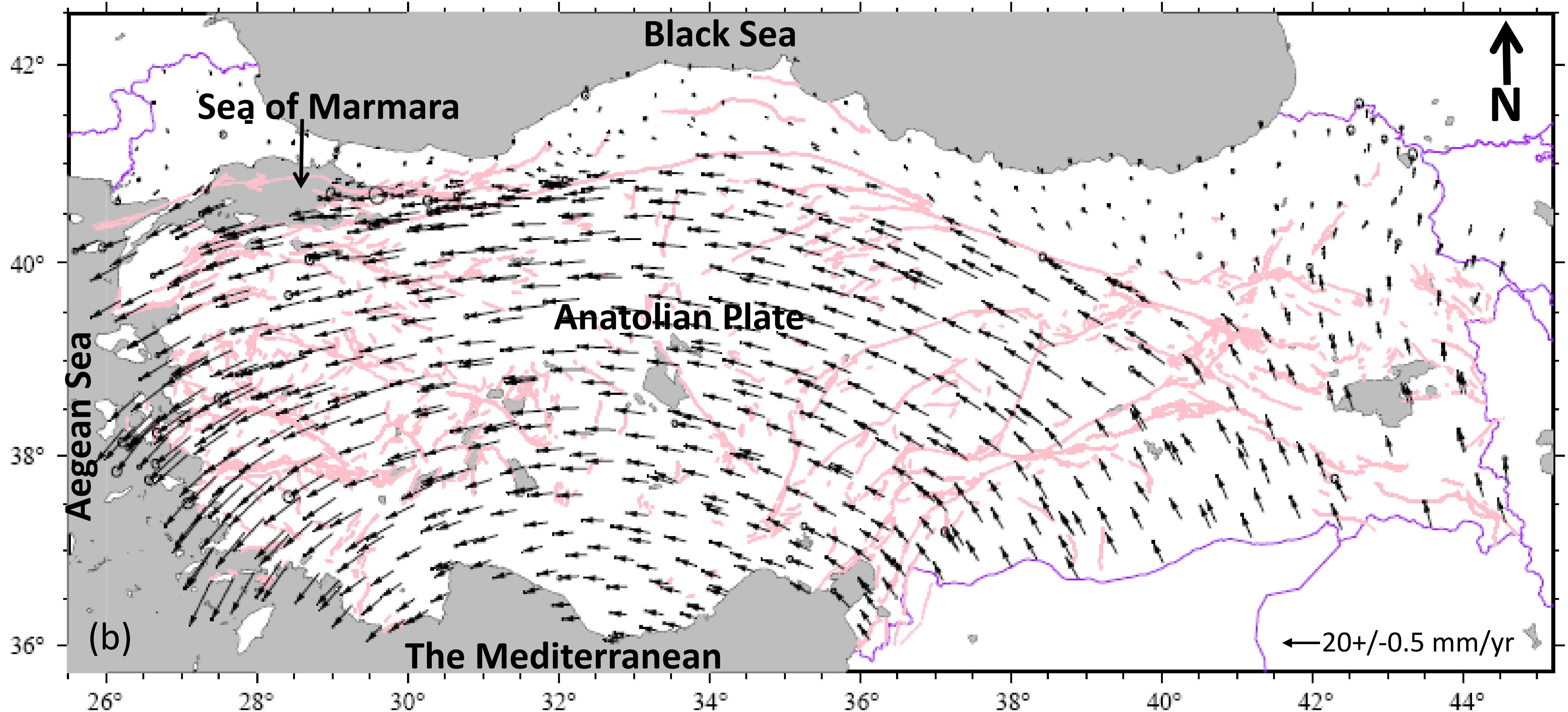


(Kurt et al., 2022)

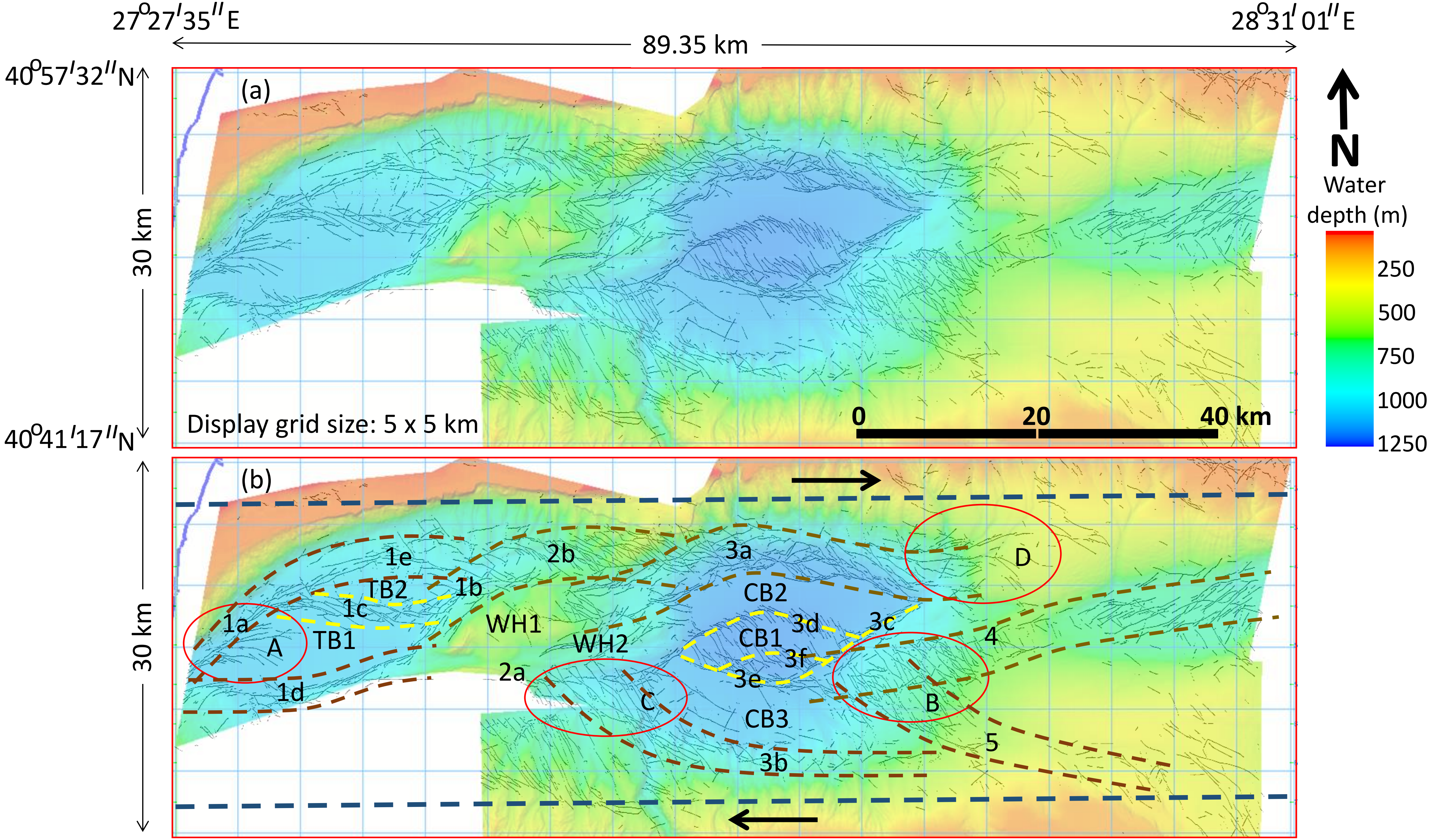
27°27′35″E
28°31′01″E
89.35 km
40°57′32″N
40°41′17″N
30 km
(a)
Display grid size: 5 x 5 km
0
20
40 km
N
Water depth (m)
250
500
750
1000
1250
(b)
30 km
1a
1b
1c
1d
1e
TB1
TB2
A
WH1
WH2
2a
2b
3a
3b
3c
3d
3e
3f
CB1
CB2
CB3
C
B
D
4
5

# Moho depth map constructed by the Airy isostasy method

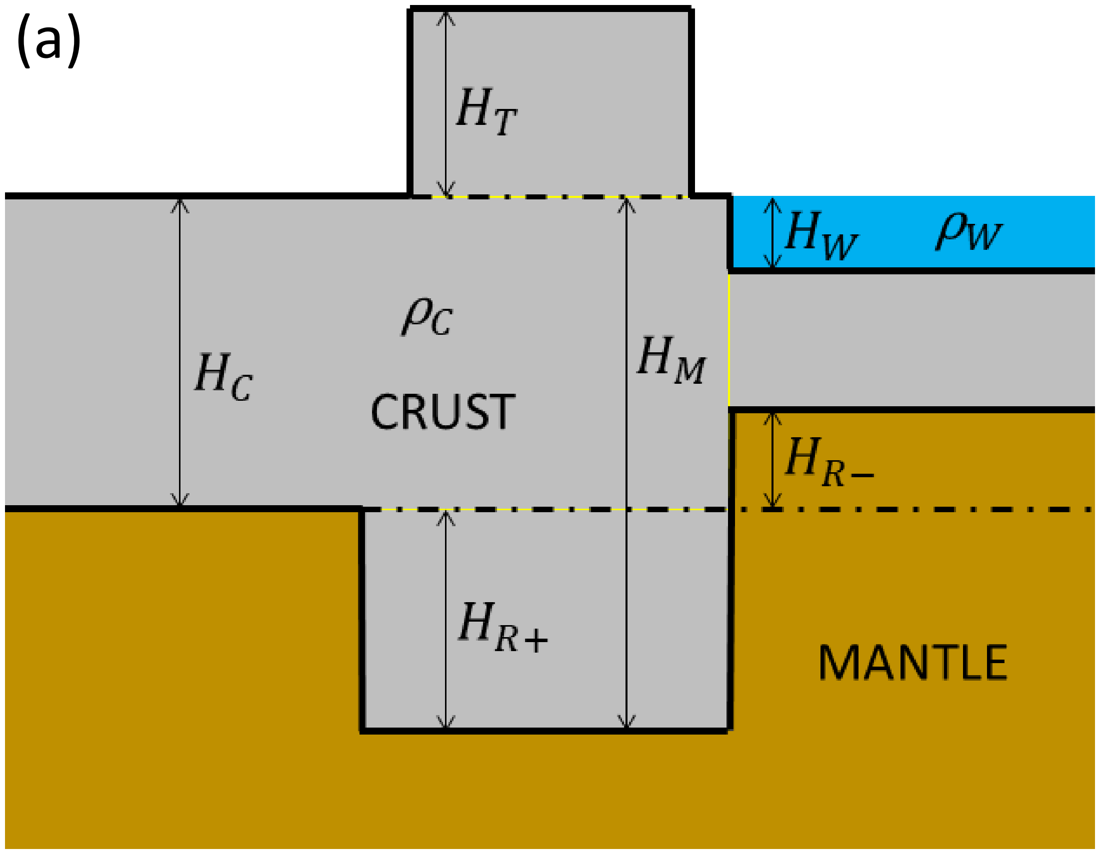


$$H_{R+} = \frac{H_T * \rho_C}{\Delta\rho_{ML}} \quad (1)$$

$$H_{R-} = \frac{H_W * (\rho_C - \rho_W)}{\Delta\rho_{MS}} \quad (2)$$

at sea: $H_M = H_C + H_{R+}$ (3)

on land: $H_M = H_C - H_{R-}$ (4)

$\rho_C = 2.67\ \mathrm{g/cm^3}$
$\rho_W = 1.03\ \mathrm{g/cm^3}$
$\Delta\rho_{ML} = 0.33\ \mathrm{g/cm^3}$
$\Delta\rho_{MS} = 0.35\ \mathrm{g/cm^3}$
$H_C = 30\ \mathrm{km}$

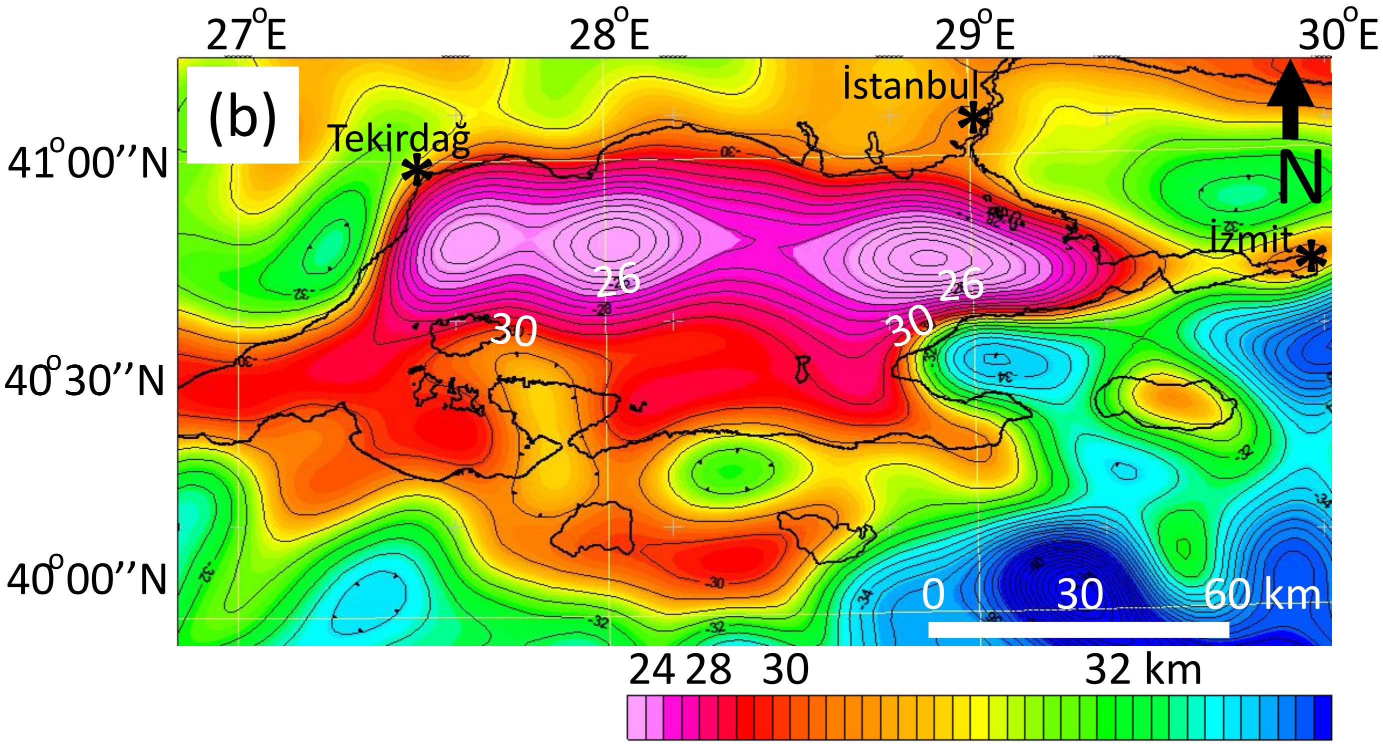

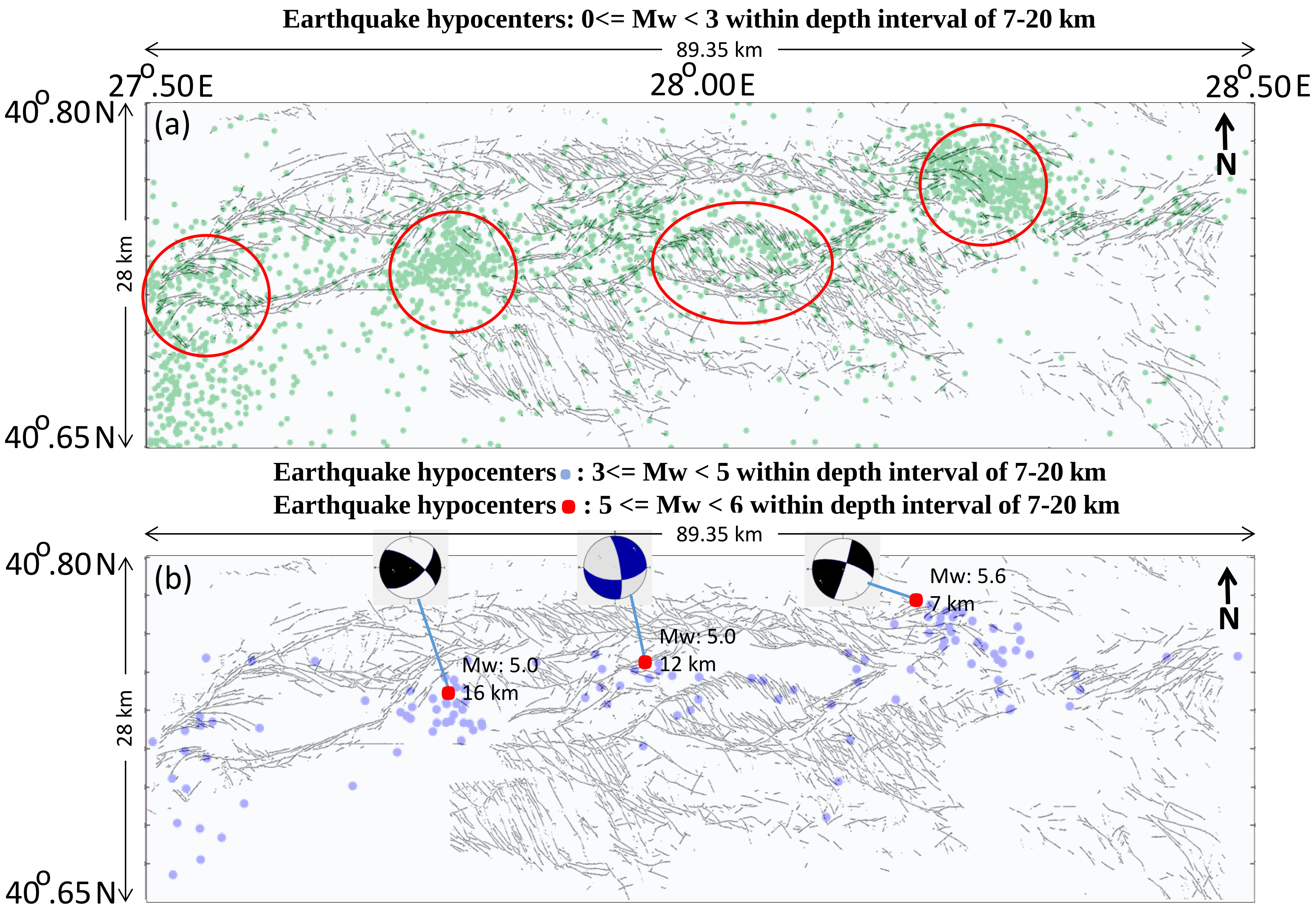
Earthquake hypocenters: 0<= Mw < 3 within depth interval of 7-20 km
89.35 km
27°.50 E
28°.00 E
28°.50 E
40°.80 N
40°.65 N
28 km
(a)
N
Earthquake hypocenters : 3<= Mw < 5 within depth interval of 7-20 km
Earthquake hypocenters : 5 <= Mw < 6 within depth interval of 7-20 km
89.35 km
40°.80 N
40°.65 N
28 km
(b)
N
Mw: 5.0
16 km
Mw: 5.0
12 km
Mw: 5.6
7 km

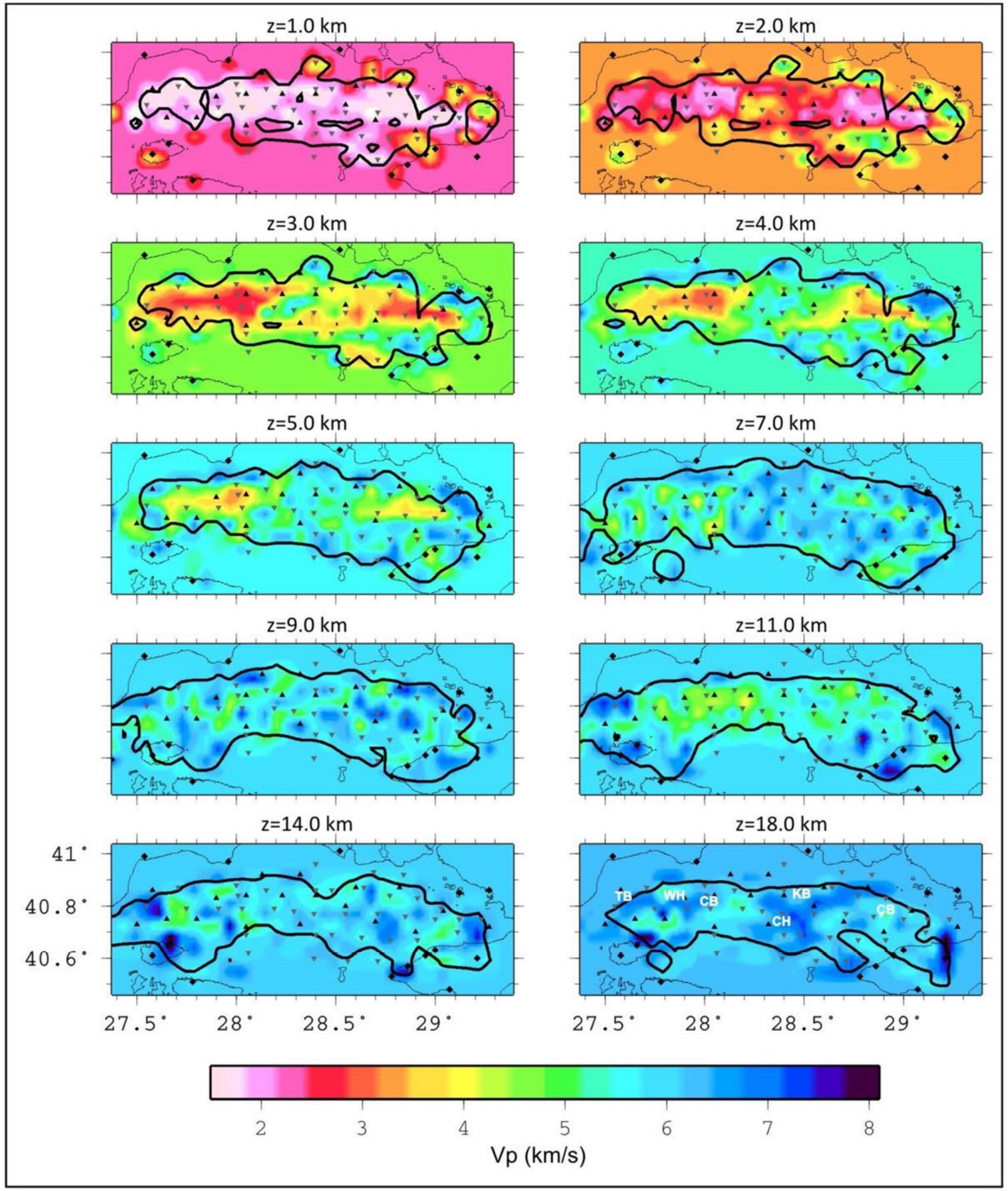


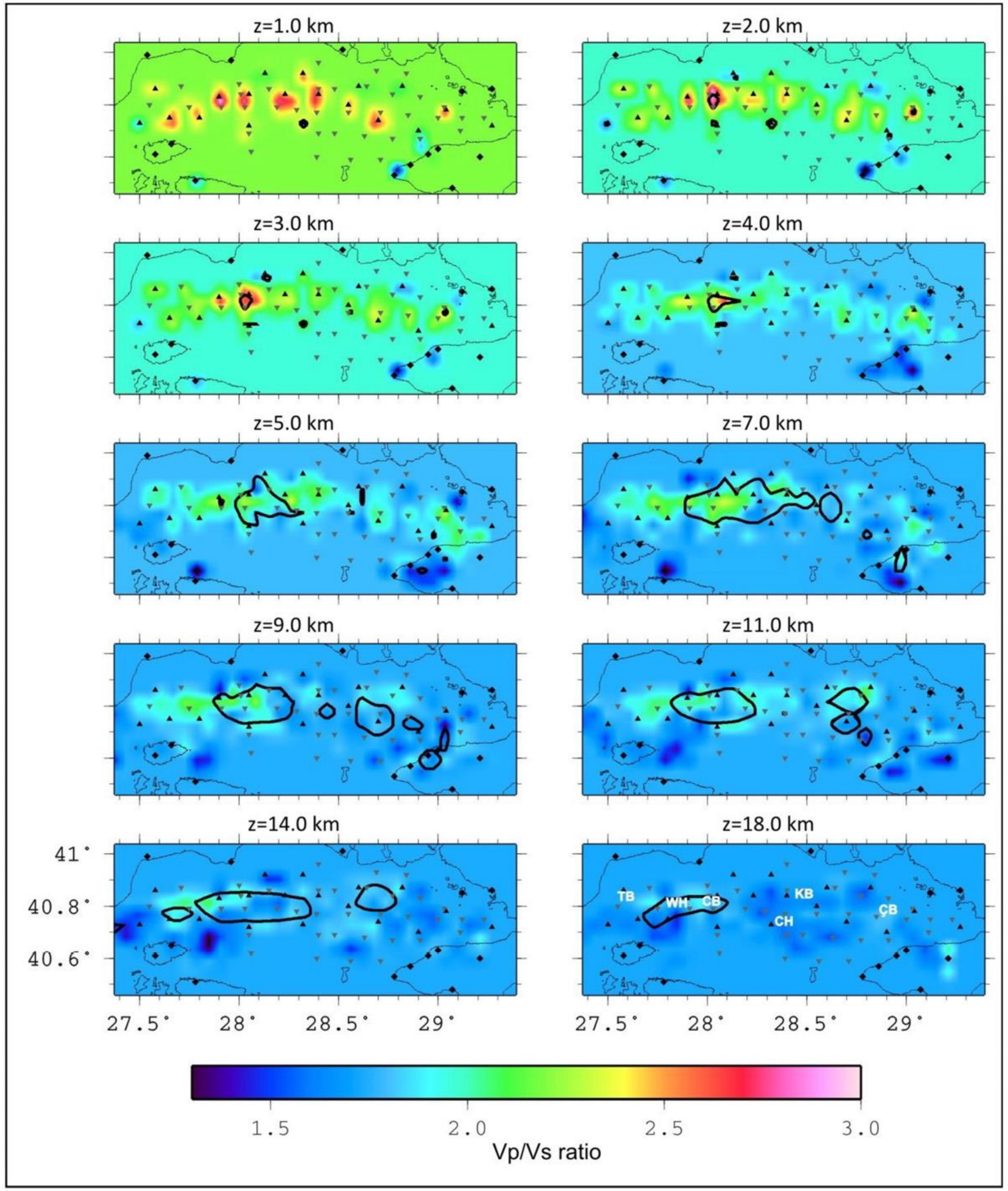


**Vp** **Tarancıoğlu et al. (2020)** **Vp/Vs**

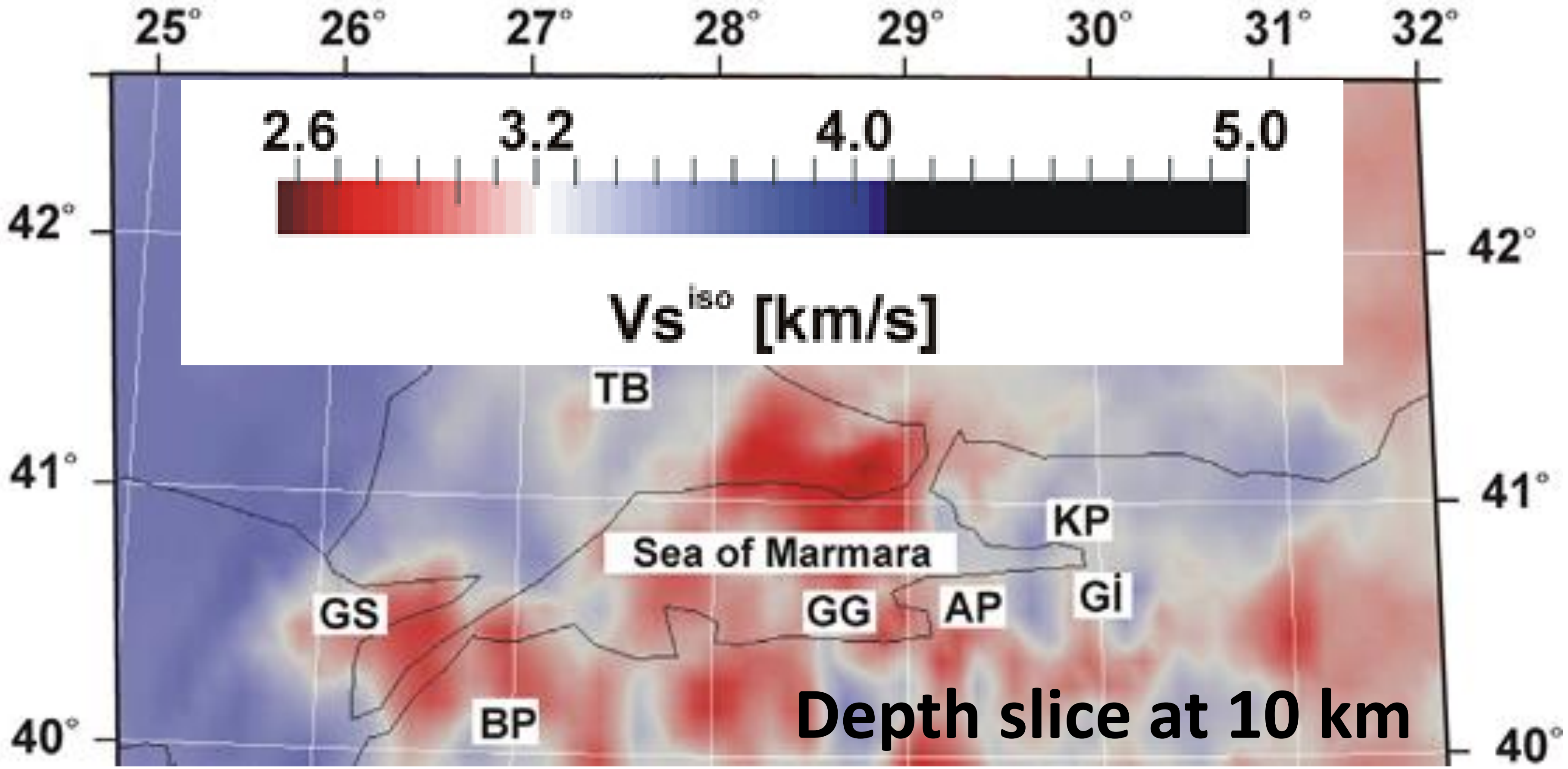


**non-linear full-waveform tomography indicating crustal heterogeneities associated with strong lateral and vertical velocity variations down to Moho depth, characteristic of highly deformed and distributed crustal features along the NAFS with its branches**

**(Çubuk-Sabuncu et al., 2017)**

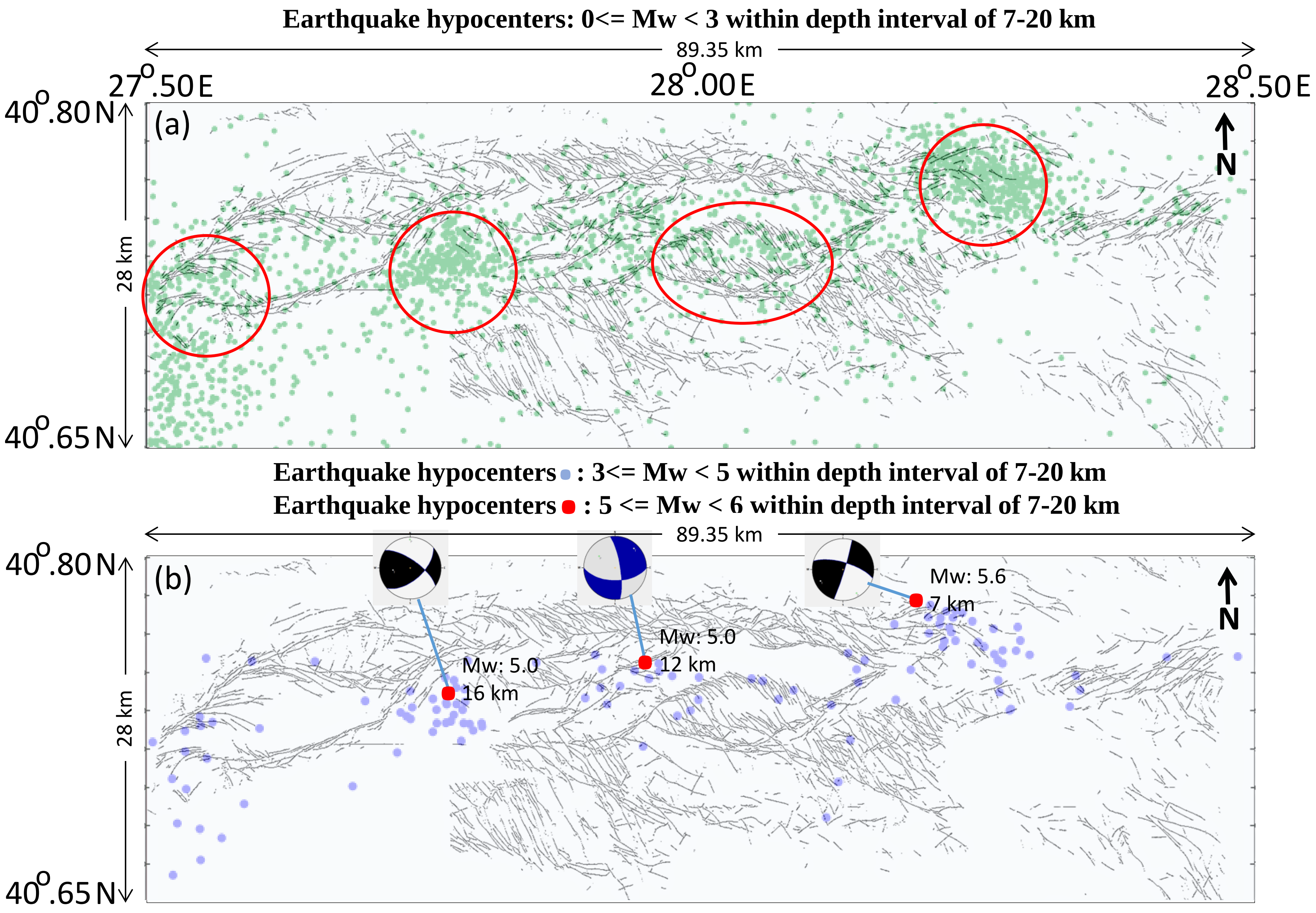
Earthquake hypocenters: 0<= Mw < 3 within depth interval of 7-20 km
89.35 km
27°.50 E
28°.00 E
28°.50 E
40°.80 N
40°.65 N
28 km
(a)
N
Earthquake hypocenters : 3<= Mw < 5 within depth interval of 7-20 km
Earthquake hypocenters : 5 <= Mw < 6 within depth interval of 7-20 km
89.35 km
40°.80 N
40°.65 N
28 km
(b)
N
Mw: 5.0
16 km
Mw: 5.0
12 km
Mw: 5.6
7 km

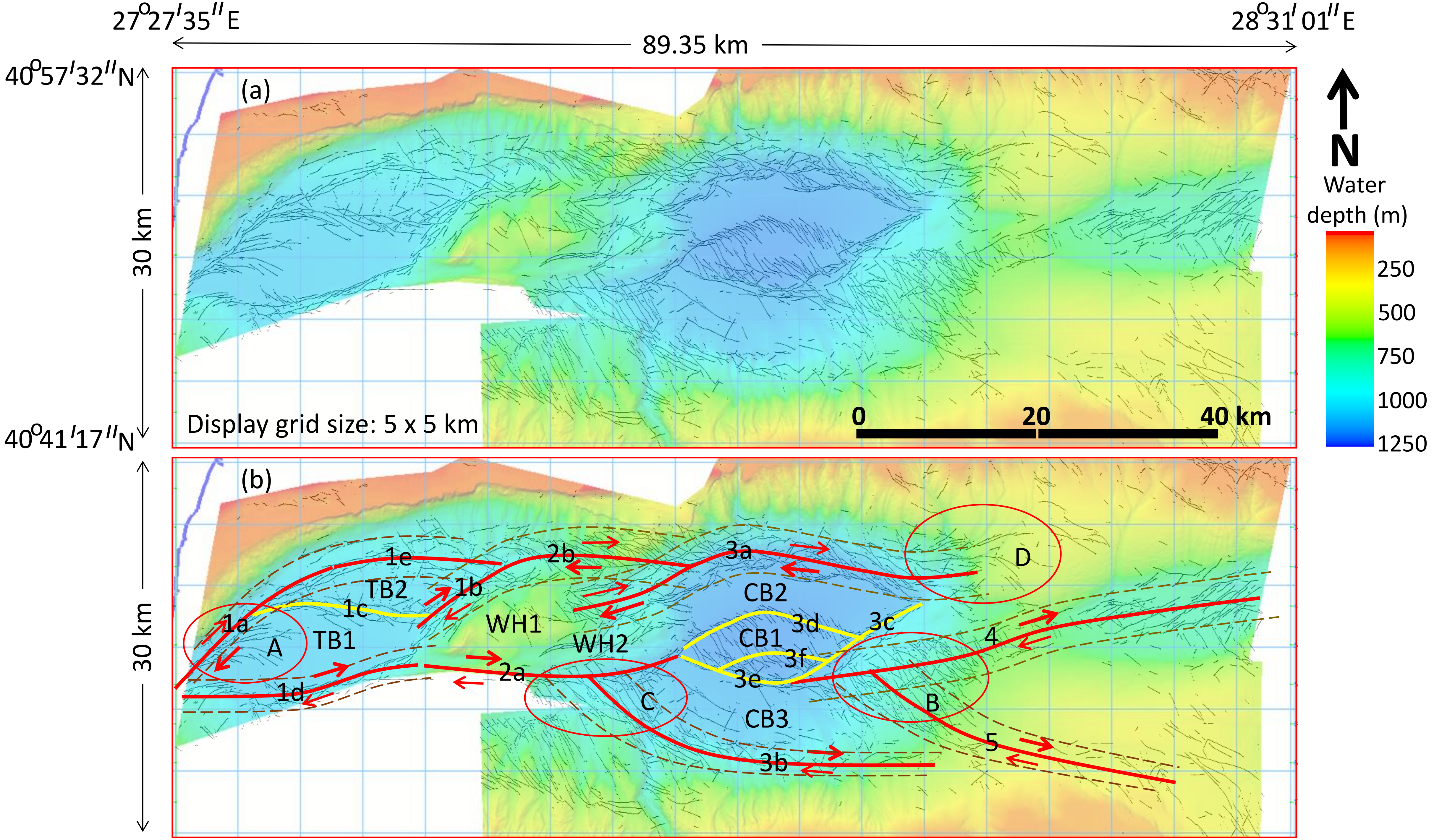

27°27′35″E
28°31′01″E
89.35 km
40°57′32″N
40°41′17″N
30 km
(a)
Display grid size: 5 x 5 km
0
20
40 km
N
Water depth (m)
250
500
750
1000
1250
(b)
1a
1b
1c
1d
1e
2a
2b
3a
3b
3c
3d
3e
3f
4
5
TB1
TB2
WH1
WH2
CB1
CB2
CB3
A
B
C
D

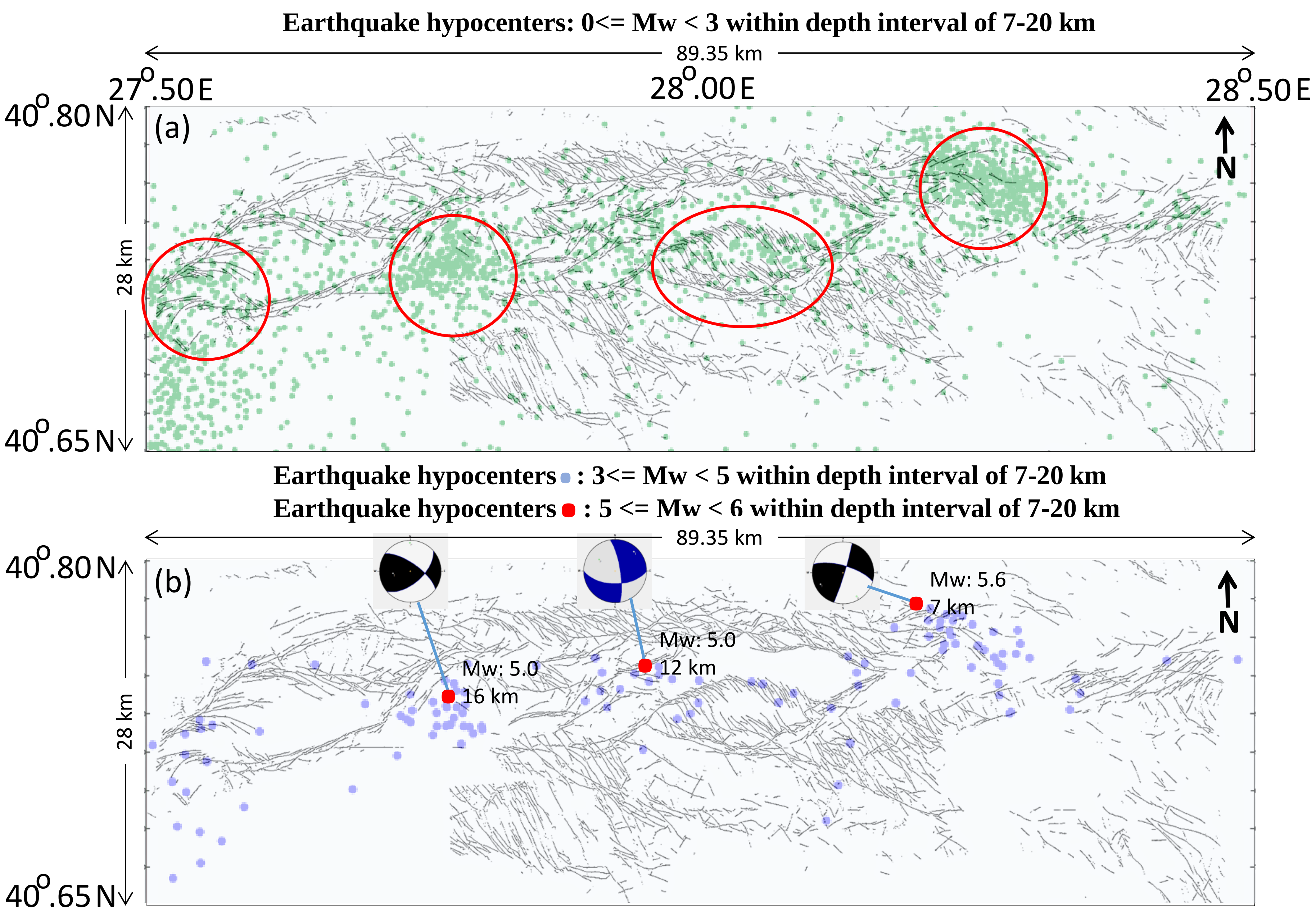

Earthquake hypocenters: 0<= Mw < 3 within depth interval of 7-20 km
89.35 km
27°.50 E
28°.00 E
28°.50 E
40°.80 N
40°.65 N
(a)
28 km
N
Earthquake hypocenters : 3<= Mw < 5 within depth interval of 7-20 km
Earthquake hypocenters : 5 <= Mw < 6 within depth interval of 7-20 km
89.35 km
40°.80 N
40°.65 N
(b)
28 km
N
Mw: 5.0
16 km
Mw: 5.0
12 km
Mw: 5.6
7 km

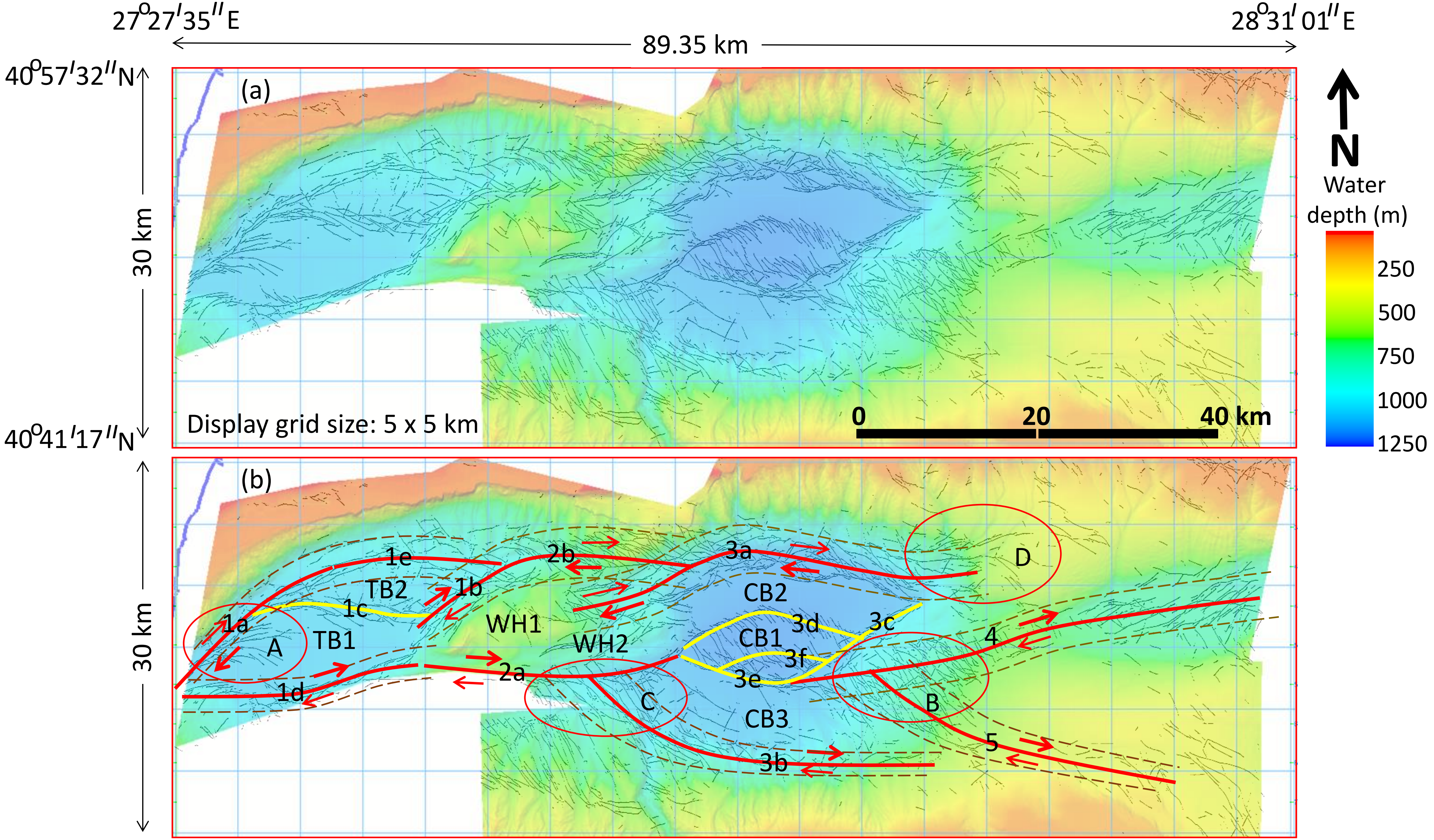

27°27′35″E
28°31′01″E
89.35 km
40°57′32″N
40°41′17″N
30 km
(a)
Display grid size: 5 x 5 km
0
20
40 km
N
Water depth (m)
250
500
750
1000
1250
(b)
1a
1b
1c
1d
1e
2a
2b
3a
3b
3c
3d
3e
3f
4
5
TB1
TB2
WH1
WH2
CB1
CB2
CB3
A
B
C
D

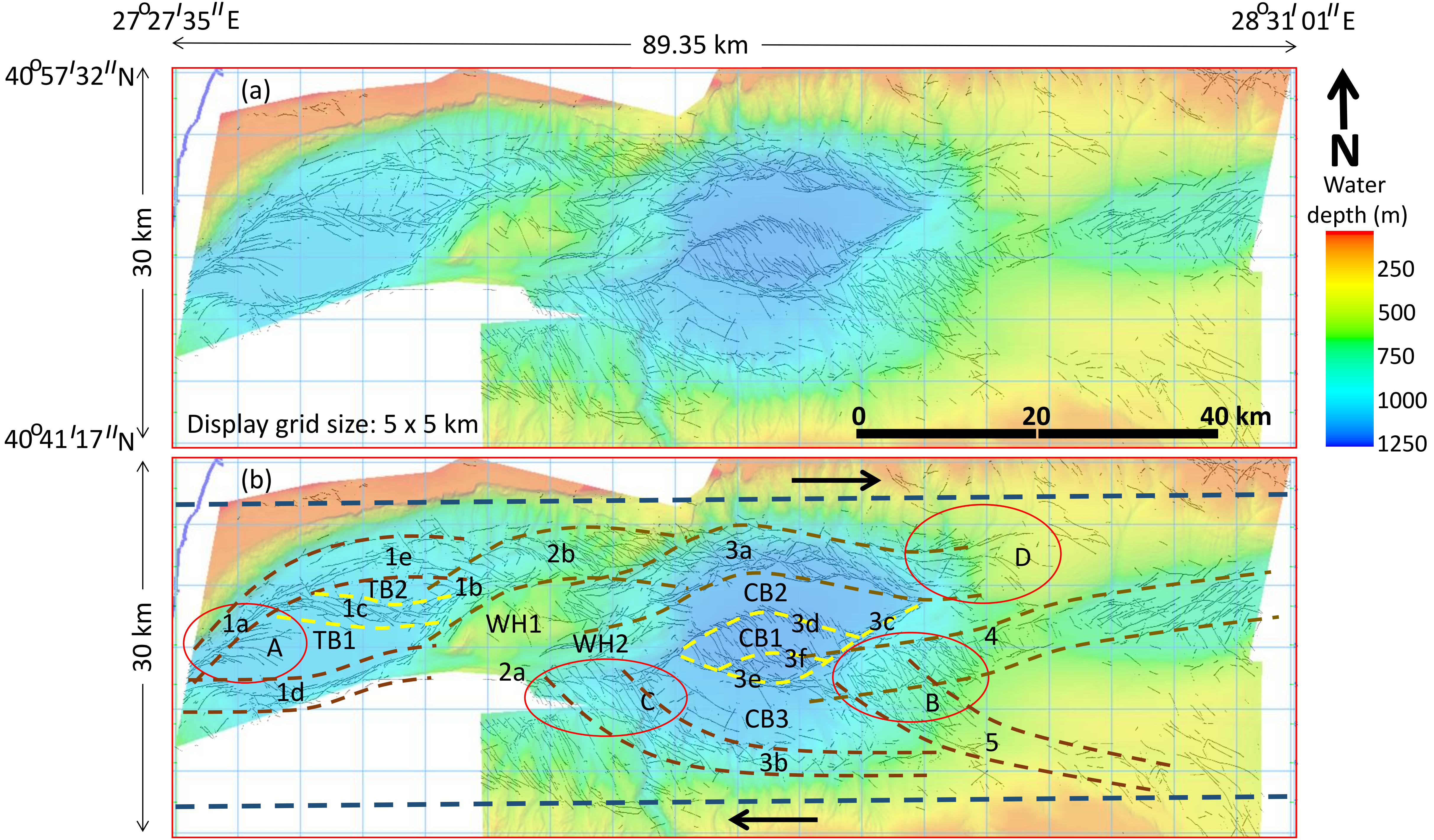

27°27′35″E
28°31′01″E
89.35 km
40°57′32″N
40°41′17″N
30 km
(a)
Display grid size: 5 x 5 km
0
20
40 km
N
Water depth (m)
250
500
750
1000
1250
(b)
1a
1b
1c
1d
1e
TB1
TB2
2a
2b
WH1
WH2
3a
3b
3c
3d
3e
3f
CB1
CB2
CB3
4
5
A
B
C
D

**I wish to conclude this presentation with a few words to the young generation of geophysicists.**

**Always honor what the real data tell you and discard the earth model and the underlying theory that is not consistent with the observed data.**

**In this regard, Nature is your best critic, but is also kind and affectionate to you.**

**Geology is your problem and physics is your solution.
As a geophysicist, you can both define the problem and solve it.**

**And Let Reason be Your Faith.**